# Design and Development of Fiber Grating Based Chemical and Bio-Sensors

*Ph D Thesis submitted to*

*Cochin University of Science and Technology*

*In partial fulfilment of the requirements for the award of the Degree of*

*Doctor of Philosophy*

**Libish T. M.**

Reg. No: 3630


**International School of Photonics**
**Faculty of Technology**
**Cochin University of Science and Technology**
**Cochin -682022, Kerala, India**

*February 2015*

# *Design and Development of Fiber Grating Based Chemical and Bio-Sensors*

**Ph D thesis in the field of Photonics**

*Author:*

**Libish T. M.**
Research Fellow
International School of Photonics
Cochin University of Science & Technology
Cochin -682022, Kerala, India
libishtm@gmail.com

*Research Advisor:*

**Dr. P. Radhakrishnan**
Professor
International School of Photonics
Cochin University of Science & Technology
Cochin -682022, Kerala, India
radhak@cusat.ac.in, padmanabhan.radhak@gmail.com

International School of Photonics
Cochin University of Science & Technology
Cochin -682022, Kerala, India
www.photonics.cusat.edu

February 2015

Cover image: Fiber Grating

*Dedicated to my Parents, Wife and Teachers……*

INTERNATIONAL SCHOOL OF PHOTONICS
COCHIN UNIVERSITY OF SCIENCE AND TECHNOLOGY
COCHIN -682022, KERALA, INDIA

**Dr. P. Radhakrishnan**
Professor

# Certificate

This is to certify that the thesis entitled **"Design and Development of Fiber Grating Based Chemical and Bio-Sensors"** submitted by **Mr. Libish T. M**., is an authentic record of research work carried out by him under my guidance and supervision in partial fulfilment of the requirement of the degree of Doctor of Philosophy of Cochin University of Science and Technology, under the Faculty of Technology and has not been included in any other thesis submitted previously for the award of any degree.

*Kochi-682022*
*07 - 02- 2015*

**Dr. P. Radhakrishnan**
*(Supervising guide)*

Phone: +91 484 2575848 Fax: 0091-484-2576714.
Email: radhak@cusat.ac.in, padmanabhan.radhak@gmail.com

INTERNATIONAL SCHOOL OF PHOTONICS
COCHIN UNIVERSITY OF SCIENCE AND TECHNOLOGY
COCHIN -682022, KERALA, INDIA

**Dr. P. Radhakrishnan**
Professor

# Certificate

This is to certify that the thesis entitled **"Design and Development of Fiber Grating Based Chemical and Bio-Sensors"** submitted by **Mr. Libish T. M.**, has incorporated all the relevant corrections and modifications suggested by the audience during the pre-synopsis seminar and recommended by the Doctoral Committee.

*Kochi-682022*
*07- 02- 2015*

**Dr. P. Radhakrishnan**
*(Supervising guide)*

Phone: +91 484 2575848 Fax: 0091-484-2576714.
Email: radhak@cusat.ac.in, padmanabhan.radhak@gmail.com

# *Declaration*

I, Libish T. M., do hereby declare that the thesis entitled **"Design and Development of Fiber Grating Based Chemical and Bio-Sensors"** is a genuine record of research work done by me under the supervision of Dr. P. Radhakrishnan, Professor, International School of Photonics, Cochin University of Science and Technology, Kochi–22, India and it has not been included in any other thesis submitted previously for the award of any degree.

*Kochi- 682022*
*07- 02- 2015*

**Libish T. M.**

# Acknowledgements

*I am indebted to many individuals who have provided assistance and support during the period of this research.*

*First and foremost, I would like to express my sincere gratitude to my supervisor Dr. P. Radhakrishnan, Professor, International School of Photonics (ISP), for giving me an opportunity to work under his guidance. His inspiration, encouragement, constant support and valuable suggestions have gone a long way in the completion of my work. His extraordinary attention to detail and endless efforts in reviewing this thesis and many manuscripts are highly appreciated.*

*I would like to thank Prof. V. P. N. Nampoori, Professor Emeritus, International School of Photonics, for his encouragement and constructive remarks in the course of my Ph D studies.*

*My sincere thanks goes to Dr. M. Kailasnath , Director, ISP, for his wholehearted support and advice during my doctoral work.*

*I gratefully thank Dr. C. P. G. Vallabhan, Dr. V. M. Nandakumaran, Dr. Sheenu Thomas and all other teachers of both ISP and Centre of Excellence in Lasers and Optoelectronic Sciences (CELOS) for the support provided during the years of my Ph D.*

*My special and sincere thanks to Mr. Palas Biswas, Dr. Somnath Bandyopadhyay, Mr. Kamal Dasgupta of Central Glass and Ceramic Research Institute, (A unit lab of CSIR), Kolkata, India, for providing most of the fiber gratings used in this work and also for helpful discussions and valuable technical support.*

*Sincere thanks go to my colleagues in Fiber lab Mr. Bobby Mathews and Mr. J. Linesh for the support and encouragement that they have provided in all my activities.*

*I would like to acknowledge other co-scholars of the ISP, in particular, Mr. S. Mathew, Mr Bejoy Varghese, Dr. Sony T George, Mr. Pradeep Chandran, Mr. Linslal, Dr. B. Nithyaja and Mr. K. J. Thomas, for all their support and for*

*creating a very vibrant environment. The group has been a source of friendship as well as good advice and collaboration.*

*I would like to thank Lab, library and administrative staff of the ISP for the assistance extended during the tenure.*

*I greatly acknowledge the Principal and Board of Governors of S. C. T college of Engineering, Pappanamcode, Trivandrum, for providing me an opportunity to carry out my Ph. D, by choosing me as a sponsored candidate.*

*I extend my sincere thanks to my colleagues of S. C. T college of Engineering, in particular, Mr. G. K. Arun, for their support during the research work.*

*I am also grateful to my parents, brother, sister and in-laws whose unfailing support and encouragement allowed me to complete this research program.*

*Finally, I would like to express my deep appreciation to my wife Fathima Zahina and son Rayhaan Libish for their unconditional support, love, care and encouragement throughout the duration of this research work.*

*Libish T. M.*

*"We still do not know one thousandth of one percent of what nature has revealed to us"*

**Albert Einstein (1879-1955)**

# *Preface*

The growing need for devices to perform fast, reliable and in situ measurements in the field of chemical and biochemical sensing is urging researchers to look for new technologies. One possibility is provided by optical refractometers, which measure the change of the refractive index (RI) associated with a chemical/biochemical reaction. The focus of this thesis is the design and development of optical fibre grating based chemical and bio sensors, mainly those with surrounding medium refractive index (SRI) sensitivities.

Optical fiber grating technologies have attracted much attention in recent years due to their numerous applications in fiber optic sensor and communication systems. Fiber gratings are prepared by creating a region of periodically varying refractive index within the fiber core and these gratings are often classified as Fiber Bragg Gratings (FBGs) or Long-Period Gratings (LPGs), according to grating period. LPGs typically have a grating period in the range 100 μm to 1 mm, whereas FBGs have period of the order of hundreds of nanometers.

Monitoring of chemical and biological species is becoming more and more important in many markets including industrial process control, energy production, health care, food industry, environment monitoring and anti-terrorism. Hence, fast, reliable and accurate chemical and biological sensors have attracted extraordinary interest in recent years. The research work reported in recent years, reveals that fiber-optic sensors have great potential in chemical and biological sensing compared with other sensors which are usually time consuming and require not only high cost equipment but also strictly trained personnel.

The thesis is divided into seven chapters and **Chapter 1** presents the general background of optical fiber sensing systems including the applications of fiber optic sensors.

**Chapter 2** presents an overview of the fundamental theory of fiber optic gratings. It begins with a review of the historical prospective of the photosensitivity mechanisms in optical fibres and provides a brief discussion on the reported photosensitization and fabrication techniques. The basic principle of FBGs, types of FBGs and sensing characteristics of FBGs are detailed in this section.

This chapter also introduces the sensing capabilities of long-period gratings. Firstly, the LPG theory and the basic principle of operation of LPG based sensors are discussed and then the mechanism behind the spectral shifts in the resonance band structure is explored.

**Chapter 3** starts by discussing the effect of grating length and annealing on the transmission spectrum of LPGs written in hydrogen loaded standard single mode fiber (SMF-28). It then presents and discusses the characterization of an LPG to measurands such as temperature and changes in the RI of surrounding medium. We also investigate the temperature sensitivity of the LPGs fabricated in SMF-28 fiber and B-Ge co doped photosensitive fiber. The difference in temperature sensitivity between the SMF-28 and B-Ge fiber is explained on the basis of the thermo-optic coefficients of the respective core and the cladding materials of the two fibers.

**Chapter 4** presents the application of the developed LPG based refractometer as an edible oil adulteration detection sensor. When the edible oils are subjected to adulteration, a change in its original refractive index occurs. Such changes cause corresponding shifts in the resonance wavelength and change in depth (amplitude) of the loss bands in the LPG. Adulteration levels can be detected by analyzing these spectral changes. A complete experimental analysis on the use of an LPG for adulteration detection in coconut oil and virgin olive oil is presented. The device performance is analyzed in terms of its sensitivity and resolution.

The fabrication method and characterization of FBGs used in this research is outlined in **Chapter 5**. This chapter also summarizes the details of RI sensing based on etched FBGs. FBGs have been extensively used as temperature and strain sensors. However, FBGs are intrinsically insensitive to surrounding refractive index of the medium since the light coupling takes place only between well-bound core modes, which are shielded from the influence of the surrounding refractive index by the fiber cladding. To make the FBG sensitive to changes in the surrounding refractive index, the cladding thickness around the grating region must be reduced. The resultant FBG is often termed as an etched, thinned or reduced cladding FBG.

Among the two main sections of the chapter, the initial part explores the fabrication of etched FBGs and the spectral response of FBGs during etching process. A reliable and stable method of etching of FBGs using a special mount is discussed. An experimental verification of the RI sensitivity of the FBGs is given in the latter part of the chapter.

In **chapter 6**, we propose a novel method for measuring the concentration of protein (Bovine Serum Albumin) present in bio-chemical samples. The bio sensor exploits the inherent characteristics of the Fiber Bragg Grating (FBG) which is coated with a biopolymer, deoxyribonucleic acid (DNA). For increased sensitivity, the fiber with FBG was etched with hydrofluoric acid (HF) prior to coating with the DNA. The etched FBGs are sensitive to an external analyte by evanescent field interaction. The sensing mechanism is based on the interaction of the protein with the biopolymer film, which changes the film refractive index resulting in a shift in the Bragg wavelength. By analyzing the Bragg wavelength shift, we can calculate the amount of protein present in the sample solutions.

**Chapter 7** deals with the summary of the findings of the present investigations and discusses the scope for future work.

This thesis also includes a list of the papers accepted for publication during the course of this Ph.D work.

# List of Publications

## *International Journals*


[1]. **T. M. Libish**, M. C. Bobby, J. Linesh, S. Mathew, C. Pradeep, V. P. N. Nampoori, P. Biswas, S. Bandyopadhyay, K. Dasgupta and P. Radhakrishnan, "Detection of adulteration in virgin olive oil using a fiber optic long period grating based sensor", Laser Physics, 23 (4), pp. 045112 (2013).

[2]. **T. M. Libish**, M. C. Bobby, C. L. Linslal, S. Mathew, C. Pradeep, S. Indu, P Biswas, S. Bandyopadhyay, K. Dasgupta, V. P. N. Nampoori and P. Radhakrishnan, "Etched and DNA coated Fiber Bragg Grating sensing system for Protein concentration measurement", Optoelectronics and Advanced Materials-Rapid Communications, 9 (11), pp. 1401-1405 ( 2015).

[3]. **T. M. Libish**, M. C. Bobby, J. Linesh, S. Mathew, P. Biswas, S. Bandyopadhyay, K. Dasgupta and P. Radhakrishnan, "The effect of annealing and temperature on transmission spectra of long period gratings written in hydrogen loaded standard single mode fiber", Optik-International Journal for Light and Electron Optics, 124 (20), pp. 4345-4348 (2013).

[4]. **T. M. Libish**, M. C. Bobby, J. Linesh, S. Mathew, C. Pradeep, V. P. N Nampoori and P. Radhakrishnan, "Refractive index and temperature dependent displacements of resonant peaks of long period grating inscribed in hydrogen loaded SMF-28 fiber", Optoelectronics Letters, 8 (2), pp. 101-104 (2012).

[5]. **T. M. Libish**, M. C. Bobby, J. Linesh, V. P. N. Nampoori and P. Radhakrishnan, "Experimental Analysis on the Response of Long Period Grating to Refractive Indices Higher and Lower than that of Fiber Cladding", Microwave and Optical Technology Letters, 54 (10), pp. 2356-2360 (2012).

[6]. **T. M. Libish**, C.B. Mathews, J. Linesh, P. Biswas, S. Bandyopadhyay, K. Dasgupta, V. P. N. Nampoori, P. Radhakrishnan, "Comparison of thermal response of LPGs written in SMF-28 and B-Ge co doped photosensitive fiber", Fiber Optics and Photonics, pp.1-3 (2012).

[7]. **T. M. Libish**, J. Linesh, M. C. Bobby, B. Nithyaja, S. Mathew, C. Pradeep and P. Radhakrishnan, "Glucose Concentration Sensor Based on Long Period Grating Fabricated from Hydrogen Loaded Photosensitive Fiber", Sensors & Transducers Journal, 129 (6), pp. 142-148 (2011).

[8]. **T. M. Libish**, M. C. Bobby, J. Linesh, P. Biswas, S. Bandyopadhyay, K. Dasgupta, P. Radhakrishnan, "The Effect of Grating Period on Refractive Index Sensitivity of Long Period Gratings Written in Hydrogen Loaded SMF-28 Fiber", Journal of Optoelectronics and advanced Materials, 13 (5), pp. 491-496 (2011).

[9]. **T. M. Libish**, M. C. Bobby, J. Linesh, P. Biswas, S. Bandyopadhyay, K. Dasgupta and P. Radhakrishnan, "Fiber optic sensor for the adulteration detection of edible oils", Optoelectronics and advanced Materials-Rapid Communications, 5, pp. 68 – 72 (2011).

[10]. **T. M. Libish**, J. Linesh, P. Biswas, S. Bandyopadhyay, K. Dasgupta and P. Radhakrishnan, "Fiber Optic Long Period Grating Based Sensor for Coconut Oil Adulteration Detection", Sensors & Transducers Journal, 114 (3), pp. 102-111 (2010).

[11]. S. Mathew, A. kumar Prasad, T. Benoy, P. P. Rakesh, M. Hari, **T. M. Libish**, V. P. N Nampoori and P. Radhakrishnan, "UV-Visible Photoluminescence of $TiO_2$ Nanoparticles Prepared by Hydrothermal Method", Journal of Fluorescence, 22 (6), pp. 1563-1569 (2012).

[12]. C. Bobby Mathews, **T. M. Libish**, J. Linesh, P. Biswas, S. Bandyopadhyay, K. Dasgupta and P. Radhakrishnan, "A Biosensor for the Detection and Estimation of Cholesterol Levels based on LongPeriod Gratings", Sensors & Transducers, 149 (2), pp. 83-88 (2013).

[13]. J. Linesh, **T. M. Libish**, M. C. Bobby, P. Radhakrishnan and V. P. N. Nampoori, "Comparison of Thermal and Refractive index Sensitivity of Symmetric and Antisymmetric modes of Long Period Fiber Gratings", AIP Conf. Proc., 1391, pp. 397-391 (2011).

[14]. J. Linesh, **T. M. Libish**, M. C. Bobby, P. Radhakrishnan and V. P. N. Nampoori "Periodically Tapered LPFG for Ethanol Concentration Detection in Ethanol-Gasoline Blend", Sensors & Transducers Journal, 125 (2), pp. 205-212 (2011).

[15]. P. P. Anish, J. Linesh, **T. M. Libish**, S. Mathew, P. Radhakrishnan, "Design and development of diaphragm based EFPI pressure sensor", Proc. Of SPIE, 8173, 81731V1-6 (2011).

## *International Conferences*

[1]. **T. M. Libish**, J. Linesh, P. P. Anish, P. Biswas, S. Bandyopadhyay, K. Dasgupta and P. Radhakrishnan, "Adulteration Detection Of Coconut Oil Using Long Period Fiber Grating", International Conference on Fiber Optics and Photonics (PHOTONICS-2010), Dec 2010, IIT Guwahati.

[2]. **T. M. Libish**, J. Linesh, Bobby Mathews, C. Pradeep and P. Radhakrishnan, "Fiber optic sensor for the adulteration detection of edible oils", International Conference on Contemporary Trends in Optics and Optoelectronics, Jan 2011, IIST Thiruvananthapuram.

[3]. **T. M. Libish**, C. Bobby Mathews, J. Linesh, P. Biswas, S. Bandyopadhyay, K. Dasgupta and P. Radhakrishnan, "Response of Hydrogen Loaded Long Period Grating Attenuation Bands During Annealing process", International Conference on Sensors and Related Networks (SENNET'12), VIT University, Vellore, India.

[4]. C. Bobby Mathews, **T. M. Libish**, P. Biswas, S. Bandyopadhyay, K. Dasgupta, P. Radhakrishnan, "A Chitosan coated Fiber Optic Long Period Grating Biosensor for the Detection and Estimation of Cholesterol", Proceedings Photonics 2014: International Conference on Fiber Optics and Photonics, OSA 2014, IIT Kharagpur.

[5]. Bobby Mathews C, **T. M. Libish**, J. Linesh, P. Biswas, S. Bandyopadhyay, K. Dasgupta and P.Radhakrishnan, "A Long Period Grating based Biosensor for the Detection and Estimation of Cholesterol", International Conference on Fiber Optics and Photonics (Photonics 2012), 2012, IIT Madras.

[6]. J. Linesh, **T. M. Libish**, M. C. Bobby, P. Radhakrishnan and V. P. N. Nampoori, "Comparison of Thermal and Refractive index Sensitivity of Symmetric and Antisymmetric modes of Long Period Fiber Gratings", Proceedings of International Conference on Light (optics'11), May 2011, NIT Calicut.

[7]. P. P. Anish, J. Linesh, **T. M. Libish**, S. Mathew and P. Radhakrishnan, "Design and Development of Diaphragm-Based EFPI Pressure Sensor", International Conference on Fiber Optics and Photonics (PHOTONICS- 2010), Dec 2010, IIT Guwahati.

[8]. J. Linesh, K. Sudeesh, **T. M. Libish**, P. Radhakrishnan and V P N Nampoori, "Optical Fiber Sensor to Determine Critical Mole Fractions Of Alcohol- Water Binary Mixtures", International Conference on Fiber Optics and Photonics (PHOTONICS-2010), Dec 2010, IIT Guwahati.

[9]. J. Linesh, **T. M. Libish**, P. Radhakrishnan and V. P. N. Nampoori, "LPFG Based Sensor to Monitor Ethanol Concentration in Ethanol Petrol Blend", International Conference on Fiber Optics and Photonics (PHOTONICS-2010), Dec 2010, IIT Guwahati.

[10]. J. Linesh, M. G. Dibin, **T. M. Libish**, M. Bobby, P. Radhakrishnan and V. P. N. Nampoori, "Optical Fiber Sensor to Determine Critical Micelle Concentration of Binary Mixtures of tert -Butyl Alcohol and Water", International Conference on Contemporary Trends in Optics and Optoelectronics, Jan 2011, IIST Thiruvananthapuram.

### *National Conferences*

[1]. **T. M. Libish**, J. Linesh, P. P. Anish, S. Mathew, V. P. N. Nampoori and P. Radhakrishnan, "Fiber Optic Sensor for Detection of Adulteration in Sunflower Oil", DAE- BRNS, National Laser Symposium (NLS)-2010, December 2010, RRCAT, Indore.

[2]. J. Linesh, V. Bejoy, **T. M. Libish**, M. C. Bobby, P. Radhakrishnan and V. P. N. Nampoori, "Fiber optic humidity sensor based on $TiO_2$ blended PVA coating", DAE-BRNS National Laser Symposium, (NLS-21) February 2013, BARC Mumbai.

[3]. J. Linesh, M. C. Bobby, **T. M. Libish**, P. Radhakrishnan and V. P. N. Nampoori, "Fiber Optic Alcometer Using Pva/Chitosan Polymer Blend", XXXVI OSI Symposium on Frontiers in Optics and Photonics (FOP11), December 2011, IIT Delhi.

[4]. P. P. Anish, J. Linesh, **T. M. Libish**, V. Bejoy and P. Radhakrishnan, "A Metal Diaphragm Based Fiber Optic EFPI Temperature Sensor", DAEBRNS National Laser Symposium (NLS), Dec 2010, RRCAT, Indore.

# *Contents*

# Chapter 1

# Introduction to fiber optic sensors

*Abstract*

*This chapter presents the general background of optical fiber based sensing systems and then discusses the specific importance of fiber gratings in optical sensor field.*

## 1.1 Introduction

The optical fiber is considered to be one of the most significant inventions of the twentieth century. As suggested by Kao and Hockham [1] during the early development stages, the optical fiber has emerged to become undeniably the most important transmission medium for light wave delivery, and has revolutionized modern communications and optical science. The award of the 2009 Nobel Prize in Physics to C. K. Kao, who first proposed the use of optical fibers for data communication, is the crowning jewel on this fantastic story. Fiber optic sensor has been one of the most benefited technologies of the remarkable developments that were achieved by optoelectronics and fiber optic communications industries. Fundamentally, a fiber-optic sensor works by modulating one or more properties of a propagating light wave, including intensity, phase, polarization, and wavelength, in response to the environmental parameter being measured [2]. Today fiber optic based devices, including fiber gratings, play a major role in optical sensor and optical communication applications. These applications include civil, mechanical, electrical, aerospace, automotive, nuclear, biomedical and chemical sensing technologies [3,4].

The following section provides an introduction to optical fiber sensors before focusing on fiber gratings and grating based sensor.

## 1.2 Fiber Optic Sensors (FOS)

Optical fiber as the light wave guiding media has been proposed and developed since 1960s. But it is not until 1980s that the first silica based low loss fiber was fabricated for optical communication system. Since then, there has been an explosive development in fiber optical communication and fiber based systems have become the backbone of the “information age”. In parallel with these developments, optical fiber sensors, which have been a major user of the

technology associated with the optoelectronics and fiber optic communications industries, have fascinated the researchers and tantalized the application engineers for over thirty years. Many components associated with optical fiber communications and optoelectronic industries have been developed for optical fiber sensor applications nowadays. The capability of optical fiber sensors to displace traditional sensors for sensing applications has been increased, since component prices have fallen and the component quality has been improved greatly.

In the 21$^{st}$ century, photonics technology has turned into one of the primary research fields. Fiber optic sensors have been used in diverse applications ranging from monitoring of natural structures for prediction of earthquakes and volcanic activity [5] to medical systems like blood oxygen monitoring [6]. For structural applications, fiber optic sensors are used for strain sensing and damage detection [7-9]. These sensors have also been used for sensing temperature, pressure, rotation, velocity, magnetic field, acceleration, vibration [2,10-13], chemical [14-16] and biological species [17-19], pH level, acoustic waves, environmental [20] sensing and many other physical parameters [4].

Optical fiber sensors may be defined as a means through which a physical, chemical, biological or other measurand interacts with light guided in an optical fiber or guided to an interaction region by an optical fiber to produce an optical signal related to the parameter of interest. The fiber sensor is illustrated diagrammatically in Fig. 1.1. Light is taken to a modulation region using an optical fiber and modulated therein by physical, chemical, or biological phenomena, and the modulated light is transmitted back to a receiver, detected, and demodulated.

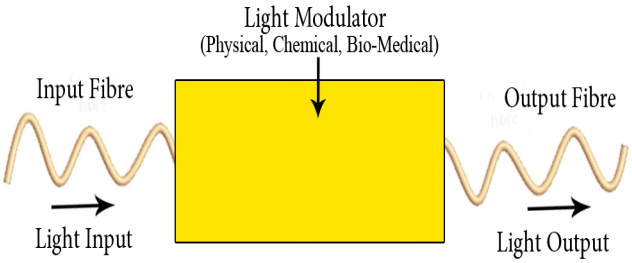


***Figure 1.1:*** *A basic fiber optic sensor system consists of an optical fiber and a light modulating arrangement.*

The advantages of fiber-optic sensing are well known and have been widely presented [3, 4, 21-23]. Comparing with the conventional electrical and electronic sensors, fiber-optic sensors (FOS) have inherent superiorities that others cannot or difficult to achieve, such as:

(i). Insensitivity to EMI (electro magnetic interference) and inability to conduct electric current;

(ii). Remote sensing: it is possible to use a segment of the fiber as a sensor gauge with a long segment of another fiber (or of the same fiber) conveying the sensing information to a remote station. Optical fiber transmission cables offer significantly lower signal loss, as compared to signal transmission in other sensors, and can maintain a high signal-to-noise ratio (SNR).

(iii). Small size and light weight: optical fibers are intrinsically small-size, which helps when building a compact measurement and acquisition system and suitable for installing or embedding into structures.

(iv). Operation in hazardous environments: optical fiber sensors have been proven to be able to work under extreme conditions, such as high

temperature, high pressure, corrosive and toxic environments, high radiation, large electromagnetic fields and other harsh environments;

(v). High sensitivity and wide bandwidth: a FOS is sensitive to small perturbations in its environment.

(vi). Distributed measurement: an optical fiber communication network allows the user to carry out measurements at different points along the transmission line without significant loss when the signal passes through it. This provides a method to monitor, control, and analyze the parameter being monitored over an extended length or area.

### 1.2.1 Classification of FOS

In general, optical fiber sensors may be categorized under two headings according to their operation [2-4, 23, 24]:

I. Extrinsic Fiber Optic Sensor

II. Intrinsic Fiber Optic Sensor

Extrinsic sensors are distinguished by the characteristic that the sensing takes place in a region outside the fiber as shown in Fig. 1.2(a). The optical fiber is only used as the means of light delivery and collection. The propagating light leaves the fiber in a way that can be detected and collected back by another or the same fiber. Intrinsic FOSs differ from extrinsic sensors, where light does not have to leave the optical fiber to perform the sensing function as shown in Fig. 1.2(b). In intrinsic FOSs, the optical fiber structure is modified and the fiber itself plays an active role in the sensing function, i.e. modulation of light takes place inside the fiber to measure a particular parameter [25-29]. So they are also called all-fiber sensors.

Extrinsic optical fiber sensors can be found in schemes such as Fabry-Perot interferometers which utilize only some of the advantages optical fibers offer over competing technologies. Intrinsic optical fiber sensors such as fiber optic gyroscope, fiber Bragg gratings, long period gratings, microbend and coated or doped fiber sensors utilise most of the advantages offered by the technology [24]. Intrinsic systems have attracted many researchers mainly due to their ability to be embedded into composite structures.

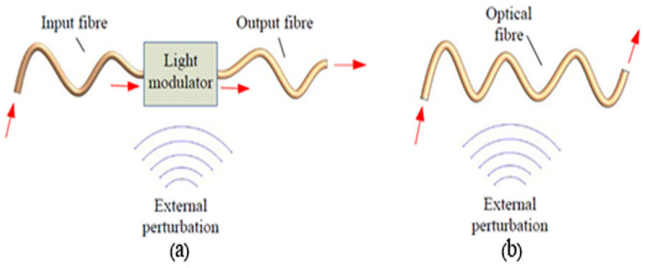


***Figure 1.2:*** *Schematic showing the general design scheme of (a) extrinsic and (b) intrinsic fiber optic sensors.*

### 1.2.2 Classification of FOS based on modulation techniques

Optical fiber sensors act as transducers and convert measurands such as temperature, strain and pressure into a corresponding change in the optical radiation. Light wave propagating along the optical fiber could be characterized in terms of four factors, which are intensity (amplitude), phase, wavelength (frequency) and state of polarization [3,4]. When the surrounding environment has certain perturbation on the sensing head, at least one of the four factors change according to the influence. By measuring the light signal variation, one could obtain useful information of the change in surrounding environment. Thus the effectiveness of the optical fiber sensor depends on its ability to convert the measurands into these parameters reliably and accurately. Based on the modulation technique FOSs are classified as follows.

- Intensity modulated FOS
- Phase modulated FOS
- Polarization modulated FOS
- Wavelength modulated FOS

Phase-modulated sensors usually use an interferometer and sense the output signal by comparing the phase of the received signal with a reference signal. Generally, this sensor employs a coherent light source such as a laser and two single mode fibers. The intensity sensors are basically incoherent in nature and are simple in construction and handling, while the interferometric sensors are quite complex in design and handling but offer better sensitivity and resolution compared to intensity modulated sensor. In the polarization modulation based sensors, a plane polarized light is launched in the fiber and the change in the state of polarization is measured as a function of the perturbing parameter of interest. In the case of commonly used wavelength modulated sensors, light from a broad band source is launched from one side of the fiber and the variation is sensed in terms of change in wavelength of reflected or transmitted spectrum.

#### 1.2.2.1 Intensity modulated sensors

In an intensity modulated FOS, the measurand modulates the intensity of transmitted light through the fiber and these variations in output light is measured using a suitable detector [24,30]. Measurements of optical power are easier than measurements of complicated optical properties like wavelength shift, polarisation state or phase interference. Various mechanisms such as transmission, reflection, micro-bending, or other phenomenon such as absorption, scattering, or fluorescence can be associated with light loss. Depending upon which mechanism changes the intensity of a signal, a wide variety of architectures are possible for these sensors. Optical fiber intensity-based reflective sensors represent one of the initial, straightforward and, maybe, the most widely used sensors [31-33]. The intensity-

based sensor requires more light and therefore usually uses multimode large core fibers. The popularity of these sensors is related to their simple configuration, low fabrication cost, possibility of being multiplexed, robustness and flexibility because no speciality components or fibers are required except a stable optical source, a reasonable photo-detector and signal processing unit. However, by adding suitable components to the architecture of these sensors, performance can be enhanced and sensing at multiple points becomes possible. Intensity-based fiber optic sensors have a series of limitations imposed by variable losses in the system that are not related to the environmental effect to be measured. Potential error sources include variable losses due to connectors and splices, micro bending loss, macro bending loss, deterioration of optical fiber and misalignment of light sources and detectors. Variations in the intensity of the light source may also lead to false readings, unless a referencing system is used [34]. Intensity modulated FOS can be found in a variety of intrinsic and extrinsic configurations.

#### 1.2.2.2 Phase modulated sensors

Phase modulated sensors use changes in the phase of light for detection. The principle attraction of optical phase modulation is its intrinsically high sensitivity to environmental modulation, so that very high resolution measurand are feasible. The optical phase of the light passing through the fiber is modulated by the field to be detected. This phase modulation is then detected interferometrically, by comparing the phase of the light in the signal fiber to that in a reference optical fiber.

In an interferometer, the light is split into two beams, where one beam is exposed to the action of the measurand and undergoes a phase shift and the other is isolated from the sensing environment and is used as a reference. Once the beams are recombined, they interfere with each other [24]. These are used to measure pressure, rotation and magnetic field, etc. Mach-Zehnder, Michelson, Fabry-Perot, Sagnac, polarimetric, and grating interferometers are the commonly used

intereferometers. These interferometric sensors have wide applications in science, engineering and technical field [4,24,35]. Mach-Zehnder interferometer is the most commonly used phase-modulated sensor. These sensors give a change in phase depending upon the change in length of an arm of interferometer or change in RI, or both. In general, the phase-based fiber optic sensor is more sensitive than the intensity-based fiber optic sensors.

#### 1.2.2.3 Polarization modulated sensors

Optical fiber is made of glass. The refractive index of the fiber can be changed by the application of stress or strain. This phenomenon is called a photo elastic effect. In addition, in many cases, the stress or strain in different directions is different, so that the induced refractive index change is also different in different directions. Thus, there is an induced phase difference between different polarization directions. In other words, under the external perturbation, such as stress or strain, the optical fiber works like a linear retarder. Therefore, by detecting the change in the output polarization state, the external perturbation can be sensed [2,24].

Polarization plays an important role in a system using single mode fiber. A variety of physical phenomena influence the state of polarization of light. They are Faraday rotation, electrogyration, electro-optic effect and photo elastic effect. Polarization modulation may also be introduced by a number of other means, such as mechanical twisting or by applying stress on the fiber. We can measure magnetic field, electric field, temperature and chemical species based on polarization effect [23, 24, 36, 37]. For example, magnetic field causes Faraday rotation of the plane polarized light by an angle proportional to the strength of the magnetic field. Liquid crystals (LCs) have polarization effects, so sensors based on LCs also exhibit polarization effects [38].

#### 1.2.2.4 Wavelength modulated sensors

Wavelength modulated sensors use changes in the wavelength of light for detection. Truly wavelength-modulated sensors are those making use of gratings inscribed inside the optical fiber. A grating is a periodic structure that causes light or incident electromagnetic energy to behave in a certain way dependent on the periodicity of the grating. The following section will give a brief introduction to fiber grating based sensors.

## 1.3 Fiber grating based sensors

Fiber sensors based on intensity modulation and phase modulation principle have some problems that need to be solved in practical applications. The problems associated with source power fluctuations, coupler losses, bending losses, mechanical losses due to misalignment and absorption effects will significantly influence measurement performance of intensity based fiber sensors [4]. Measurement accuracy of phase-based fiber sensors is often compromised due to the existence of temperature drifts and vibration. Among the spectrally modulated fiber sensors the most promising developments are those based on grating technology.

A fiber optic grating is formed by inducing a periodic refractive index perturbation along the length of an optical fiber core [39]. The periodical perturbation of the effective refractive index allows the coupling of a core mode into forward or backward propagating modes, depending on the grating period [40]. The fiber gratings are classified into two categories depending on the grating period and type of mode coupling:

**Fiber Bragg Gratings (FBGs)** - also called reflection or short period gratings, where the coupling takes place between two modes travelling in opposite directions [39].

**Long Period Gratings (LPGs)** - also called transmission gratings, where the coupling take place between core and cladding modes travelling in the same direction [41-44]. These cladding modes attenuate rapidly on propagation and result in loss bands at distinct wavelengths in the grating transmission spectrum. When broadband source is injected, a specific wavelength is reflected back and rest are transmitted. Whenever the environmental measurand affects the grating region, it shifts the peak wavelength. In FBG the reflected spectrum is studied, while in LPG the transmitted spectrum is studied [45,46].

The most widely used wavelength based sensor is the Bragg grating sensor. FBGs have revolutionized modern telecommunications and subsequently that of optical fiber based sensor technology. In the latter case, FBGs are an excellent sensing element due to their high sensitivity, multiplexing ability and reasonable fabrication cost. In addition, several distinct types of FBGs have been developed in order to meet certain scientific needs. The principle of operation of an FBG sensor is based on the shift of the Bragg wavelength when it is under the influence of a measurand [46,47]. Strain and temperature are the two basic parameters that can directly tune the Bragg wavelength of FBG [48]. Since the light coupling takes place between well-bound core modes that are screened from the influence of the surrounding medium refractive index by the cladding, normal FBGs are intrinsically insensitive to SRI. So normal FBGs cannot be used as chemical sensors or biosensors. To use the FBG as an effective refractometric sensor element, the cladding radius around the grating region must be reduced, allowing the effective refractive index of the fiber core to be significantly affected by the refractive index of external medium [49]. As a consequence, shifts are expected in the Bragg wavelength combined with a modulation of the reflected amplitude. The resultant FBG is often termed as an etched, thinned or reduced cladding FBG [50,51]. A very simple method to reduce the cladding can be the uniform chemical

etching of the Bragg grating section of the fiber using hydrofluoric acid. The sensitivity of the sensor depends on the change in the effective index of the core mode, which is related to the change in the refractive index of a biological or chemical sample under test. To date, a number of surrounding refractive index (SRI) sensors have been realized using etched FBG structures to measure concentrations of some chemicals or bio samples [52,53].

The first LPG successfully inscribed in an optical fiber was described in 1996 by Vengsarkar *et al*. and was used as a band-rejection filter [43]. In the same year Bhatia presented the first LPG device acting as an optical sensor [54]. Since then, LPGs have found many applications in optical communication and sensing. In optical communication systems, LPGs are applied as gain equalizers [55], dispersion compensators [56], optical switches [57], components in wavelength division multiplexing (WDM) systems [58], band rejection filters [9] and mode converters [59]. The attenuation bands of LPG is a strong function of external perturbations like strain, temperature, bending and surrounding refractive index [54,60]. Presence of these external perturbations affects the coupling strength between the core and cladding modes, which could lead to both amplitude and wavelength shift of the attenuation bands in the LPG transmission spectrum. Measurement of these spectral parameters in response to environment, surrounding the grating region is the basis of sensing with LPGs [45]. In an LPG the guided light interacts with the external medium and the effective index of the excited cladding modes depends on the refractive index of the core, cladding and external medium materials.

Long-period fiber gratings have been demonstrated to have high sensitivity to the refractive index of the ambient media. However, their multiple resonance peaks and broad transmission spectra (typically tens of nanometers) limit the measurement accuracy and their multiplexing capabilities. In addition, the

relatively long length of the grating limits their application as point sensor devices. In conventional fiber Bragg gratings, for refractive- index sensing, etching of the cladding is required for the evanescent field of the guided mode to be accessed. This reduces the strength and durability of the sensor and makes it susceptible to damage under harsh environmental conditions. Long period grating (LPG) refractive index sensors retain their endurance, as the integrity of the fiber is not violated.

At present, the refractive index sensing based on the fiber grating is an extraordinarily important subject in the biochemical sensing area which attracts significant research interest. FBGs are generally less sensitive to the variations in the refractive index of the surrounding medium as the fiber core is well covered by the cladding layer. This limits the application of FBGs in chemical and bio-sensing. Therefore, Long Period Gratings (LPGs) [54,60] and etched FBGs (eFBGs) [49-52] have been utilized for chemical and bio-sensing applications.

The forthcoming chapters of this thesis discuss the design and development of different LPG and FBG based sensors in detail.

Chapter 2 of the thesis has been devoted to the fundamental theory of fiber optic gratings, fabrication technology and principle of operation of FBG and LPG based sensors. In chapter 3, the fabrication of LPG and experimental analysis of its transmission spectra with variation in refractive index and temperature of surrounding medium have been presented. Chapter 4 presents the application of the developed LPG based refractometer as an edible oil adulteration detection sensor. Chapter 5 of the thesis deals with the fabrication of etched FBGs and refractive index sensing using etched FBGs. In chapter 6, we propose a novel method for measuring the concentration of protein (Bovine Serum Albumin) present in bio-

chemical samples using FBG. Finally, chapter 7 gives a summary of the present work and a few future studies for various medical diagnostic applications.

## 1.4 Summary

This first chapter presented an overview of the optical fiber sensors, its classifications, the advantages and the applications. The chapter also introduced the relatively new class of fiber optic sensors, the fiber grating sensors, and discussed the advantages that they offer over conventional fiber optic sensors. The chapter also presented the distinguishing features of the two different classes of fiber grating, the fiber Bragg grating and the long period grating.

## References

[1]. K. C. Kao and G. A. Hockham, "*Dielectric-fiber surface waveguides for optical frequencies*", Proceedings of the Institution of Electrical Engineers, **113**, pp. 1151-1158 (1966).

[2]. S. Yin, P. B. Ruffin and F. T. S. Yu, "*Fiber optic sensors*", 2nd edn, Taylor & Francis Group, CRC Press (2008).

[3]. B. Culshaw and J. Dakin, "*Optical Fiber Sensors System and Applications*", Vol 2, Artech House (1989).

[4]. Eric Udd and William B. Spillman, "*Fiber Optic Sensors: An Introduction for Engineers and Scientists*", John Wiley & Sons (2011).

[5]. E. Udd, R. G. Blom, D. Tralli, E. Saaski and R. Dokka, "*Application of the Sagnac Interferometer Based Strain Sensor to an Earth Movement Detection System*", Proceedings of the SPIE, 2191, pp. 126-136 (1994).

[6]. J. R. Griffiths and S. P. Robinson "The OxyLite: a *Fiber- Optic oxygen Sensor*", The British Journal of Radiology, pp. 627-630 (1999).

[7]. K. Hotate and S. L. Ong, "*Distributed dynamic strain measurement using a correlation-based Brillouin sensing system*", IEEE Photonics Technology Letters, **15**, pp. 272–274 (2003).

[8]. S. Villalba and J R Casas, *"Application of optical fiber distributed sensing to health monitoring of concrete structures",* Mechanical Systems and Signal Processing, **39**, pp. 441–451 (2013).

[9]. C. K. Y Leung, N. Elvin, N. Olson, T.F. Morse and H. Yi Fei, "*A novel distributed optical crack sensor for concrete structures"*, Engineering Fracture Mechanics, **65**, pp. 133-148 (2000).

[10]. Y. Dong, X. Bao, L. Chen, "*Distributed temperature sensing based on birefringence effect on transient Brillouin grating in a polarization-maintaining photonic crystal fiber",* Optics Letters, **34**, pp. 2590–2592 (2009).

[11]. D. Zhou, Z. Qin, W. Li, L. Chen and X. Bao, "*Distributed vibration sensing with time-resolved optical frequency-domain reflectometry*", Optics Express, **20,** pp.13138–13145 (2012).

[12]. Y. Dong, L. Chen and X. Bao, "*High-spatial-resolution simultaneous strain and temperature sensor using Brillouin scattering and birefringence in a polarization-maintaining fiber*", IEEE Photonics Technology Letters, **22**, pp. 1364–1366 (2010).

[13]. B. Culshaw and A.D. Kersey, "*Fiber optic sensors: an historical perspective*", Journal of Lightwave Technology, **26**, pp. 1064-1078 (2008).

[14]. G. Stewart, W. Jin and B. Culshaw, "*Prospects for fiber-optic evanescent-field gas sensors using absorption in the near-infrared*", Sensors and Actuators B: Chemical, **38**, pp. 42-47 (1997).

[15]. F. B. Xiong, W. Z. Zhu, H. F. Lin, X. G. Merg, "*Fiber-optic sensor based on evanescent wave absorbance around 2.7 μm for determining water content in polar organic solvents",* Applied Physics B, **115**, pp. 129-135 (2014).

[16]. H. Jiang, R. Yang, X. Tang, A. Burnett, X. Lan, H. Xiao and J. Dong, "*Multilayer fiber optic sensors for in situ gas monitoring in harsh environments"*, Sensors and Actuators B: Chemical, **177**, pp. 205–212 (2013).

[17]. O. S. Wolfbeis, "Fiber-optic chemical sensors and biosensors," Analytical Chemistry, **76**, pp. 3269-3284 (2004).

[18]. J. A. Ferguson, T. C. Boles, C. P. Adams and D. R. Walt, "*A fiber-optic DNA biosensor microarray for the analysis of gene expression*", Nature Biotechnology, **14**, pp. 1681-1684 (1996).

[19]. B. G. Healy, L. Li, and D. R. Walt, "*Multianalyte biosensors on optical imaging bundles",* Biosensors and Bioelectronics, **12**, pp. 521-529 (1997).

[20]. A. M. Dietrich, J. N. Jensen and W. F. Da Costa, "*Measurement of pollutants:chemical species*", Water environmental research, **68**, pp. 391-406 (1996).

[21]. T. G. Giallorenzi, J. A. Bucaro, A. Dandridge, J. H. Cole, S. C. Rashley and R. G. Priest, "*Optical Fiber Sensor Technology*", IEEE Transactions on Microwave Theory and Techniques, **30**, pp. 472-511 (1982).

[22]. B. Lee, "*Review of the Present Status of Optical Fiber Sensors"*, Optical Fiber Technology, **8**, pp. 57-79 (2003).

[23]. K. T. V Grattan and B. T. Meggitt, "*Optical Fiber Sensor Technology: Applications and Systems*", **3**, Kluwer Academic Publishers (1999).

[24]. B. D. Gupta, Gupta and Banshi Das, "*Fiber Optic Sensors: Principles and Applications*", New India Publishing (2006).

[25]. M. Archenault, H. Gagnaire, J. P. Goure and N. Jaffrezic-Renault, "*A simple intrinsic optical fiber refractometer*," Sensors and Actuators B: Chemical, **5**, pp. 173-179 (1991).

[26]. J. Yuan and M. A. El-Sherif, "*Fiber-optic chemical sensor using polyaniline as modified cladding material*", IEEE Sensors, **3**, pp. 5-12 (2003).

[27]. S. Trolier McKinstry, G. R. Fox, A. Kholkin, C. A. P. Muller and N. Setter, "*Optical fibers with patterned ZnO/electrode coatings for flexural actuators*", Sensors and Actuators A: Physical, **73**, pp. 267-274 (1999).

[28]. C. Egami, K. Takeda, M. Isai and M. Ogita, "*Evanescent-wave spectroscopic fiber optic pH sensor",* Optics Communications, **122**, pp. 122-126 (1996).

[29]. H. Guo and S. Tao, "*An active core fiber-optic temperature sensor using an Eu(III)-doped sol-gel silica fiber as a temperature indicator*", IEEE Sensors Journal, **7**, pp. 953-954 (2007).

[30]. J. Zhang and S. Albin, "*Self-referenced reflective intensity modulated fiber optic displacement sensor*", Optical Engineering, **38**, pp. 227-232 (1999).

[31]. S. Jhonson, "*Fiber displacement sensor for metrology and control",* Optical Engineering, **24**, pp. 961-965 (1985).

[32]. H. S. Haddock, P. M. Shankar and R. Mutharasan, "*Evanescent sensing of bimolecules and cells"*, Sensors and Actuators B: Chemical, **88**, pp. 67-74 (2003).

[33]. P.V. Preejith, C. S. Lim, A. Kishen, M. S. John and A. Asundi, "*Total protein measurement using a fiber optic evanescent wave based biosensor*", Biotechnology Letters, **25**, pp.105-110 (2001).

[34]. J. R. Casas, and J. S. Paulo, "*Fiber Optic Sensors for Bridge Monitoring*", Journal of Bridge Engineering, **8**, pp. 362-373 (2003).

[35]. B. Culshaw, "*Fiber Optics in Sensing and Measurement*", IEEE J. Selected Topics in Quantum Electronics, **6**, pp. 1014-1021 (2000).

[36]. S. M. Jeon, Y.P. Kim, "*Temperature measurement using fiber optic polarization interferometer*", Optics and Laser Technology, **36**, pp. 181-185 (2004).

[37]. Y. Lung Lo, T. Chih Yu, "*A polarimetric glucose sensor using a liquid-crystal polarization modulator driven by a sinusoidal signal*", Optics Communications, **259**, pp. 40-48 (2006).

[38]. D. A. Krohn, "*Fiber Optic Sensors: Fundamentals and Applications"*, 3rd edition, Instrumentation Systems (2000).

[39]. R. Kashyap, "*Fiber Bragg Gratings*", 2nd Edition, Academic Press (2010).

[40]. A. Othonos, "*Fiber Bragg gratings*", Review of Scientific Instruments, **68**, pp.4309-4341 (1997).

[41]. T. Erdogan, "*Fiber grating spectra*", Journal of Lightwave Technology, **15**, pp. 1277-1294 (1997).

[42]. T. Erdogan, "*Cladding-mode resonances in short- and long-period fiber grating filters*", J. Optical Society of America A, **14**, pp. 1760–1773 (1997).

[43]. A. M. Vengsarkar, P. J. Lemaire, J. B. Judkins, V. Bhatia, T. Erdogan and J. E. Sipe, "*Long-period fiber gratings as band-rejection filters*", Journal of Lightwave Technology, **14**, pp. 58-65 (1996).

[44]. S. W. James and R.P. Tatam, "*Optical fiber long-period grating sensors: characteristics and applications",* Measurement Science and Technology, **14**, pp. 49-61 (2003).

[45]. X. Shu, L. Zhang and I. Bennion, "*Sensitivity characteristics of long-period fiber gratings*", J. of Lightwave Technology, **20**, pp. 255-266 (2002).

[46]. Y. J. Rao, "*In-fiber Bragg grating sensors*", Measurement Science and Technology, **8**, pp. 355-375 (1997).

[47]. A. D. Kersey, M. A. Davis, H. J. Patrick, "*Fiber grating sensors"*, Journal of Lightwave Technology, **15**, pp. 1442-1463 (1997).

[48]. X. Shu, Y. Liu, D. Zhao, B. Gwandu, F. Floreani, L. Zhang and I. Bennion, "*Dependence of temperature and strain coefficients on fiber grating type and its application to simultaneous temperature and strain measurement"*, Optics Leters, **27,** pp. 701–703 (2002).

[49]. A. Iadicicco, A. Cusano, S. Campopiano, A. Cutolo and M. Giordano, "*Thinned fiber Bragg gratings as refractive index sensors*", IEEE Sensor Journal, **5**, pp. 1288-1295 (2005).

[50]. A. N. Chryssis, S. M. Lee, S. B. Lee, S. S. Saini and M. Dagenais, "*High sensitivity etched core fiber Bragg grating sensors*", IEEE Photonics Technology Letters, **17**, pp. 1253–1255 (2005).

[51]. A. Asseh, S. Sandgren, H. Ahlfeldt, B. Sahlgren, R. Stubbe and G. Edwall, "*Fiber optical Bragg grating refractometer*", Fiber and Integrated Optics, **17**, pp. 51–62(1998).

[52]. A. Cusano, A. Iadicicco, S. Campopiano, M. Giordano and A. Cutolo, "*Thinned and micro-structured fiber Bragg gratings: towards new all fiber high sensitivity chemical sensors*", Journal of Optics A: Pure and Applied Optics, **7**, pp. 734-741 (2005).

[53]. G. Ryu, M. Dagenais, M. T. Hurley and P. Deshong, "*High specificity binding of lectins to carbohydrate-functionalized fiber Bragg gratings: A newmodel for biosensing applications*", IEEE Journal of Quantum Electronics, **16**, pp. 647–653 (2010).

[54]. V. Bhatia and A. M. Vengsarkar, "*Optical fiber long period gratings sensors"*, Optics Letters, **21**, pp. 692 – 694 (1996).

[55]. A. M. Vengsarkar, J. R. Pedrazzani, J. B. Judkins, P.J. Lemaire, N. S. Bergano and C. Davidson, "*Long-period fiber-grating-based gain equalizers*", Optics Letters, **21**, pp. 336–338 (1996).

[56]. M. Das and K. Thyagarajan, "*Dispersion compensation in transmission using uniform long period fiber gratings*", Optics Communications, **190**, pp. 159- 163 (2001).

[57]. B. J. Eggleton, R. E. Slusher, J. B. Judkins, J. B. Stark and A. M. Vengsarkar, "*All-optical switching in long-period fiber gratings"*, Optics Letters, **22**, pp. 883-885 (1997).

[58]. Y. Zhu, C. Lu, B. M. Lacquet, P. L. Swart, S. J. Spammer, "*Wavelength tunable add/drop multiplexer for dense wavelength division multiplexing using long-period gratings and fiber stretchers*", Optics Communications, **208**, pp. 337-344 (2002).

[59]. F. Bilodeau, K. O. Hill, B. Malo, D. C. Jonson and I. M. Skinner, "*Efficient, narrowband $LP_{01}\leftrightarrow LP_{02}$ mode convertors fabricated in photosensitive fiber: spectral response"*, Electronics Letters, **27**, pp 682–684 (1991).

[60]. C.C. Ye, S. W. James and R. P. Tatam, "*Long period fiber gratings for simultaneous temperature and bend sensing*", Optics Letters, **25**, pp. 1007-1009 (2000).

Chapter 2

# Fiber Gratings: Basic Theory and Sensing Principle

*Abstract*

*This chapter begins with a review of the historical prospective of the photosensitivity mechanisms in optical fibers and a brief discussion on the reported photosensitization techniques. The chapter presents an overview of the fundamental theory of fiber optic gratings and their development. It also provides a review of the sensing applications of FBGs and LPGs with a particular emphasis on their application as refractive index sensors for chemical and bio-sensing applications. This chapter provides the basis for the following chapters in which applications of gratings with different structures are proposed and demonstrated.*

## 2.1 Introduction

The significant discovery of photosensitivity in optical fibers led to the development of a new class of in-fiber components called fiber gratings. Photosensitivity refers to a permanent change of RI of the fiber core while exposed to light with characteristic wavelength and intensity depending on the core material. In recent years, owing to the numerous advantages of fiber gratings in a wide range of applications, they have attracted great attention over other conventional fiber optic devices. Applications in which FBG structures are employed use the coupling between the forward and backward propagating core modes in the fiber while those using LPGs utilize the core mode to cladding mode coupling.

## 2.2 Bragg grating history

Fiber Bragg gratings (FBGs) are formed by constructing a periodic or a quasi-periodic modulation of refractive index inside the core of an optical fiber. This change in index of refraction is typically created by exposing the fiber core to an intense interference pattern of UV energy. The exposure produces a permanent increase in the refractive index of the fiber's core, creating a fixed index modulation according to the exposure pattern. This fixed index modulation is called a grating [1]. A small amount of light is reflected at each period. All the reflected light signals combine coherently to one large reflection at a particular wavelength. This is referred to as the Bragg condition, and the wavelength at which this reflection occurs is called the Bragg wavelength [2,3]. Only those wavelengths that satisfy the Bragg condition are affected and strongly back reflected through the same core of the fiber.

The formation of permanent grating structures in optical fiber was first demonstrated by Hill and co-workers in 1978 at the Canadian Communications

Research Centre (CRC) in Ottawa, Ontario, Canada [4,5]. In groundbreaking work, they launched high intensity Argon-ion laser radiation (488 nm) into germanium doped fiber and observed an increase in reflected light intensity. After exposing the fiber for a period of time it was found that the reflected light had a particular wavelength. After the exposure, spectral measurements were taken, and confirmed that a permanent narrowband Bragg grating filter had been created in the area of exposure. This was the beginning of a revolution in communications and sensor technology using FBG devices.

The Bragg grating is named after William Lawrence Bragg who formulated the conditions for X-ray diffraction (Bragg's Law). The gratings first written at CRC, initially referred to as "Hill gratings", were actually a result of research on the nonlinear properties of germanium-doped silica fiber. At this early stage, gratings were not fabricated from the "side" (external to the fiber) as commonly practiced now, but written by creating a standing wave of radiation interference within the fiber core introduced from the end of the fiber. This fabrication method was known as internal inscription method. As the light reflected from the grating has the same wavelength as that used to write the grating, this technique is limited to applications using wavelength at or near the writing wavelength.

Almost a decade later, in 1989, Meltz and co-workers showed that it was possible to write gratings from outside the optical fiber using a wavelength of 244nm [6]. This proved to be a significant achievement as it made possible future low cost fabrication methods of fiber Bragg gratings. With this external writing method, it was discovered that a grating made to reflect any wavelength of light could be created by illuminating the fiber through the side of the cladding with two beams of coherent UV light. By using this holographic method the interference pattern and therefore the Bragg wavelength could be controlled by the angle between the two beams, something not possible with the internal writing method.

Since the discovery of photosensitivity in optical fiber by Hill and the developments of the holographic writing method by Meltz, hundreds of articles have been published concerning photosensitivity and fiber Bragg gratings.

To overcome the limitations of two-beam holographic technique, phase mask technique for fabricating gratings was reported by Hill *et al.* [7] in 1993. This new techniques has removed the complexity in the manufacturing process of FBGs, making them reproducible at lower costs.

Nowadays, the phase mask technique has become the most popular and one of the most effective methods for the fabrication of FBGs. This technique makes use of phase mask as a key component of the interferometer to generate the interference pattern. The use of high power femtosecond laser sources for inscribing Bragg gratings has attained significant interest in recent years[8,9]. The principal advantage of high-energy pulses is their ability of grating inscription in any material type without pre-processing, such as hydrogenation or special core doping with photosensitive materials. The refractive index change in femtosecond-inscribed gratings is initiated by a nonlinear reaction through the multiphoton process. The commercial products of fiber Bragg gratings have been available since early 1995. Today, FBGs have become almost synonymous with the field itself and most fiber optic sensor systems make use of Bragg grating technology.

## 2.3 Basics of FBG

A fiber Bragg grating consists of a periodic modulation of the refractive index in the core of a single-mode optical fiber. Schematic and operation of basic FBG are illustrated in Fig. 2.1. When light from a broadband source is launched from one side of the fiber, only a particular wavelength which satisfies Bragg condition will be reflected while the remainder is transmitted without any loss. Periodic RI variations reflect the incoming wave front and constructively form a

back reflected power peaked at a centre wavelength defined by the grating characteristics. The wavelength for which the incident light is reflected with maximum efficiency is called the Bragg wavelength [1,3,10,11]. In optical fiber gratings, the phase matching condition is given by [1]:

$$\beta_1 - \beta_2 = \Delta\beta = \frac{2\pi}{\Lambda} \quad \text{.....(2.1)}$$

where $\beta_1$ and $\beta_2$ are the propagation constants of the modes being coupled and $\Lambda$ is the grating period. In the case of FBGs, the forward propagating core mode ($LP_{01}$) couples to the reverse propagating core mode. i.e. Propagation constants remain the same but with a negative sign.

$$\beta_2 = -\beta_1 = \beta \quad \text{..... (2.2)}$$

Therefore the phase matching condition becomes

$$\beta - (-\beta) = \frac{2\pi}{\Lambda} \quad \text{.....(2.3)}$$

$$2\beta = \Delta\beta = \frac{2\pi}{\Lambda} \quad \text{.....(2.4)}$$

Since $\Delta\beta$ is large in this case, the grating periodicity will be small, typically less than 1μm.

But

$$\beta = \frac{2\pi}{\lambda} n_{eff} \quad \text{.....(2.5)}$$

where $n_{eff}$ is the effective refractive index of fiber core. Now the equation (2.4) becomes

$$2\left(\frac{2\pi}{\lambda} n_{eff}\right) = \frac{2\pi}{\Lambda} \quad \text{.....(2.6)}$$

Thus the Bragg wavelength can be written as:

$$\lambda_B = 2.\ n_{eff}.\Lambda \quad \text{.....(2.7)}$$

where $n_{eff}$ is effective refractive index of the fiber core and $\Lambda$ is the grating period. So any change in the effective refractive index or the grating period will cause a shift in the reflected Bragg wavelength. The wavelengths, other than $\lambda_B$ will experience weak reflection at each of the grating planes because of the phase mismatch over the length of the grating. The grating spacing can be changed, during manufacturing, to create Bragg gratings of different center wavelengths. Comprehensive explanation of FBG basic principles can be found in several references [4,11]. In some papers, the coupled-mode theory [12] is used as a technique for the detailed theoretical analysis of FBGs, because it is simple and accurate in simulating the optical behavior and in modeling the optical property of most the fiber gratings.

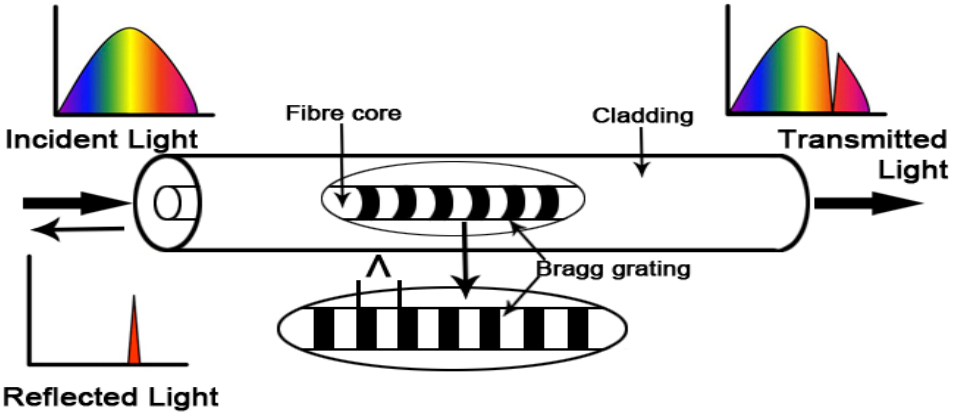


***Figure 2.1:*** *Schematic representation of a Bragg grating inscribed into the core of an optical fiber. The period of the index of refraction variation is represented by* $\Lambda$.

### 2.3.1 The Bragg condition

The Bragg grating resonance condition is the requirement to satisfy both energy and momentum conservation, in which the energy conservation $(hw_i=hw_f)$ requires that the frequency of the reflected radiation should be the same as that of the incident radiation. The momentum conservation requires that the sum of

incident wave vector ($\vec{k}_i$) and the grating wave vector ($\vec{K}$) should be equal to the wave vector of the scattered radiation ($\vec{k}_f$). This can be expressed as

$$\vec{k}_i + \vec{K} = \vec{k}_f \quad \text{.....(2.8)}$$

where the grating wave vector K, has a direction normal to the grating plane with a magnitude $2\pi/\Lambda$, with $\Lambda$ being the grating spacing [3,13]. The diffracted wave vector is equal in magnitude and opposite in direction with regard to the incident wave vector and hence the momentum conservation condition can be represented as [3,10]

$$2\left(\frac{2\pi n_{eff}}{\lambda_B}\right) = \frac{2\pi}{\Lambda} \quad \text{.....(2.9)}$$

This simplifies to the first order Bragg condition

$$\lambda_B = 2\, n_{eff}\, \Lambda \quad \text{.....(2.10)}$$

where $\lambda_B$ is the Bragg wavelength and $n_{eff}$ is effective refractive index of the fiber core. If the Bragg condition is not satisfied, the reflected light from each subsequent plane in the grating becomes out of phase progressively and gradually cancel out. Also, light that is not coincident with the Bragg wavelength will simply get transmitted and experience very little reflection.

### 2.3.2 Induced refractive index change

The simplest uniform fiber Bragg grating structure in optical fiber is an axial (x) and periodic change of the refractive index of the core with a refractive index profile given by[3,13]:

$$n_{eff}(x) = n_0 + \Delta n \cos\left(\frac{2\pi x}{\Lambda}\right) \quad \text{.....(2.11)}$$

where Δn is the amplitude of the induced refractive index perturbation, $n_0$ is the averag index of the fiber core, x is the distance along the fiber's longitudinal axis and Λ is the grating period.The typical value of Δn varies in the range $10^{-5}$ to$10^{-2}$.

### 2.3.3 Bragg grating reflectivity

The reflectivity of a grating with constant modulation amplitude and period can be expressed using the coupled mode theory of Lam and Garside as [3,14]

$$R(l,\lambda) = \frac{\Omega^2 \sinh^2(sl)}{\Delta k^2 \sinh^2(sl) + s^2 \cosh^2(sl)} \quad \text{.....(2.12)}$$

where R(l, λ) is a fraction between 0 and 1 of the propagating optical power reflected by a grating of length *l* at a given wavelength λ. $\Delta k = k - \frac{\pi}{\lambda}$ is the detuning wave vector, $k = \frac{2\pi n_0}{\lambda}$ is the propagation constant and $s = \sqrt{\Omega^2 - \Delta k^2}$. The coupling coefficient, Ω, for a sinusoidally varying index modulation along the fiber axis is given by:

$$\Omega = \frac{\pi \Delta n \eta(V)}{\lambda} \quad \text{.....(2.13)}$$

where Δn is the amplitude of the induced refractive index at a given wavelength λ and η (V) is a function of the normalized frequency V of the fiber that represents the fraction of the fiber mode power contained in the core, η (V ) $\approx 1 - {}^{1}/_{V^2}$ . The normalized frequency V can be expressed as [14]

$$V = \frac{2\pi}{\lambda}\, a\, (n_{co}^2 - n_{cl}^2)^{1/2} \quad \text{.....(2.14)}$$

where a is the fiber core radius, $n_{co}$ and $n_{cl}$ are the core and cladding refractive indices, respectively. The fiber is single mode at wavelengths for which

$V \leq 2.405$ [6]. At the Bragg grating center wavelength, there is no wave vector detuning and $\Delta k$ equals zero. Therefore, the expression for the reflectivity becomes

$$R(l, \lambda) = \tanh^2(\Omega l) \quad \text{.....(2.15)}$$

### 2.3.4 Spectral reflectivity dependence on grating parameters

Bragg grating has the property of reflecting light within a narrow band of wavelengths and transmitting the entire wavelength outside that band. The reflectivity increases with the change in the induced refractive index. It can also be found that the reflectivity increases with the increase in the length of the grating.

#### *A. Grating strength*

The reflectivity of the fiber Bragg grating depends on the grating strength according to Eqn.2.15. It implies that the reflectivity of the Bragg gratings can be increased by increasing the magnitude of the refractive index change [3]. A refractive index modulation of $10^{-3}$ in silica fibers is normally achievable.

#### *B. Grating length*

The length of a Bragg grating is dependent on the size of the fabrication system and is normally limited to a few centimeters. An FBG close to 100% reflection of the Bragg wavelength can be obtained by increasing the length of the grating [3].

### 2.3.5 Full-width at half-maximum (FWHM)

The full-width at half-maximum (FWHM) bandwidth of a grating [15,16] is the difference between two wavelengths on either side of Bragg wavelength where reflectivity drops to half of its maximum. An increase in length of grating results in

reduced FWHM bandwidth. A general expression for the approximate full width at half-maximum bandwidth of a grating is given by

$$\Delta\lambda_{FWHM} = \lambda_B \alpha \sqrt{\left(\frac{1}{2}\frac{\Delta n}{n}\right)^2 + \left(\frac{1}{N}\right)^2} \quad \text{.....(2.16)}$$

where N is the number of grating planes present in grating structure, $\alpha \approx 1$ for strong gratings(for grating with near 100% reflection) and $\alpha \approx 0.5$ for weaker gratings [17].

## 2.4 Sensing principle

Fiber gratings are excellent elements in sensing applications, which is the main topic of this thesis. The basic principle of operation commonly used in an FBG based sensor system is to monitor the shift in Bragg wavelength, $\lambda_B$ with the changes in the measurand. The Bragg wavelength of an optical fiber grating is a function of the grating period ($\Lambda$) and the effective refractive index ($n_{eff}$) of the fiber core and is represented by equation (2.7).

$$\lambda_B = 2\, n_{eff}\, \Lambda$$

Thus any change in refractive index or the grating period due to external measurands will change the Bragg wavelength of the device and can be detected in either the reflected or transmitted spectrum of FBGs. Strain ($\varepsilon$) and temperature (T) are the two basic parameters that can directly tune the center wavelength of FBG [1,3]. i.e. the Bragg wavelength is a function of both the strain and temperature, $\lambda_B = \lambda_B(\varepsilon, T)$ and they are considered as independent variables [18,19]. Since the measurand field induces a differential change in the wavelength, the differential of $\lambda_B$ is taken. It can be represented as

$$d\lambda_B = \frac{\partial \lambda_B}{\partial \varepsilon} d\varepsilon + \frac{\partial \lambda_B}{\partial T} dT$$

$$= \left[\frac{\partial}{\partial \varepsilon} (2\, n_{eff}\, \Lambda)\right] d\varepsilon + \left[\frac{\partial}{\partial T} (2\, n_{eff}\, \Lambda)\right] dT \quad \text{.....(2.17)}$$

$$= \left[2\, n_{eff} \frac{\partial \Lambda}{\partial \varepsilon} + 2 \frac{\partial\, n_{eff}}{\partial \varepsilon} \Lambda\right] d\varepsilon + \left[2\, n_{eff} \frac{\partial \Lambda}{\partial T} + 2 \frac{\partial\, n_{eff}}{\partial T} \Lambda\right] dT$$

Dividing the equation by $\lambda_B = 2\, n_{eff}\, \Lambda$ becomes,

$$\frac{d\lambda_B}{\lambda_B} = \left[\frac{1}{\Lambda} \frac{\partial \Lambda}{\partial \varepsilon} + \frac{1}{n_{eff}} \frac{\partial\, n_{eff}}{\partial \varepsilon}\right] d\varepsilon + \left[\frac{1}{\Lambda} \frac{\partial \Lambda}{\partial T} + \frac{1}{n_{eff}} \frac{\partial\, n_{eff}}{\partial T}\right] dT \quad \text{.....(2.18)}$$

This equation shows how the Bragg wavelength is shifted by the strain and temperature.

The first term in Eq. 2.18 represents the strain effect and the second term represents the temperature effect on optical fiber grating.

### 2.4.1 Strain sensitivity of Bragg gratings

The basic operation of FBG strain sensor is based on the measurement of the peak wavelength shift induced by the applied strain [19]. FBGs can provide extremely sensitive strain measurements for various materials and structures. Strain sensing is an important part in a health monitoring system for civil, mechanical, and aerospace applications. The idea of using FBGs for strain measurement was first introduced by Bertholds *et al*. in 1988 [20], where the strain-optic coefficient of optical fibers has been determined.

The strain induced shift of the fiber Bragg grating results from two effects (former part of Eq.2.18); the physical elongation of the optical fiber corresponding to a change in grating spacing and the change in the effective refractive index due to photo elastic (strain-optic) effects [21,22,23]. The Bragg wavelength shift due to

strain optic effect alone can be expressed in terms of the photoelastic coefficient as [17, 20]

$$\Delta\lambda_B = (1 - p_e)\,\lambda_B\,\varepsilon \quad \text{.....(2.19)}$$

where the term ε is axial strain experienced by the fiber in micro-strain (με), $\Delta\lambda_B$ is the shift in wavelength (nm) and $p_e$ is the photoelastic coefficient (effective strain-optic constant) of the fiber given by

$$p_e = \left(\frac{n_{eff}^2}{2}\right)\left[p_{12} - \nu(p_{11} + p_{12})\right] \quad \text{.....(2.20)}$$

where $p_{11}$ and $p_{12}$ are the components of strain-optic tensor, and ν is Poisson's ratio.

Figure 2.2 shows the shifts of the wavelength and the grating pitch length before and after the strain is added on both ends of the fiber. Strain measurements based on FBG is a rapidly developing technology which is driven by its performance accuracy and versatility and is being used for structural monitoring and smart structure applications [24-30].

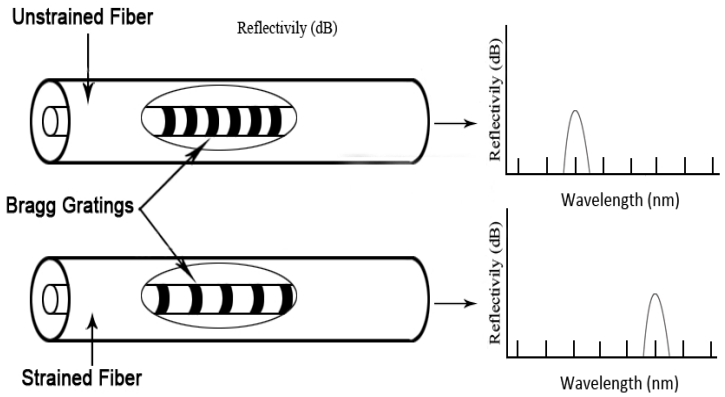


***Figure 2.2:*** *Wavelength shift and pitch length shift when strain is added on the FBG.*

### 2.4.2 Temperature sensitivity of Bragg gratings

The temperature response of the Bragg wavelength is due to two factors (latter part of Eq.2.18), the thermal expansion of the fiber resulting in a change in the grating spacing and the change in the effective refractive index of the fiber due to the thermo-optic effect. Thus the Bragg wavelength shift due to temperature change can be expressed as

$$\Delta\lambda_B = (\alpha + \xi)\,\lambda_B\,\Delta T \quad \text{.....(2.21)}$$

where $\alpha = \left(\frac{1}{\Lambda}\right)\left(\frac{\partial\Lambda}{\partial T}\right)$ is the coefficient of thermal expansion, $\xi = \left(\frac{1}{n_{eff}}\right)\left(\frac{\partial n_{eff}}{\partial T}\right)$ represents the thermo-optic coefficient of the fiber and $\Delta T$ is the change in temperature. Both parameters $\alpha$ and $\xi$ are functions of temperature and have been observed to be non-linear at high temperatures [22,24]. Most materials expand when the temperature increases. If the fiber expands with increase in temperature then the grating spacing increases and the Bragg wavelength will shift towards positive side (red-shift). For silica fibers, the thermo-optic effect is the dominant factor accounting for approximately 95% of the observed shift in the Bragg wavelength. The thermal expansion accounts for only 5% of the total effect. Various authors have reported the use of FBGs for temperature sensing applications [31-34].

### 2.4.3 Strain and temperature sensing

As discussed above, FBGs respond to changes in both strain and temperature. The strain directly affects the FBG as it expands or contracts the grating period and thus the refractive index is modified whereas, the temperature sensitivity of an FBG mainly occurs because of the change in induced refractive index [3]. Therefore if a FBG sensor is subjected simultaneously to both strain and temperature changes, the combined Bragg wavelength shift can be expressed as

$$\Delta\lambda_B = \left[\left(1 - p_e\right)\varepsilon + (\alpha + \xi)\,\Delta T\right]\lambda_B \quad \text{.....(2.22)}$$

Thus the Bragg wavelength shift can be rewritten using the above defined variables as

$$\Delta\lambda_B = \left(\left\{1 - \left(\frac{n_{eff}^2}{2}\right)\left[p_{12} - V(p_{11} + p_{12})\right]\right\}\varepsilon + \left\{\left(\frac{1}{\Lambda}\right)\left(\frac{\partial\Lambda}{\partial T}\right) + \left(\frac{1}{n}\right)\left(\frac{\partial n}{\partial T}\right)\right\}\Delta T\right)\lambda_B \quad \text{.....(2.23)}$$

So, it is necessary to discriminate strain and temperature effects in order to reveal each physical parameter, and various methods have been proposed [35-40]. A straightforward method, as proposed by Y. J. Chiang *et al*. in [41] involves using a pair of FBGs, both susceptible to temperature effect, with one of them being protected from strain. In this case, it is desirable that both FBGs experience the same sensitivity to temperature and its effect can be isolated from the strain effect.

Another method is to use two FBGs with a large difference in their Bragg wavelengths, which show different responses to the same measurand [42]. FBGs written on fibers of different diameters have also been proposed, which give different strain responses, while the temperature responses remain the same [43,44]. By writing FBG with close wavelengths in undoped and boron co-doped fibers, different temperature sensitivities are obtained while the strain sensitivities remain the same [45]. In these reported techniques, it is necessary to use special fibers (specialty fibers with different doping elements, microstructured fibers, and photonic crystal fibers) or special spectroscopic techniques (fluorescence and interferometry) in order to distinguish temperature and strain, which result in bulky sensor systems targeting for the sole purpose of simultaneous measurement of temperature and strain only [46-48]. Another method involves using nonlinear effects such as stimulated Brillouin scattering to discriminate temperature from strain measurements [49]. Lu *et al*. reported an approach to resolve the cross-sensitivity between temperature and strain of FBGs [50], in which acrylate and

polyimide polymers were used as the coating materials for different FBGs to achieve simultaneous measurement of axial strain and temperature.

### 2.4.4 Refractive index sensitivity

In standard single mode optical fibers, the fundamental mode is strongly shielded by the cladding layer avoiding any influence of the surrounding medium refractive index on the guiding properties. So the effective refractive index is not influenced by the external one, thus leading to no sensitivity to surrounding medium refractive index. However, if cladding diameter is reduced partially or totally along the grating region, the effective refractive index is significantly affected by the surrounding medium [51-53]. As a direct consequence, strong changes in the spectral response of the FBGs occur in etched optical fiber. This effect can be useful in chemical as well as in bio sensing applications [54-58]. The first demonstration of an FBG as a refractometer was done in 1997 by Asseh *et al*. [59], and it was based on the application of chemical etching to the fiber region where the grating was located. Usage of chemically etched fiber Bragg grating as refractive index sensor is discussed in detail in chapter 5 of this thesis.

## 2.5 Photosensitivity in optical fibers

The photosensitivity in optical fibers refers to a permanent change in the refractive index of the core of the optical fiber when exposed to light radiation with characteristic wavelength and intensity that depends on the fiber material [1,60]. The significant discovery of photosensitivity in optical fibers led to the development of a new class of in-fiber components called fiber gratings. The existence of high photosensitivity within a fiber core is crucial to the fabrication of high quality Bragg gratings. Photosensitivity in fiber was discovered by Hill *et al*. [4] in 1978 while they were studying the nonlinear effects in a specially designed high silica optical fiber using 488nm radiation and since then, several published

studies have explained the photosensitivity mechanisms. The refractive index change reported by Hill was due to two photon absorption and was determined by Lam and Garside [13]. They concluded that using a UV light source would be more effective in the fabrication of fiber gratings. Since then, photosensitivity in optical fibers remained dormant for several years, mainly due to limitations of the writing technique. However, a renewed interest has risen with the demonstration of the side writing technique by Meltz *et al*. [6] almost ten years later.

Numerous studies have been conducted to understand the mechanism of photosensitivity of optical fiber. Studies have also been conducted to discover for fibers of higher photosensitivity and more efficient FBG fabrication techniques. In the early research, it was believed that the photosensitivity exists only in germanium doped fibers [61], but later studies reported the photosensitivity in a wide range of different fibers, that contain dopants other than germanium and which contained no germanium at all [62,63]. However, germanium doped fibers are still the most interesting photosensitive fibers for grating fabrication due to their extensive applications in optical sensor and telecommunication area. Photosensitivity is also detected when the fiber is exposed to different wavelengths of radiations (157nm, 193nm, 244nm, 248nm, 255nm, 266 nm, 325nm, 351nm etc.) [64-66].

### 2.5.1 Photosensitivity models

Regardless of the worldwide interest into the subject, there is still no single model to explain the Photosensitivity in all cases, but it has been realized that the photosensitivity depends on a number of factors, including the core material, the wavelength and intensity of the radiating light. Several models have been proposed for these photoinduced refractive index changes, such as colour-centre model [67], compaction model [68], stress relief model [69], dipole model [70], electron charge migration model [71], ionic migration model [72] and Soret effect [73].

These models have been reviewed extensively in many papers [1,3,74]. To date, the colour centre model is the most widely accepted model for the formation mechanism of fiber gratings. According to the colour centre model, photosensitivity is related to defects present in glass.

The colour centre model is based on the breaking of the germanium-oxygen vacancy defect bonds in germanium-doped silica on absorption of UV radiation around the 244 nm wavelength band. On absorption of a photon, the GeO defect bond breaks forming a colour centre characterized by the presence of a $Si^{+}$ hole and a released electron that is free to move within the glass matrix and can be retrapped at the original site or at some other defect site. The newly trapped electron causes a reconfiguration of the shape of the molecule which changes the absorption properties of doped silica in the UV region of the spectrum, leading to an increase in the refractive index given by the Kramers-Kronig relationship [74]. The colour centre model for photosensitivity was supported by many experiments [75-77]. The compaction model or densification model [78] suggests that the UV radiation breaks bonds in the glass network causing the glass structure to compress and its density to increase, producing the refractive index change. The stress-relaxation model is based on the assumption that breaking of chemical bonds on exposure to UV radiation results in the relief of compressive internal stress which is frozen within the core of the fiber during the fiber drawing process. Thus the change in refractive index is characterized by the photo elastic process of stress relief during fabrication [69]. The electron charge migration model is based on the appearance of a periodic electric field by photoexcitation of fiber defects.

### 2.5.2 Photosensitivity enhancement techniques

Since the discovery of photosensitivity and the first demonstration of grating formation in germonosilicate fiber by Hill in 1978, considerable efforts have been made to understand and increase the photosensitivity in optical fibers. The

developed photosensitization techniques, including hydrogen loading, flame brushing and co-doping in fiber core are able to increase the photoinduced index modulations in the fiber core up to the order of $10^{-3}$ - $10^{-2}$. This section discusses different techniques available to enhance the photosensitivity in optical fibers

### 2.5.2.1 Hydrogen Loading or Hydrogenation Technique

Hydrogen loading of optical fibers is the most commonly used technique for achieving high UV photosensitivity in germanosilicate and germanium-free optical fibers and was first developed by Lemaire *et al*. in 1993 [79,80]. Hydrogen loading is carried out by diffusing hydrogen molecules into the fiber core at high pressure and temperature. This method is beneficial in that it allows any optical fiber to have Bragg gratings inscribed in them. Under UV laser radiation, the hydrogen that is diffused into the fiber reacts with the Ge-O-Si bonds in the glass, forming additional OH species. This raises the level of oxygen-deficiency in the glass matrix and hence increases the amount of absorption at 240nm. The time required for hydrogenation of fiber to achieve a certain photosensitivity level varies with the pressure and temperature. It normally takes a week of hydrogen soaking at room temperature in order to obtain the desired photosensitivity in optical fiber. The required time can be decreased to a few days by raising the temperature or the pressure during the hydrogen loading process. But it should be noticed that high pressure hydrogen is dangerous and demands special precautions.

There are several advantages with hydrogenation technique. It offers a very simple and effective way to substantially increase a fiber's photosensitivity. Fabrication of FBG is possible in any germanosilicate fibers, and even in germanium-free fiber when shorter wavelength UV light is used (typically 193 nm). Additionally, permanent refractive index changes occur only in regions that are UV irradiated. The fiber loses its photosensitivity when hydrogen molecules diffuse out. Therefore, by thermally diffusing out the hydrogen molecules after

the index change, the grating will have high photo-stability even in the UV wavelength region. The hydrogen loading technique also removes the necessity of using UV wavelengths, coinciding with defect absorption bands for accessing photosensitivity [81].

The major disadvantages of this process are that it uses high pressure hydrogen, which in itself is very dangerous and requires special precautions. Another drawback of this method is the strong absorption near the 1550 nm telecommunication window which arises due to increase O-H bond formation during hydrogenization. Thermal annealing process diffuses out the excess hydrogen present in the fiber. But this process can shift the resonance peak up to a few nanometers, thus causing difficulties in reproducing the same Bragg resonance wavelength repeatedly. The Bragg wavelength caused by the out diffusion of hydrogen molecules can also affect the stability of gratings used in elevated temperature sensing applications.

#### 2.5.2.2 The flame brushing

This technique is based on brushing the fiber repeatedly with a flame fuelled with hydrogen and a small amount of oxygen at a temperature of approximately 1700°C to achieve photosensitization [82]. At this temperature, hydrogen diffuses into fiber core very quickly and it takes only approximately 20 minutes to photosensitize a fiber completely. The principle of flame brushing technique is the same as hydrogen loading technique. Hydrogen molecules are used to create defects that strongly absorb at UV wavelength, and increase photosensitivity. Highly localized photosensitivity can be obtained in fiber because of the fact that the flame can be made very small in size. The effect only targets the core of the fiber while the cladding properties remain unaffected. The flame brushing technique has been used to increase the photosensitivity of

standard optical fiber by a factor greater than 10, achieving refractive index changes of greater than $10^{-3}$. The major advantage of the flame brushing technique over hydrogen loading is that the increased photosensitivity is permanent when the fiber has been flame brushed, whereas hydrogen loaded fiber loses photosensitivity as the hydrogen diffuses out of the fiber. The biggest disadvantage of this technique is that the exposure to high temperature flame greatly reduces the mechanical property and durability of the fiber which increases the likelihood of the fiber breaking.

### 2.5.2.3 Co- doping Technique

The other schemes for increasing the photosensitivity in optical fibers include, increasing the concentration of germanium in germanosilicate fiber or codoping of the fiber preforms with co-dopants such as boron [83], europium [84], cerium [85], erbium [86], phosphorous [87], antimony [88] and tin [89] which exhibit different degrees of sensitivity in silica host optical fiber. Germanium doping increases the intrinsic photosensitivity but also enhances the refractive index of the silica. For communication fibers, the refractive indices of the core and cladding and numerical aperture are standardized.

Studies have shown that fiber co-doped with boron to be much more photosensitive than fiber with higher germanium concentration and without boron co-doping. Addition of boron oxide to silica results in a compound glass that has a lower refractive index than silica. So boron co-doping reduces the RI of the core and makes it softer than before. Fiber indices may be matched with high concentrations of germanium as long as the boron concentration is sufficient. The absorption measurements suggest that in contrast to hydrogen loading and flame-brushing techniques, boron co-doping does not enhance the fiber photosensitivity through the creation of oxygen-germanium deficiency centers.

Instead, it is believed that boron co-doping increases the photosensitivity of the fiber by allowing photo induced stress relaxation to occur, which seems likely to be initiated by the breakage of bonds by UV light. Tin co-doped fibers exhibit similar photosensitivity as those doped with boron. But the Sn co-doped fibers also benefit from some advantages over boron doped fibers including the grating survival at high temperature and their induced refractive index changes are more stable with time [90].

## 2.6 FBG Fabrication Technology

Since the discovery of photosensitivity in optical fibers, there has been a growing interest for fabrication of Bragg gratings within the core of an optical fiber. Direct optical inscription of high quality gratings into the cores of optical fibers has been actively pursued by many research laboratories and various techniques have been reported. Different FBG fabrication techniques can be classified as internal inscription and external inscription techniques [3,4]. Adopted primarily during the earlier years, internally writing technique uses relatively simple experimental setup in which the standing wave inside the optical fiber photo imprints a Bragg grating with the same pattern as the standing wave. In recent years, the internal inscription technique has been superseded by the external inscription technique due to the inefficiency of the writing process. In this, gratings are side written into the core of a photosensitive fiber by exposure to a UV light source and generally have greater reflectance due to the large index modulation. Currently, there are three basic external writing techniques for FBGs fabrication in photosensitive optical fibers with the necessary accuracy namely: Interferometric technique [6,85,91,92]**,** Phase Mask Technique[93-108] and Point-by-Point Inscription method [109-110]. These techniques differ in the principle of writing and consequently, in the equipment used in the grating writing process.

The interferometric fabrication technique, the first external writing technique to inscribe Bragg gratings in photosensitive fibers, was demonstrated by Meltz *et al*. in 1989 [6], in which a single laser beam is split into two components, which are subsequently recombined at the fiber to produce an interference pattern. Bragg gratings can be written interferometrically by amplitude-splitting [6,90] or by wavefront-splitting [14,91,92].

The first demonstration of the point-by-point technique for writing FBG was reported by Malo *et al*. in 1993 [109]. This technique uses a UV pulse laser or femtosecond laser [110] to inscribe individual grating planes one step at a time along the core of the fibre. A single pulse of light passes through a slit and then is focused onto the core of the optical fiber to produce an index change at one point. After the refractive index at the irradiation point is changed, the fibre is translated by a distance $\Lambda$, which corresponds to the grating period, from the original place by a precision translation stage. The movement of the translation stage is computer controlled. This procedure is repeated until the desired grating length is obtained.

The phase mask method is the most widely used and effective method for inscribing FBGs in photosensitive fibers [90]. This technique makes use of phase mask as a key component of the interferometer to generate the interference pattern. A Phase mask is a corrugated grating etched in a silica substrate produced either by holographic or by electron-beam lithography method [93,94]. The phase mask is normally placed in contact or near contact with the fiber. The laser beam passes through the mask and is spatially diffracted to form an interference pattern. This interference pattern photo imprints a refractive index modulation in the core of the photosensitive optical fiber as shown in Fig.2.3.

With a normally incident UV radiation, the phase mask diffracts the incident beam into several orders, m=0, ±1, ±2 ... and the diffraction angle of the positive and negative orders are equal. The superpositions of the different plus and minus diffraction orders form an inference pattern, which can be used to inscribe Bragg gratings in optical fibers. Normally, the near field interference fringe pattern, generated by ±1 order diffraction is employed for grating fabrication. Phase masks for FBG fabrication are usually designed such that the zero order diffracted beam is suppressed to less than few percent (typically less than 3%) of the transmitted light when the light is incident on the mask. The diffracted plus and minus first (±1) orders are maximized, each containing, typically more than 35% of the transmitted power [14].

Important features in a phase mask are the period of the etched grooves and the etch depth. The period of the grating ($\Lambda_g$) written in the core of the fiber is one half of the phase mask period ($\Lambda_{pm}$) and does not depend on the wavelength of the writing beam or its incident angle on the phase mask.

$$\Lambda_g = \frac{1}{2}\ \Lambda_{pm} \quad \text{.....(2.24)}$$

To achieve the minimization of the zero order diffraction, the etching depth d of the relief grating in phase mask is controlled to be:

$$\mathrm{d} = \frac{\lambda_{uv}}{2} \quad \text{.....(2.25)}$$

where $\lambda_{uv}$ is the wavelength of UV irradiation. From this equation, it can be concluded that in FBG inscription, for each UV laser source working at a different wavelength, a different phase mask needs to be used. This is the major disadvantage of the phase mask based fabrication method. The wavelength of the UV light source is selected based on the absorbance spectra of the doped optical fiber core – thereby maximizing the source's efficiency in FBG writing.

KrF excimer lasers (248nm) are the most common UV sources used to fabricate Bragg gratings with a phase mask. Different lasers have been used for the manufacture of gratings in fibers using phase mask, ranging from fluorine lasers (157nm) [95,96], ArF lasers(193nm) [97], frequency-doubled argon-ion lasers (244 nm) [98], copper vapour lasers (211 and 255nm) [99], frequency quadrupled diode-pumped $Nd^{3}$+:YLF laser (262 nm) [100], fourth harmonic of Nd:YAG ( 266nm) [101], 351 nm light from an Ar ion laser [102], near UV lasers at 334nm [103], tripled Nd: YAG laser at 355nm [104] and femtosecond lasers [105,106] etc. The phase-mask technique can also be used to fabricate complex grating structures such as chirped and apodized gratings [107,108].

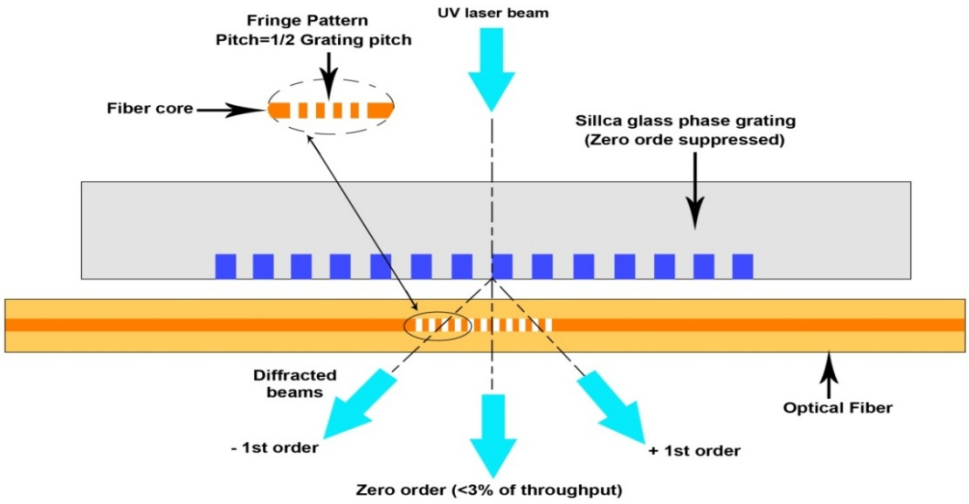


***Figure 2.3:*** *Phase-mask geometry for inscribing Bragg gratings in optical fibers.*

The phase mask technique has been used to fabricate FBGs for the experiments undertaken in the present thesis work. The experimental set up is explained in detail in chapter 5 of this thesis. This technique was selected primarily due to the reduced complexity of the fabrication system.

## 2.7 Long Period Gratings (LPGs)

Significant research efforts have been devoted to the study of Long Period Gratings (LPGs) since it was first reported in 1996 [111,112]. An LPG can be formed by the introduction of a periodic modulation to the optical properties of the fiber with a pitch of the order of 100μm [113]. The periodic modulation can be realized by a permanent modification of the refractive index of the fiber core or by a physical deformation of the fiber. The transmission spectrum of a typical LPG consists of a number of attenuation bands at specific wavelengths (resonance wavelengths), each of which corresponds to the coupling between the guided core mode and a particular cladding mode [114]. The study of the LPG's attenuation bands has yielded many potential applications in fiber-optic communication and sensing fields. The centre wavelengths of the attenuation bands are dependent on the composition of the fiber, and are influenced by environmental factors such as temperature [114,115], strain [116-118], refractive index [119-121] of the material surrounding the fiber and bend radius [117,122]. Thus it may be used for multi-parameter sensing applications. The principle of operation mechanism of long-period grating sensors is based on the modulation of the effective indices of the core and cladding modes and/or the grating periodicity by the external perturbation [123]. In comparison with fiber Bragg gratings (FBGs), LPGs offer a number of advantages, including easy fabrication, low insertion loss, and better wavelength tunability.

This section introduces the sensing capabilities of long-period gratings based on the above mentioned principle. Firstly, the LPG theory and the basic principle of operation of LPG based sensors are discussed and then the mechanism behind the spectral shifts in the resonance band is explored. It is shown that for a given LPG, the wavelength shifts are strong functions of the grating period and the order of the corresponding cladding mode. The temperature and strain sensitivity of the

LPG is discussed and furthermore long-period gratings are shown to be highly sensitive to index changes of the medium surrounding the bare cladding.

### 2.7.1 Mode Coupling in LPG

In optical fiber gratings, the phase matching condition is given by [111]:

$$\beta_1 - \beta_2 = \Delta\beta = \frac{2\pi}{\Lambda} \quad \text{.....(2.26)}$$

where $\beta_1$ and $\beta_2$ are the propagation constants of the modes being coupled and $\Lambda$ is the grating period [124,125].

In the case of LPGs, the forward propagating core mode couples to the co-propagating cladding modes of order m. Then

$$\beta_{co} - \beta_{cl,m} = \Delta\beta = \frac{2\pi}{\Lambda} \quad \text{.....(2.27)}$$

where $\beta_{co}$ is the propagation constant of core and $\beta_{cl,m}$ is that of $m^{th}$ order cladding mode. In this case $\Delta\beta$ is small and hence the grating periodicity will be very large compared to FBG grating period. Substituting the values as done in the case of FBG, we will get the resonance wavelength condition as [111,112]:

$$\lambda_m = \left[n_{eff}^{co} - n_{eff,m}^{cl}\right]\Lambda \quad \text{.....(2.28)}$$

where $\lambda_m$ is the resonance wavelength corresponding to coupling to the $m^{th}$ cladding mode, $\Lambda$ is the grating period, $n_{eff}^{co}$ is the effective index of the fundamental core mode ($LP_{01}$), $n_{eff,m}^{cl}$ is the effective index of the $m^{th}$ order cladding mode ($LP_{0m}$). Comprehensive explanation and analysis of mode coupling in fiber gratings and theory of LPGs can be found in several books [72,126,127], and in published literature [114,123,124,128,129].

### 2.7.2 Phase Matching Curve (PMC)

The $n_{eff}$ for each resonant wavelength can be calculated after identifying the modes in simulation software (eg: OptiGrating). Using this $n_{eff}$, corresponding to each cladding modes for various wavelengths, grating period versus wavelength can be plotted using the equation (2.28). Therefore

$$\Lambda = \frac{\lambda_m}{[n_{eff}^{co} - n_{eff,m}^{cl}]} \quad \text{.....(2.29)}$$

Thus for various modes, period versus resonant wavelength can be plotted. This plot is called Phase Matching Curve (PMC). The phase matching curve for LPGs in SMF-28 fiber is shown in Fig. 2.4.

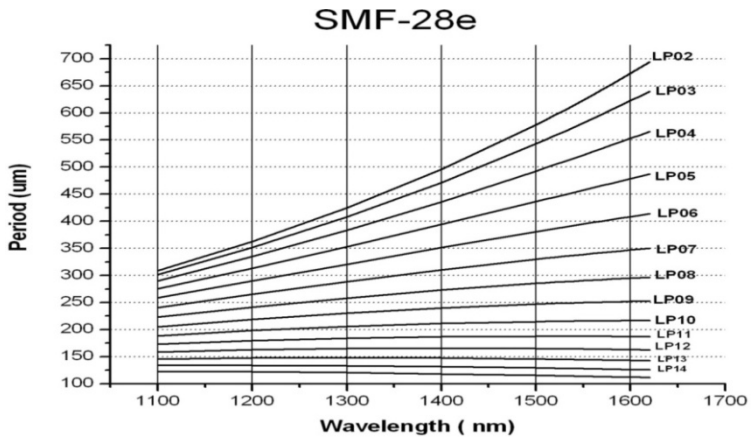


***Figure 2.4:*** *The phase matching curve for SMF-28 fiber. The PMCs represent the grating period, Λ as a function of the resonant wavelength, $\lambda_{res}$.*

The slope, $d\lambda/d\Lambda$ from the phase matching curves is indicative of the sensitivity of the cladding mode to external measurands. The highest order cladding mode with the largest $d\lambda/d\Lambda$ will exhibit the greatest sensitivity [123-125]. If we are taking a particular period, there will be a corresponding resonance wavelength. The

intersection of the curve with period of grating gives the corresponding wavelength of attenuation.

From Fig. 2.4 several important observations can be made: (1) For a specific grating period, the LPG can couple the energy of the fundamental mode into multiple other modes simultaneously at different resonant wavelengths; (2) For a certain resonant wavelength, a particular grating period can be chosen to allow the LPG to couple the fundamental mode into a certain fiber mode; (3) The higher the coupled fiber mode order, the shorter the grating period required to achieve mode coupling; (4) The slope, $d\Lambda/d\lambda_{res}$ progressively decreases from the lower order modes to the higher order modes. Consequently, $d\lambda_{res}/d\Lambda$ progressively increases from lower order mode to higher order mode. This shows that the change in $\lambda_{res}$ as a result of the change in $\Lambda$ gets larger as the order of the coupled fiber mode increases for the same LPG. The change in $\Lambda$ can result from the change in strain on the grating or the change in ambient temperature. Consequently, the sensitivity of the LPG to strain or temperature increases with increase in fiber mode order for the same LPG.

The simulations made (using Optigrating software by Optiwave) for two LPGs of grating period of 550 μm and 415 μm are shown in Fig.2.5. The sensitivity to a particular measurand is dependent on the core-cladding refractive index contrast, the core-cladding dimension, and the order of the cladding mode to which the fundamental core mode is coupled to. Therefore, different cladding modes exhibit different sensitivities.

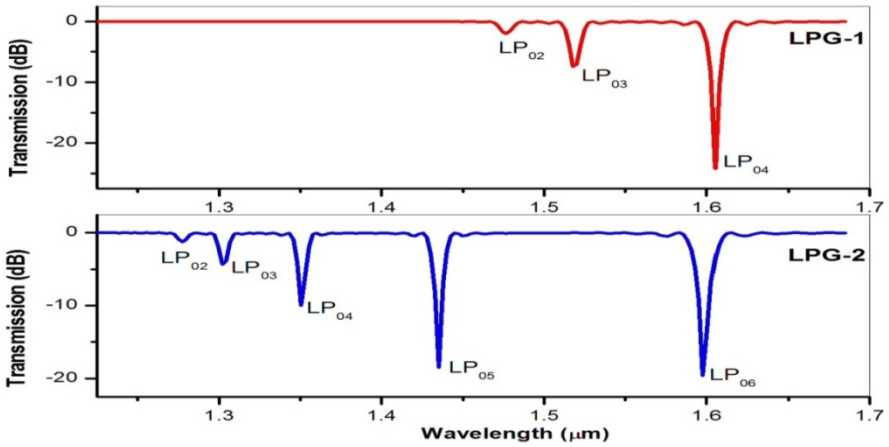


***Figure 2.5:*** *Simulated transmission spectra of LPG-1 with a grating period of 550 μm and LPG-2 with a grating period of 415 μm using Optigrating software by Optiwave.*

## 2.8 Principle of operation of LPG based sensor

An LPG is a periodic modulation of the fiber core refractive index produced along its length. The basic function of the LPG is to couple light from the fundamental guided mode (i.e. the $LP_{01}$ mode present in the core) to co-propagating cladding modes ($LP_{0m}$ mode with m =2, 3, 4 . . .) in the fiber and is shown in Fig.2.6.

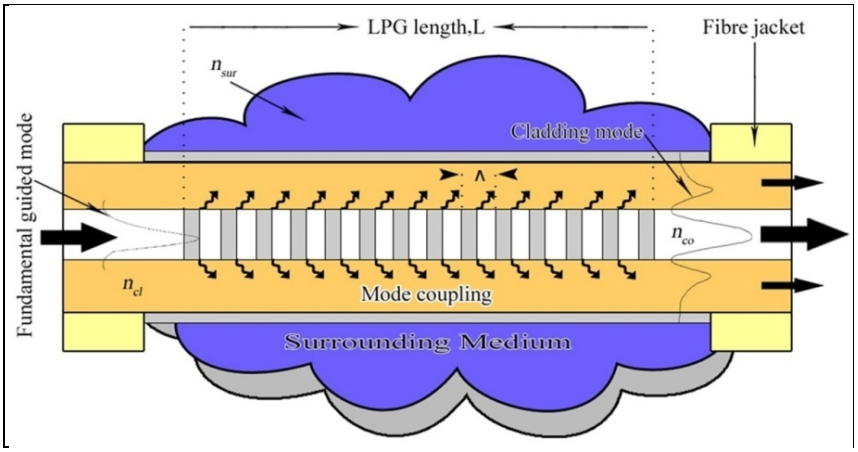


***Figure 2.6:*** *Mode coupling in a Long Period Grating.*

As the cladding modes are weakly guided and suffer from high attenuation, the transmission spectrum of a typical LPG consists of a series of attenuation bands at discrete wavelengths. The wavelength at which the guided mode couples to the cladding modes can be obtained through the phase-matching equation [113,130]:

$$\lambda_m = \left[n_{eff}^{co} - n_{eff,m}^{cl}\right]\Lambda$$

We can also write

$$\lambda_m = (\delta n_{eff})\,\Lambda \quad \text{.....(2.30)}$$

where $\delta n_{eff}$ is the differential effective index between the guided and cladding mode $(n_{eff}^{co} - n_{eff,m}^{cl})$ at wavelength $\lambda_m$. For a typical long period grating, more than one cladding mode can satisfy the phase matching condition at different wavelengths, and the guided mode will be coupled to all those cladding modes. The strength of transmission of the attenuation bands [113] can be written as

$$T_m = 1 - \sin^2(k_m L) \quad \text{.....(2.31)}$$

where L is the length of LPG and $k_m$ is the coupling coefficient for $m^{th}$ cladding mode. Therefore, the coupled power % depends on L and $k_m$. The parameter $k_m$ however depends on the specific cladding mode and also the amplitude of refractive index modulation ($\Delta n_{co}$) induced in the fiber core.

The resonance wavelength of LPG is a strong function of external perturbations like strain [115], temperature [117], bending [111] and SRI [119]. Presence of these external perturbations affects the coupling strength between the core and cladding modes, which could lead to both amplitude and wavelength shift of the attenuation bands in the LPG transmission spectrum [131,132]. Measurement of these spectral parameters in response to environment, surrounding the grating region is the basis of sensing with LPGs. The shift in the coupling wavelength can

be determined using an optical spectrum analyser(OSA) to produce a simple LPG based sensor. A complete analysis of the sensitivity of LPGs to external ambient is necessary prior to practical device design. In 2002, Shu *et al*. [133] have presented a complete investigation of the shift in the center of the resonance wavelength of the LPG due to temperature, strain and external refractive index variations, and can be expressed as

$$\Delta\lambda_m = \left(\frac{d\lambda_m}{dT}\right)\Delta T + \left(\frac{d\lambda_m}{d\varepsilon}\right)\Delta\varepsilon + \left(\frac{d\lambda_m}{dn_{sur}}\right)\Delta n_{sur} \quad \text{.....(2.32)}$$

where $\left(\frac{d\lambda_m}{dT}\right)$, $\left(\frac{d\lambda_m}{d\varepsilon}\right)$ and $\left(\frac{d\lambda_m}{dn_{sur}}\right)$ are the temperature, strain and surrounding refractive index sensitivity of the resonant wavelength, respectively. In the following sections a detailed expression for such sensitivities will be discussed.

### 2.8.1 Wavelength dependence of long-period gratings on temperature

The temperature sensitivity of LPGs arises from two major contributions: 1) changes in the differential refractive index of the core and the cladding due to thermo-optic effects, 2) changes in the LPG's period with the temperature. The sensitivity of an LPG to temperature, T, can be explained by taking the temperature derivation of the phase matching condition to give [114, 133-135]

$$\frac{d\lambda_m}{dT} = \frac{d\lambda_m}{d(\delta n_{eff})}\left[\frac{dn_{co}^{eff}}{dT} - \frac{dn_{cl,m}^{eff})}{dT}\right] + \Lambda\frac{d\lambda_m}{d\Lambda}\frac{1}{L}\frac{dL}{dT} \quad \text{..... (2.33)}$$

where T is the temperature, L is the length of LPG, and $\delta n_{eff}$ is the effective differential refractive index between the core mode and the cladding mode ($n_{co}^{eff}$- $n_{cl,m}^{eff}$). The wavelength shift is mainly influenced by the grating period [4], the order of the cladding mode to which coupling takes place [114] and by the composition of the optical fiber [133].

The right hand side of the equation (2.33) contains two terms that may be separated as two contributing terms to the wavelength response. The first term represents a thermo-optic effect and is described as the material contribution. It is related to the change in the differential refractive index of the core and cladding arising from the thermo-optic effect. This contribution is dependent upon the composition of the fiber, i.e. different fiber types having different thermo-optic coefficients. It is also dependent upon the order of the cladding mode. Different temperature dependent spectral response can be observed when coupling occurs with lower-order cladding modes as opposed to modes of higher order [114,115,136]. For coupling to lower order cladding modes, which are accessed using a large grating period (in excess of 100 μm), the material effect dominates. On the other hand, coupling to higher-order cladding modes takes place in LPGs with relatively short periods (less than 100μm). When these shorter period LPGs are exposed to temperature fluctuations the material contribution can become negligible. The second term on the right hand side of equation (2.33) is the waveguide contribution. This contribution arises from changes in the grating periodicity and can be negative or positive depending on the order of cladding mode [123].

Shu *et al*. [133,135] also derived an equation for the temperature sensitivity of the resonance wavelengths of LPGs as

$$\frac{d\lambda_m}{dT} = \lambda_m \gamma\left(\alpha + \Gamma_T\right) \quad \text{..... (2.34)}$$

where T is the temperature, α is the thermal expansion coefficient of silica, $\gamma$ is the contribution of the waveguide dispersion and $\Gamma$ is a measurand-specific factor, which reflects the influence of the measurand on the dispersion of the LPG. The specific sensitivity factor for temperature, $\Gamma_T$ and $\gamma$ are given by [137,138]

$$\gamma = \frac{\frac{d\lambda_m}{d\Lambda}}{n_{co}^{eff} - n_{cl,m}^{eff}} \quad \text{.....(2.35)}$$

$$\Gamma_T = \frac{\xi_{co} n_{co}^{eff} - \xi_{cl} n_{cl,m}^{eff}}{n_{co}^{eff} - n_{cl,m}^{eff}} \quad \text{.....(2.36)}$$

where $\xi_{co}$ and $\xi_{cl}$ are the thermo optic coefficients of the core and the cladding, respectively. $\Gamma_T$ is determined by the temperature dependence of the refractive index of the core, which depends on the composition of the fiber( $SiO_2$, $GeO_2$, $B_2O_3$ etc.).

As $\alpha$ has a small value at room temperature, it is negligible compared with $\Gamma_T$ and the temperature sensitivity is determined by the term $\gamma\,\Gamma_T$. Equation (2.33) highlights the importance of the relative temperature dependencies of the effective refractive indices and therefore the magnitudes of the core and cladding thermo-optic coefficients (respectively $\xi_{co}$ = $dn_{co}/dT$ and $\xi_{cl}$ = $dn_{cl}/dT$) [139] in determining LPG wavelength sensitivity to external temperature fluctuations.

The direction of attenuation band shift depends on the relative magnitudes of the core and cladding thermo-optic coefficients [133,140]. The thermo optic coefficient of the core depends on the concentration of the dopants in silica. $GeO_2$ has a larger thermo optic coefficient than that of $SiO_2$, whereas $B_2O_3$ has a negative thermo optic coefficient. In the case of standard fiber, the core contains $SiO_2$ and $GeO_2$ and the cladding contains only $SiO_2$. So the thermo optic coefficient of the core will be higher than that of the cladding ($\xi_{co} n_{co}^{eff} > \xi_{cl} n_{cl,m}^{eff}$ and $\Gamma_T > 0$). As a result when the temperature increases, these fibers will show a wavelength shift towards longer wavelengths [135,140]. On the other hand, the boron co-doped fibers will show a wavelength shift towards shorter wavelengths due to the

negative thermo optic coefficient of the boron dopant ($\xi_{co} n_{co}^{eff} < \xi_{cl} n_{cl,m}^{eff}$ and $\Gamma_T < 0$) [133,140,141]. Thus, it is to be expected that the thermal responses of LPFGs produced in different fiber types will exhibit different trends. The temperature sensitivity of the resonance wavelength of LPGs can be increased by coating the LPGs with polymer materials that have large thermal-optic coefficients [142,143] or by etching the fiber cladding [144]. Long-period gratings written in microstructure fiber with large holes in the cladding that were filled with polymer also demonstrated higher temperature sensitivity [145].

### 2.8.2 Wavelength dependence of long-period gratings on strain

Strain induces significant variations in the core and cladding refractive indices of an optical fiber and, unlike the temperature, it also induces significant changes in the dimensions of an optical fiber. In an LPG the deviation of these parameters from the unperturbed state gives rise to different coupling of the light between the propagating modes and, as consequence, corresponding variations in the transmission spectrum. These variations can be detected and related to the strain intensity.

The strain response of a long-period fiber grating arises due to the physical elongation of the fiber, changing the grating pitch and the effective refractive index of the core and cladding due to the elastooptic effect [145]. Differentiation of the phase-matching condition with respect to axial strain, ε, provides an equation for the shift in resonant wavelength with axial strain [114,115,136].

$$\frac{d\lambda_m}{d\varepsilon} = \frac{d\lambda_m}{d(\delta n_{eff})}\left[\frac{dn_{co}^{eff}}{d\varepsilon} - \frac{dn_{cl,m}^{eff})}{d\varepsilon}\right] + \Lambda\frac{d\lambda_m}{d\Lambda} \quad \text{..... (2.37)}$$

Similar to the temperature sensitivity (equation 2.33), there are two terms which influence the axial strain sensitivity: material and waveguide effects. The

first term on the right hand side of the equation is the material contribution and the second is the waveguide contribution. The material effects are the change in dimension of the fiber (Poisson's effect) and the strain-optic effect (refractive index changes); while the waveguide effect is a function of the slope of the dispersion term, $\frac{d\lambda_m}{d\Lambda}$, for a specific cladding mode [115,136]. In short, the shift in resonant wavelength ($\lambda_m$) of the LPG transmission spectrum is dependent on the order of the relevant cladding mode(m) that participates in coupling, as well as the grating period ($\Lambda$).

The polarity of the strain coefficient depends on whether the material or waveguide contribution provides the dominating effect. The two contributions to the total strain induced wavelength shift can be either positive or negative depending on the period of the LPG and the order of the cladding mode. For LPGs with a periodicity > 100μm the material contribution is negative and the waveguide contribution is positive. When the LPG period is less than 100 μm, both material and waveguide contributions to the strain sensitivity will be negative. The relative magnitudes of these contributions will therefore determine if the overall effect creates an attenuation peak shift to longer or shorter wavelengths. For the case where the material and waveguide effects cancel each other completely – their magnitudes are equal but opposite in sign – that particular resonant band becomes insensitive to axial strain. i.e. By choosing appropriate grating period and fiber composition, it is possible to get an attenuation band with positive, negative or zero sensitivity to strain [115,136]. Thus the ability to design an LPG's response to strain and temperature opens up the possibility of sensing multi-parameter devices with the option of isolating either of the measurands. Shu *et al.* [133,135] derived an equation for the strain sensitivity of the resonance wavelengths of LPGs as

$$\frac{d\lambda_m}{d\varepsilon} = \lambda_m \gamma \left(1 + \Gamma_S\right) \quad \text{.....(2.38)}$$

where $\gamma$ is the general sensitivity factor which describe the waveguide dispersion, and it relates the sensitivity of the LPG to all forms of external perturbation including strain, temperature and surrounding refractive index [133,138]. The specific sensitivity factor, $\Gamma_S$ for strain is given by

$$\Gamma_S = \frac{\eta_{co} n_{co}^{eff} - \eta_{cl} n_{cl,m}^{eff}}{n_{co}^{eff} - n_{cl,m}^{eff}} \quad \text{.....(2.39)}$$

where $\eta_{co}$ and $\eta_{cl}$ are the elastooptic coefficients of the core and cladding materials, respectively. So, the LPG sensitivity to strain can be expressed as follows

$$\frac{d\lambda_m}{\mathrm{d}\varepsilon} = \lambda_m \gamma \left( 1 + \frac{\eta_{co} n_{co}^{eff} - \eta_{cl} n_{cl,m}^{eff}}{n_{co}^{eff} - n_{cl,m}^{eff}} \right) \quad \text{.....(2.40)}$$

It can be seen form eq. (2.40) that an LPG is strain-insensitive when the second term in the parenthesis is equal to -1.

The effect of strain on the wavelength shift of an LPG is different from that of a fiber Bragg grating. Qualitatively, the FBG and LPG responses are different. The FBG wavelength is linearly proportional to the grating period multiplied by the effective index of refraction of the core, the LPG wavelength is proportional to the grating period multiplied by the difference in index of refraction between the core and the cladding. Furthermore, the effect of strain on the long-period grating is more dependent on the fiber type.

### 2.8.3 LPG Sensitivity to the refractive index of the surrounding medium

Conventional fiber optic refractive index sensors typically use some form of modification of the cladding to gain access to the evanescent field of the guided mode. For example, surface plasmon sensors require polishing the fiber cladding

and depositing a thin layer of appropriate metal on the polished fiber surface [146]. Limitations of this device include questionable repeatability and mechanical strength. In an LPG the guided light interacts with the external medium so there is no need to modify the fiber. In this section we will show that long-period gratings are highly sensitive refractive index sensors and can be implemented without sacrificing the integrity of the fiber [111].

The attenuation spectrum of an LPG is highly sensitive to the ambient refractive index. The refractive index sensitivity of an LPG arises from the dependence of the phase matching condition on the effective refractive index of the cladding modes, which are determined by the refractive index of the cladding material and that of the medium surrounding the cladding. LPG is very useful as a surrounding medium refractive index sensor when the refractive index of the external medium changes. The change in ambient index changes the effective index of the cladding mode and will lead to both amplitude and wavelength shifts of the resonance dips in the LPG transmission spectrum. The RI sensitivity of LPGs has been exploited to form RI sensors, biosensors, liquid sensors and chemical concentration sensors by measuring the small shift in the resonant wavelength with a change in ambient refractive index [111,120,133,147-149]. The effect of refractive index of the surrounding medium on the resonance wavelength is expressed by [114]:

$$\frac{d\lambda_m}{dn_{sur}} = \frac{d\lambda_m}{dn_{eff,m}^{cl}} \left[\frac{dn_{eff,m}^{cl}}{dn_{sur}}\right] \quad \text{..... (2.41)}$$

where $n_{sur}$ is the refractive index of the surrounding material. For each cladding mode, the term $\left[\frac{dn_{eff,m}^{cl}}{dn_{sur}}\right]$ is distinct and hence an LPG is expected to have a strong dependence on the order of the coupled cladding mode. Higher order cladding modes tend to show greater sensitivity to changes in external refractive index

because these modes extend further out into the area exterior to the fiber [114,120,133]. Shu *et al*. [133,134] derived an equation for the RI sensitivity of the resonance wavelengths of LPGs as

$$\frac{d\lambda_m}{dn_{sur}} = \lambda_m . \gamma . \Gamma_{sur} \quad \text{.....(2.42)}$$

The specific sensitivity factor, $\Gamma_{sur}$ for surrounding RI is given by

$$\Gamma_{sur} = -\frac{u_m^2 \lambda_m^3 n_{sur}}{8\pi r_{cl}^3 n_{cl} (n_{co}^{eff} - n_{cl,m}^{eff})(n_{cl}^2 - n_{sur}^2)^{3/2}} \quad \text{.....(2.43)}$$

Where $u_m$ is the $m^{th}$ root of the zeroth-order Bessel function of the first kind, $r_{cl}$ and $n_{cl}$ are the radius and refractive index of the fiber cladding, respectively. From equation (2.43), it is evident that the sensitivity is greater for higher order cladding modes and it can be enhanced by reducing the cladding radius since the term in parenthesis is dependent on ($r_{cl}^{-3}$) [133,150].

The spectral change of LPG sensors can be characterized in terms of external RI as follows. If the SRI is lower than the refractive index of the cladding ($n_{sur} < n_{cl}$), mode guidance can be explained using total internal reflection. In this case, typically strong resonance peaks are observed and the attenuation dips shift towards shorter wavelengths (blue shift) when the external medium refractive index increases up to the fiber cladding refractive index [133,148]. The closer the refractive index of the external medium to the cladding, the higher the grating sensitivity and leads to larger wavelength shift. When the value of the ambient refractive index matches with that of the cladding, the cladding layer acts as an infinitely extended medium and thus supports no discrete cladding modes. In this case, a broadband radiation mode coupling occurs with no distinct attenuation bands [151]. In short, when the external RI becomes equal to

the RI of the cladding, rejection bands disappear, and the transmission spectrum gets flattened. Once the SRI is higher than the refractive index of the cladding ($n_{sur} > n_{clad}$), the cladding modes no longer experience total internal reflection and Fresnel reflection can be used to explain the mode structure [147]. Whatever may be the value of the external index ($> n_{clad}$), a part of the energy is reflected at the interface of the cladding and the external medium. The ratio of the energy reflected will be determined by the Fresnel coefficients. In this case the resonance peaks reappear at slightly longer wavelengths (red shift) compared to those measured with air as the surrounding medium [152,153]. The depth of each attenuation peak steadily increases with increase in refractive index of the surrounding medium, owing to larger Fresnel reflection coefficients that yield improved reflection at the cladding boundary [151,154]. So, chemical concentration changes can also be measured by studying the amplitude changes in the LPG attenuation dips. Refractive index sensing is important for biological, chemical and biochemical applications since a number of substances can be detected through the measurements of refractive index [118,155-159].

Etching of the cladding diameter is a simple method to improve the refractive index sensitivity of a long-period gratings following the fabrication process [144,150]. The sensitivity to the ambient refractive index of an LPG can also be improved by coating the fiber grating with a thin film of material with higher refractive index than that of the fiber cladding [131,160-167]. As an example, an opto-chemical sensor employing LPGs coated with polymeric sensitive overlays (syndiotactic polystyrene (sPS) in the nanoporous crystalline δ form) has been proposed [168]. A monolayer of colloidal gold nano-particles has also been proposed for improving the spectral sensitivity and detection limit of LPGs [169].

## 2.9 Fabrication methods for Long Period Gratings

The fabrication of an LPG relies on the introduction of a periodic modulation of the optical properties of the fiber, which can be in the form of index modulation along the fiber core [112] or physical deformation along the fiber [113]. It has been seen that long-period gratings could be fabricated by a number of methods, which belong to either the UV exposure or non-UV exposure. In the UV exposure, there is either the point-by-point writing method [182-184] or amplitude mask technique [112,173,174]. The former method is flexible for fabricating LPGs with different spectral characteristics but not suitable for mass production, whereas the amplitude mask techniques could be used for mass production of LPGs. UV-induced index modulation is typically achieved in germanosilicate optical fibers using wavelengths between 193 nm and 266 nm [113,175]. The major UV sources are, radiation from a KrF excimer laser (242-248 nm) [2, 176-178], the second harmonic radiation of a continuous-wave (CW) Ar ion laser (244 nm) [179], nanosecond pulses from a ArF excimer laser (193 nm) [180], frequency quadrupled and tripled Nd:YAG lasers (266nm and 355nm outputs, respectively) [112,181] etc. UV exposure is the most widely utilized method for the fabrication of LPGs. Fibers with high UV photosensitivity have been developed by co-doping the core with boron and germanium [182] and by hydrogen loading [173].

Non-UV methods include $CO_2$ laser irradiation [183,184], electric arc discharge [185,186], infrared femtosecond laser pulse irradiation [187,188], mercury-arc lamp [189], ion implantation (bombardment) [190,191] and dopant diffusion in nitrogen-doped fibers [192]. Advantages of the ion and proton implantation techniques include the fabrication of LPGs by inducing high refractive index changes in the core and the possibility to write LPGs in almost any kind of silica-based fibers. These fabrication techniques have the disadvantage of increasing the average cladding effective index, leading to losses in the spectrum

and requiring specialized equipment to fabricate LPGs. A periodic physical deformation along the fiber can also be produced by mechanical methods [193-196] or tapering the fiber [197] or deformation of the core [198] or the cladding [199]. A simple method to create temporary LPG is to press a periodically grooved plate onto a fiber, and this is based on the physical deformation to the optical fiber which can also change the refractive index profile of the fiber core [141,200]. In addition, dynamic LPGs with controllable transmission characteristics have been implemented by using coil heaters [201], mechanical loading [202], and liquid-crystal filled hollow-core fibers [203]. A temporary LPG can also be created using acoustical modulation of a length of optical fiber (acousto-optic modulation) [204,205].

Long period gratings have been virtually written in all kind of optical fibers, namely, in standard single mode communications fibers [112], in non-photosensitive fibers [185,206,207] for EDFAs gain equalisation and sensing, in multimode fibers for chemical sensing [208], in polarization maintaining fibers [209], in D-fibers for enhanced RI measurements [210], in specially designed fibers like dispersion compensating [211], depressed inner cladding [212], dual core [213], twin core [214] fibers with particular properties for optical communications and sensing. Recent advances have been focused in the research of LPGs induced in photonic crystal fibres (PCFs) which consist of a pure-silica core, and a microstructured air-silica cladding [215,216]. Because the microstructured cladding consists of air holes, a PCF's cladding index shows strong wavelength dependence. LPGs have also been fabricated in planar waveguides for compactness and mass production [217].

A big problem with the UV inscription method is the LPGs fabricated by this method cannot survive at high temperature. When the temperature goes much beyond room temperature, the UV written LPG starts to fade and eventually loses the modal coupling. Among the techniques mentioned above, femtosecond laser, $CO_2$ laser irradiation and electric discharge are able to fabricate survival LPG at a temperature up

to 1000°C [185]. But femtosecond lasers are too expensive to be used in LPG fabrication; and $CO_2$ laser irradiation and electric discharge method may significantly affect the mechanical strength of the optical fibers. A detailed review of the above fabrication techniques and mechanisms can be found in the review paper [113].

The LPGs used in our experiments were fabricated using a 248 nm KrF excimer laser source, employing point-by-point writing method [182-184]. A great advantage of the point-by-point method is that it is a highly flexible technique, since the grating periodicity and length can be individually adjusted to meet the desired LPG specifications and corresponding spectral characteristics.

## 2.10 Annealing of long-period gratings

In the case of fiber gratings fabricated using hydrogen loaded fibers, the amount of hydrogen present in an optical fiber will be far in surplus of that required to achieve a given refractive index change. Thus, at the end of the writing process, there is a finite amount of unused hydrogen remaining in the cladding that can significantly influence the grating transmission spectrum. Hydrogen diffusion leads to wavelength shift of the attenuation bands in the case of UV written LPG. Hydrogen out diffusion also causes a change in resonance strength of the LPGs after UV inscription. From this point of view, after the UV writing, it is necessary to anneal the grating in order to stabilize the optical properties of long period grating [112,218-220]. In 1995, Williams *et al*. studied the thermal stability of in fiber gratings and reported that annealing ensures the stability of the gratings for about 25 years at room temperature [221]. Later in 1997 the creditability of this work was further confirmed by Kannan *et al*. [222].

There are two purposes for the annealing process: 1) to anneal out the unreacted hydrogen, which would increase the average refractive index of the fiber and temporarily shift the LPG attenuation bands to longer wavelength (red shift)

and 2) to anneal out the portion of the UV created sites which would be thermally unstable over long periods at a normal operating temperature [112]. Appropriate annealing conditions will depend on the fiber and grating type, the anticipated operating temperature and the required stability of a grating device. The annealing process involves heating the gratings to an elevated temperature for a period of time dependent on the expected lifetime of the device [123]. The annealing temperature varies from 150$^{o}$C to 200$^{o}$C while the duration of this thermal treatment is 10 to 48 hours. Since the removal of hydrogen and UV sites causes the effective index of the guided mode to be reduced, the resonance wavelengths move to lower wavelengths (blue shifts) after annealing.

## 2.11 Summary

This chapter discussed fiber Bragg gratings, theory behind the gratings and their applications. Measurement of various measurands using FBG such as strain, temperature and refractive index were presented in detail. Brief overview of photosensitivity in optical fiber and different methods to enhance the photosensitivity has been presented in this chapter. Widely employed FBG writing techniques in photosensitive optical fibers were also introduced and discussed. Although fiber Bragg gratings and long-period fiber gratings are similar in terms of the introduction of an index modulation in the fiber core, a few fundamental differences exist between them in terms of the operating principle and spectral response. The chapter also outlined the characteristics and the mechanism of mode coupling in FBGs and LPGs.

This chapter has also discussed the origin of the sensitivity of LPGs to measurands such as temperature, strain and RI, and how the attenuation bands have differing sensitivities to the various measurands. The ability to tune the sensitivity by virtue of the fiber composition and LPG period has also been discussed. Continuing with more practical aspects concerning LPGs, a number of reported

grating fabrication techniques in the literature were presented. The fabrication of LPGs relies upon the introduction of a periodic modulation of the optical properties of the fiber. This may be achieved by permanent modification of the RI of the core of the optical fiber or by physical deformation of the fiber. Finally the effects of residual hydrogen diffusion from the LPG after fabrication and the method of annealing were discussed. This method emphasized the importance of stabilizing a grating structure after grating fabrication.

To enhance the richness of these discussions, the results of experiments conducted on LPGs and FBGs are presented and discussed in chapter 3 and chapter 5 of this thesis.

## References


[1]. R. Kashyap, "*Fiber Bragg Gratings*", 2nd Edition, Academic Press (2010).

[2]. Raman Kashyap, J. M. Lopez Higuera, "*Handbook of optical fiber sensing technology; Fiber Grating Technology: Theory, Photosensitivity, Fabrication and characterization*", John Wiley & Sons, pp. 349-377 (2002).

[3]. Andreas Othonos, "*Fiber Bragg gratings*", Review of Scientific Instruments, **68**, pp. 4309-4341 (1997).

[4]. K. O. Hill, Y. Fujii, D. C. Johnson and B. S. Kawasaki, *"Photosensitivity in optical fiber waveguides: Application to reflection filter fabrication",* Applied Physics Letters, **32**, pp. 647-649 (1978).

[5]. B. S. Kawasaki, K. O. Hill, D. C. Johnson and Y. Fujii, "*Narrow-band Bragg reflectors in optical fibers*", Optics Letters, **3**, pp. 66-68 (1978).

[6]. G. Meltz, W.W. Morey and W.H. Glenn, "*Formation of Bragg gratings in optical fibers by a transverse holographic method*", Optics Letters, **14**, pp. 823-825 (1989).

[7]. K. O. Hill, B. Malo, F. Bilodeau, D.C. Johnson and J. Albert, "*Bragg gratings fabricated in monomode photosensitive optical fiber by UV exposure through a phase mask*", Applied Physics Letters, **62**, pp. 1035-1037 (1993).

[8]. D. Grobnic, C. Smelser, S. Mihailov, R. Walker and P. Lu, "*Fiber Bragg gratings with suppressed cladding modes made in SMF-28 with a femtosecond IR laser and a phase mask*," IEEE Photonics Technology Letters, **16**, pp. 1864–1866 (2004).

[9]. Y. Li, C. R. Liao, D. N. Wang, T. Sun and K. T. V. Grattan, "*Study of spectral and annealing properties offiber Bragg gratings written in $H_2$-free and $H_2$-loaded fibers by use of femtosecond laser pulses*", Optics Express, **16**, pp. 239–247 (2008).

[10]. K. O. Hill and G. Meltz, "*Fiber Bragg grating technology fundamentals and overview*", IEEE J. Lightwave Technology, **15**, pp. 1263-1276 (1997).

[11]. T. Erdogan, "*Fiber grating spectra*", Journal Lightwave Technology, **15**, pp. 1277-1294 (1997).

[12]. D. Sengupta, "*Study on discrete and continuous liquid level measurements using fiber bragg gratings*", Ph.D. Thesis, NIT, Warangel (2012).

[13]. D.K.W. Lam and B.K. Garside, "*Characterization of single-mode optical fiber filters",* Applied Optics, **20**, pp. 440-445 (1981).

[14]. H. G. Limberger, P.Y. Fonjallaz and R.P. Salathe, "*Spectral characterisation of photoinduced high efficiency Bragg gratings in standard telecommunication fibers",* Electronics Letters, **29**, pp. 47-49 (1993).

[15]. I. Bennion, J. A. R. Williams, L. Zhang, K. Sugden and N. J. Doran, "*UVwritten in-fiber Bragg gratings"*, Optical and Quantum Electronics*,* **28**, pp. 93-135 (1996).

[16]. P. Russell, J. L. Archambault and L. Reekie, "*Fiber gratings*", Physics World, **6**, pp. 41-46 (1993).

[17]. Y. J. Rao, "*In-fiber Bragg grating sensors*", Measurement Science and Technology, **8**, pp. 355-375(1997).

[18]. Y.J. Rao and D.A. Jackson, "*Recent progress in fiber optic low-coherence interferometry*", Measurement Science and Technology, **7**, pp. 981-999 (1996).

[19]. A.D. Kersey, M.A. Davis and H.J. Patrick, *"Fiber grating sensors",* Journal of Lightwave Technology, **15**, pp. 1442 -1463 (1997).

[20]. A. Bertholds, R. Dandliker *"Determination of the individual strain-optic coefficients in singlemode optical fibers",* Journal of Lightwave Technology, **6**, pp. 17-20 (1988).

[21]. V. M. Murukeshan, P. Y. Chan, L. S. Ong and A. Asundi, "*Intracore fiber Bragg gratings for strain measurement in embedded composite structures*", Applied Optics, **40**, pp. 145-149 (2001).

[22]. S. Pal, T. Sun, K. T. V. Grattan, S. A. Wade, S. F. Collins, G. W. Baxter, B. Dussardier and Monnom G, "*Strain-independent temperature measurement using a type-I and type IIA optical fiber Bragg grating combination*", Review of Scientific Instruments,**75**, pp. 1327-1331(2004).

[23]. L. Ren, J. Chen, H. N. Li, G. Song and X. Ji, "*Design and application of a fiber Bragg grating strain sensor with enhanced sensitivity in the small-scale dam model*", Smart Materials and Structures, **18**, pp. 035015 (2009).

[24]. W.L. Schulz, E. Udd, J.M. Seim and G.E. McGill, "*Single and multi axis fiber grating strain sensor applications for bridges and highways*", SPIE Proc., 3325, pp. 212–221(1998).

[25]. E. Rivera and D.J. Thomson, "*Accurate strain measurements with fiber Bragg sensors and wavelength references*", Smart Materials and Structures, **15**, pp. 325–330 (2006).

[26]. H.N. Li, D.S. Li and G. Song, "*Recent applications of fiber optic sensors to health monitoring in civil engineering*", Engineering Structures, **26,** pp. 1647–57 (2004).

[27]. Y. Lo, Y. Lin and Y. Chen, "*A thermal fiber Bragg grating strain gauge with metal coating in measurement of thermal expansion coefficient*", Sensors and Actuators A, **117**, pp. 103–109 (2005).

[28]. P. Moyo, J.M.W. Brownjohn, R. Suresh and S.C. Tjin, "*Development of fiber Bragg grating sensors for monitoring civil Infrastructure*", Engineering Structures, **27**, pp. 1828–1834 (2005).

[29]. X. F. Zhao, S. Z. Tian, Z. Zhou, L. B. Wan and J. P. Ou, "Experimental study on strain monitoring of concrete using a steel slice packaged fiber grating", J. Optoelectronics Laser, **14**, pp. 171–174 (2003).

[30]. Y. B. Lin, K. C. Chang, J. C. Chern and L. A. Wang, "*Packaging methods of fiber-Bragg grating sensors in civil structure applications*", IEEE Sensors Journal, **5**, pp. 419–24 (2005).

[31]. S. Pal, J. Mandal, T. Sun, K.T.V. Grattan, M. Fokine, F. Carlsson, P.Y. Fonjallaz, S.A. Wade and S.F. Collins, "Characteristics of potential fiber Bragg grating sensor-based devices at elevated temperatures", Measurement Science and Technology, **14**, pp.1131–1136 (2003).

[32]. S. Gupta, T. Mizunami, T. Yamao, T. Shimomura, "*Fiber Bragg grating cryogenic temperature sensors*", Applied Optics, **35**, pp. 5202–5205 (1996).

[33]. T. Mizunami, H. Tatehata and H. Kawashima, "High-sensitivity cryogenic fiber-Bragg-grating temperature sensors using Teflon substrate", Measurement Science and Technology, **12**, pp. 914–917 (2001).

[34]. M. B. Reid and M. Ozcan, "*Temperature dependence of fiber optic Bragg gratings at low temperatures*", Optical Engineering, **37**, pp. 237–240 (1998).

[35]. Y. Zhao and Y. Liao, "*Discrimination methods and demodulation techniques for fiber Bragg grating sensors*", Optics and Lasers in Engineering, **41**, pp. 1–18 (2004).

[36]. X. Shu, Y. Liu, D. Zhao, B. Gwandu, F. Floreani, L. Zhang and I. Bennion, "*Dependence of temperature and strain coefficients on fiber grating type and its application to simultaneous temperature and strain measurement*", Optics Letters, **27**, pp. 701–703 (2002).

[37]. W.C. Du, X.M. Tao and H.Y. Tam, "*Fiber Bragg grating cavity sensor for simultaneous measurement of strain and temperature*", IEEE Photonics Technology Letters, **11**, pp. 105–107 (1999).

[38]. M.G. Xu, L. Dong, L. Reekie, J.A. Tucknott, and J.L. Cruz, "*Temperature-independent strain sensor using a chirped Bragg grating in a tapered optical fiber*", Electronics Letters, **31**, pp. 823–825 (1995).

[39]. S. Kim, J. Kwon, S. Kim and B. Lee, "*Temperature-independent strain sensor using a chirped grating partially embedded in a glass tube*", IEEE Photonics Technology Letters, **12**, pp.678–680 (2000).

[40]. S.E. Kanellopoulos, V.A. Handerek and A.J. Rogers, "*Simultaneous strain and temperature sensing with photogenerated in-fiber gratings*", Optics Letters, **20**, pp. 333–335 (1995).

[41]. Y. J. Chiang, L. Wang, H. Chen, C. Yang and W. F. Liu, "*Multipoint temperature-independent fiber-Bragg-grating strain-sensing system employing an optical-power-detection scheme*", Applied Optics, **41**, pp. 1661-1667 (2002).

[42]. M. G. Xu, J. L. Archambault, L. Reekie and J.P. Dakin, "*Discrimination between strain and temperature effects using dual-wavelength fiber grating sensors*", Electronics Letters, **30**, pp. 1085–1087 (1994).

[43]. S. W. James, M. L. Dockney and R. P. Tatam, "*Simultaneous independent temperature and strain measurement using in-fiber Bragg gratings sensors*", Electronics Letters, **32**, pp.1133–1134 (1996).

[44]. M. Song, B. Lee, S.B. Lee and S.S. Choi, "*Interferometric temperature insensitive strain measurement with different-diameter fiber Bragg gratings*", Optics Letters, **22**, pp. 790–792 (1997).

[45]. P. M. Cavaleiro, A. M. Ara´ujo, L. A. Ferreira, J. L. Santos and F. Farahi, "*Simultaneous measurement of strain and temperature using Bragg gratings written in germanosilicate and boron-codoped germanosilicate fibers*", IEEE Photonics Technology Letters, **11**, pp. 1635–1637 (1999).

[46]. J. Jung, H. Nam, J.H. Lee, N. Park and B. Lee, "Simultaneous measurement of strain and temperature by use of a single-fiber Bragg grating and an erbium-doped fiber amplifier", Applied Optics, **38**, pp. 2749–2751 (1999).

[47]. D.I. Forsyth, S.A. Wade, T. Sun, X. Chen and K.T.V. Grattan, "*Dual temperature and strain measurement using the combined fluorescence lifetime and Bragg wavelength shift approach in doped optical fiber*", Applied Optics, **41**, pp. 6585–6592 (2002).

[48]. L. A. Ferreira, F. M. Araujo, J. L. Santos and F. Farahi, "*Simultaneous measurement of strain and temperature using interferometrically interrogated fiber Bragg grating sensors*", Optical Engineering, **39**, pp. 2226–2234, (2000).

[49]. M. N. Alahbabi, Y. T. Cho and T. P Newson, "*Long-range distributed temperature and strain optical fiber sensor based on the coherent detection of spontaneous Brillouin scattering with in-line Raman amplification*", Measurement Science and Technology, **17**, pp. 1082-1090 (2006).

[50]. P. Lu, L. Men and Q. Chen, "*Resolving cross sensitivity of fiber Bragg gratings with different polymeric coatings*", Applied Physics Letters, 92, 171112 (2008).

[51]. A. Iadicicco, A. Cusano, S. Campopiano, A. Cutolo and M. Giordano, "Thinned fiber Bragg gratings as refractive index sensors", IEEE Sensors Journal, **5**, pp. 1288-1295 (2005).

[52]. A. N. Chryssis, S. M. Lee, S. B. Lee, S. S. Saini, and M. Dagenais, "High sensitivity etched core fiber Bragg grating sensors," IEEE Photonics Technology Letters, **17**, pp. 1253–1255 (2005).

[53]. A. Iadicicco, A. Cusano, A. Cutolo, R. Bernini and M. Giordano, "*Thinned fiber Bragg gratings as high sensitivity refractive index sensor*", IEEE Photonics Technology Letters, **16**, pp. 1149-1151 (2004).

[54]. A. Iadicicco, S. Campopiano, A. Cutolo, M. Giordano, and A. Cusano, "*Self temperature referenced refractive index sensor by non-uniform thinned fiber Bragg gratings*", Sensors and Actuators B, **120**, pp. 231–237 (2006).

[55]. H. Xue Feng, C. Zhe Min, S. Li Yang, C. Ke Fa, S. De Ren, C. Jun and Z. Hao, "*Design and characteristics of refractive index sensor based on thinned and microstructure fiber Bragg grating*", Applied Optics, **47**, pp. 504-511 (2008).

[56]. G. Tsigaridas, D. Polyzos, A. Ioannou, M. Fakis and P. Persephonis, "Theoretical *and experimental study of refractive index sensors based on etched fiber Bragg gratings*", Sensors and Actuators A: Physical, **209**, pp. 9-15 (2014).

[57]. A. Cusano, A. Iadicicco, S. Campopiano, M. Giordano and A. Cutolo, "*Thinned and micro-structured fiber Bragg gratings: towards new allfiber high-sensitivity chemical sensors*", J. Opt. A: Pure Applied Optics, **7**, pp. 734-741 (2005).

[58]. G. Ryu, M. Dagenais, M. T. Hurley and P. Deshong, "*High specificity binding of lectins to carbohydrate-functionalized fiber Bragg gratings: A newmodel for biosensing applications*", IEEE J. Quantum Electronics, **16**, pp. 647–653 (2010).

[59]. A. Asseh, S. Sandgren, H. Ahlfeldt, B. Sahlgren, R. Stubbe and G. Edwall, "*Fiber optical Bragg grating refractometer*", Fiber and Integrated Optics, **17**, pp. 51–62 (1998).

[60]. A. Othonos and K. Kalli, "*Fiber Bragg Gratings: Fundamentals and Applications in Telecommunications and Sensing*", Artech House (1999).

[61]. J. Stone, "*Photorefractivity in $GeO_2$ doped silica fibers*", Applied Physics, **62**, pp. 4371-4374 (1987).

[62]. M. M. Broer, A. J. Bruce and W. H. Grodkiewicz, "*Photoinduced refractive-index changes in several $Eu^{3+,}$ $Pr^{3+,}$ and $Er^{3+}$ doped oxide glasses*", Physical Review B, **45**, pp.7077-7083 (1992).

[63]. G. M. Williams, Tsung Ein Tsai, Celia I. Merzbacher and E. Joseph Friebele "*Photosensitivity of Rare Earth doped ZBLAN Fluoride glasses*", J. Lightwave Technology, **15**, pp.1357-1362 (1997).

[64]. P. R. Herman, K. Beckley and S. Ness, "*157nm photosensitivity in germanosilicate waveguides*", Conference on Lasers and Electro-Optics: California, Technical Digest Series, pp. 513 (1998).

[65]. J. Albert, B. Malo, F. Bilodeau, D. C. Johnson, K. O. Hill, Y. Hibino and M. Kawachi, "*Photosensitivity in Ge doped silica optical waveguides and fibers with 193nm light from an ArF excimer laser*", Optics Letters, **19**, pp.387-389 (1994).

[66]. R. M. Atkins and R. P. Espindola, "*Photosensitivity and grating writing in hydrogen loaded germanosilicate core optical fibers at 325 and 351nm*", Applied Physics Letters, **70**, pp. 1068-1069 (1997).

[67]. D. P. Hand and J. S. Russell, "*Photoinduced refractive index changes in fiber Bragg gratings",* Applied Physics Letters, **15**, pp. 102-104 (1990).

[68]. H.G Limberger, P.Y. Fonjallaz, R.P. Salathe and F. Cochet, "*Compaction and photoelastic induced index changes in fiber Bragg gratings", Applied* Physics Letters, **68**, pp. 3069-3071 (1996).

[69]. D. Wong, S. B. Poole, and M. G. Sceats, "*Stress-birefringence reduction in elliptical-core fibers under ultraviolet irradiation*", Optics Letters, **17**, pp. 1773-1775 (1992).

[70]. D. L. Williams, "*Photosensitive index changes in germania doped silica fibers and waveguides*", Photosensitivity and Self Organisation in Optical Fibers and Waveguides, Quebec, Canada, Proceedings SPIE, **2044**, pp. 55-68 (1993).

[71]. A. Attard, "*Fermi level shift in $Bi1_2SiO_20$ via photon induced trap level occupation*", Applied Physics, **71**, pp. 933-937 (1992).

[72]. N. Lawandy, "*Light induced transport and delocalisation in transparent amorphous systems,*" Optics Communication, **74**, pp. 180-184 (1989).

[73]. A. Miotello and R. Kelly, "*Laser irradiation effects in $Si^+$-implanted $SiO_2$*", nuclear instruments & methods in physics research. Sect. B, **65**, pp. 217-222 (1992).

[74]. M. Douay, W. X. Xie, T. Taunay, P. Bernage, P. Niay P, P. Cordier, B. Poumellec, L. Dong, J. F. Bayon, H. Poignant and E. Delevaque, "*Densification involved in the UV-based photosensitivity of silica glasses and optical fibers*", J. Lightwave Technoogy, **15**, pp. 1329-1342 (1997).

[75]. R. M. Atkins, V. Mizrahi and T. Erdogan, "*248 nm induced vacuum UV spectral changes in optical fiber preform cores: support for a colour centre model of photosensitivity*", Electronics Letters, **29**, pp. 385-387 (1993).

[76]. K. D. Simmons, S. LaRochelle, V. Mizrahi, G. I. Stegeman and D. L. Griscom. "*Correlation of defect centers with a wavelength-dependent photosensitive response in germania-doped silica optical fibers*", Optics Letters, **16**, pp. 141-143 (1991).

[77]. R. M. Atkins and V. Mizrahi, "*Observations of changes in UV absorption bands of singlemode germanosilicate core optical fibers on writing and thermally erasing refractive index gratings*", Electronics Letters, **28**, pp.1743-1744 (1992).

[78]. B. P. Poumellec, M. Niay, Douay and J.F. Bayon, "*The UV-induced refractive index grating in $Ge:SiO_2$ preforms: Additional CW experiments and the macroscopic origin of the change in index*", Applied Physics, **29**, pp. 1842-1856 (1996).

[79]. P. J. Lemaire, R. M. Atkins, V. Mizrahi and W. A. Reed, "*High pressure $H_2$ loading as a technique for achieving ultrahigh UV photosensitivity and thermal sensitivity in $GeO_2$ doped optical fibers*", Electronics Letters, **29**, pp. 1191-1193 (1993).

[80]. R. M. Atkins, P. J. Lemaire, T. Erdogan and V. A. Mizrahi, "*Mechanisms of enhanced UV photosensitivity via hydrogen loading in germanosilicate glasses*", Electronics Letters, **29**, pp. 1234-1235 (1993).

[81]. V. Grubsky, D. S. Starodubov, J. Feinberg, "*Photochemical reaction of hydrogen with germanosilicate glass initiated by 3.4 - 5.4-eV ultraviolet light*", Optics Letters, **24**, pp. 729-731 (1999).

[82]. F. Bliodeau, B. Malo, J. Albert, DC. Johnson, KO. Hill, Y. Hibino, Y. Abe and M. Kawachi, "*Photosensitisation of optical fiber and silica on silicon/silica waveguides*", Optics Letters, **18**, pp. 953-955 (1993).

[83]. D. L. Williams, B. J. Ainslie, J. R. Armitage, R. Kashyap and R. Campbell, "*Enhanced UV photosensitivity in boron codoped germanosilicate fibers",* Electronics Letters, **29**, pp. 45-47 (1993).

[84]. K. O. Hill, B. Malo, F. Bilodeau, D. C. Johnson, J. F. Morse, A. Kilian, L. Reinhart and K. Oh," Photosensitivity in $Eu^{2+}$ : $Al_2O_3$ doped core fiber", Proceedings of the Conference on Optical Fiber Communication," Optical Society of America, **14**, pp. 14-21 (1991).

[85]. M. M. Broer, R. L. Cone and J. R. Simpson, "*Ultraviolet-induced distributed feedback gratings in $Ce^{3+}$ -doped silica optical fibers*", Optics Letters, **16**, pp. 1391-1393 (1991).

[86]. F. Bilodeau, D. C. Johnson, B. Malo, K. A. Vineberg, K. O. Hill, T. F. Morse, A. Kilian and L. Reinhart, "*Ultraviolet-Light Photosensitivity in $Er^{3+}$ -Ge-doped optical fiber*," Optics Letters, **15**, pp. 1138-1140 (1990).

[87]. L. Dong, L. Reekie, L. Cruz and D. N. Payne, "*Grating formation in a phosphorus doped germanosilicate fiber*", Conference on Optical Fiber Communication, pp. 82-83 (1996).

[88]. K. Oh, P. S. Westbrook, R.M. Atkins, P. Reyes, R.S. Windeler, W.A. Reed, T.E. Stockert, D. Brownlow and D. DiGiovanni, "*Ultraviolet photosensitive response in an antimony-doped optical fiber",* Optics Letters, **27**, pp. 488-490 (2002).

[89]. ]. L. Dong, J. L. Cruz, L. Reekie, M. G. Xu and D. Payne, "*Enhanced photosensitivity in tin-co doped germanosilicate optical fibers*", IEEE Photonics Technology Letters, **7**, pp. 1048-1050 (1995).

[90]. M. L. Dockney, J.W. James and R. P. Tatam, "*Fiber Bragg grating fabricated using a wavelength tuneable source and a phase-mask based interferometer*", Measurement Science and Technology, **7**, pp. 445-448 (1996).

[91]. R. Kashyap, J. R. Armitage, R. W. Wyatt, S. T. Davey and D. L. Williams, "*All-fiber narrow-band reflection gratings at 150 nm*", Electronics Letters, **26**, pp.730-732 ( 1990).

[92]. B. J. Eggleton, P. A. Krug and L. Poladian: "*Experimental demonstration of compression of dispersed optical pulses by reflection from self-chirped optical fiber Bragg gratings*," Optics Letters, **19**, pp. 877-880 (1994).

[93]. D. Z. Anderson, V. Mizrahi, T. Erdogan and A.E. White, "*Production of in-fiber gratings using a diffractive optical element*", Electronics Letters, **29**, pp. 566-568 (1993).

[94]. J. Albert, S. Theriault, F. Bilodeau, D. Johnson, K. Hill, P. Sixt and M. Rooks, "*Minimization of phase errors in long fiber Bragg grating phase masks made using electron beam lithography*," IEEE Photonics Technology Letters, **8**, pp. 1334–1336 (1996).

[95]. P. R. Herman, K. Beckley and S. Ness, "*157 nm Photosensitivity in germanosilicate and fused-silica glasses",* Conf. on Lasers and Electro-Optics, San Francisco, CA, 4-8 (1998).

[96]. K. P. Chen, P. R. Herman and R. Tam, "*Strong Fiber Bragg Grating Fabrication by Hybrid 157- and 248-nm Laser Exposure*", IEEE photonics technology letters, **14**, pp 170-172 (2002).

[97]. L. Dong, W.F.Liu and L.Reekie, "*Negative-index gratings formed by a 193-nm excimer laser*", Optics Letters, **21**, pp. 2032- 2034 (1996).

[98]. H. Patric and S.L. Gilbert, "*Growth of Bragg gratings produced by continuous-wave ultraviolet light in optical fibers*", Optics Letters, **18**, pp. 1484-1486 (1993).

[99]. C. J. Paddison, J. M. Dawes, D. J. W. Brown, M. J. Withford, R. I. Trickett, P. A. Krug, "*Multiple fiber gratings fabricated using frequency-doubled copper vapour lasers*", Electronics Letters, **34**, pp. 2407-2408 (1998).

[100]. J. R. Armitage, "*Fiber Bragg reflectors written at 262nm using a frequency quadrupled diode-pumped $Nd^{3+}$:YLF laser*", Electronics Letters, **29**, pp. 1181-1183 (1993).

[101]. C.Y. Wei, C. C. Ye, S.W. James, R.P. Tatam and P.E. Irving. "*The influence of hydrogen loading and the fabrication process on the mechanical strength of optical fibre Bragg gratings*", Optical Materials, **20**, pp. 241–51 (2002).

[102]. R. M. Atkins, R.P. Espindola, "*Photosensitivity and grating writing in hydrogen loaded germanosilicate core optical fibers at 325 and 351 nm*", Applied Physics Letters, **70**, pp. 1078-1069 (1997).

[103]. D. S. Starodubov, V. Grubsky, J. Feinberg, "*Bragg grating fabrication in germanosilicate fibers by use of near-UV light: a new pathway for refractive index changes*", Optics Letters, **22**, pp. 1086-1088 (1997).

[104]. J. Blows, D. Y. Tang, "Gratings written with tripled output of Q-switched Nd;YAG laser", Electronics Letters, **36**, pp. 1837-1839 (2000).

[105]. J. Thomas, E. Wikszak, T. Clausnitzer, U. Fuchs, U. Zeitner, S. Nolte and A. T¨unnermann,"*Inscription of fiber Bragg gratings with femtosecond pulses using a phase mask scanning technique*", Applied Physics A, **86**, pp. 153–157 (2007).

[106]. S. J. Mihailov, D. Grobnic, C. W. Smelser, P. Lu, R. B. Walker, H. Ding, "*Bragg grating inscription in various optical fibers with femtosecond infrared lasers and a phase mask*", Optical Materials Express, **1**, pp. 754–765 (2011).

[107]. J. Thomas, C. Voigtländer, D. Schimpf, F. Stutzki, E. Wikszak, J. Limpert, S. Nolte and A. Tünnermann, "*Continuously chirped fiber Bragg gratings by femtosecond laser structuring*", Optics Letters, **33**, pp. 1560–1562, (2008).

[108]. C. Voigtländer, J. Thomas, E. Wikszak, P. Dannberg, S. Nolte and A. Tünnermann, **"***Chirped fiber Bragg gratings written with ultrashort pulses and a tunable phase mask***",** Optics Letters, **34**, pp. 1888-1890 (2009).

[109]. B. Malo, K. O. Hill, F. Bilodeau, D. C. Johnson and J. Albert, "*Point-by-point fabrication of micro-Bragg gratings in photosensitive fiber using single excimer pulse refractive index modification techniques*", Electronics Letters, **29**, pp.1668-1669 (1993).

[110]. A. Martinez, I. Y. Khrushchev and I. Bennion, "*Thermal properties of fiber Bragg gratings inscribed point-by-point by infrared femtosecond laser*", Electronics Letters, **41**, pp.176–178 (2005).

[111]. V. Bhatia and A. M. Vengsarkar, "*Optical fiber long period gratings sensors*", Optics Letters, **21**, pp. 692 – 694 (1996).

[112]. A. M. Vengsarkar, P. J. Lemaire, J. B. Judkins, V. Bhatia, T. Erdogan and J. E. Sipe, "*Long-period fiber gratings as band-rejection filters*", J. Lightwave Technology, **14**, pp. 58-65 (1996).

[113]. S.W. James and R.P. Tatam, "*Optical fiber long-period grating sensors: characteristics and applications*", Measurement Science and Technology, **14**, pp. 49-61 (2003).

[114]. V. Bhatia, "*Applications of long-period gratings to single and multi-parameter sensing*", Optics Express, **4**, pp. 457-466 (1999).

[115]. V. Bhatia, D. K. Campbell, D. Sherr, T. G. D. Alberto, N. A. Zabaronick, G. A. Ten Eyck, K. A. Murphy and R. A. Claus, "*Temperature insensitive and strain insensitive long period grating sensors for smart structures*", Optical Engineering, **36**, pp. 1872-1876 (1997).

[116]. Y. Liu, L. Zhang and I. Bennion, "*Fiber optic load sensors with high transverse strain sensitivity based on long-period gratings in B/Ge co-doped fiber*", Electronics Letters, **35**, pp. 661-662 (1999).

[117]. H. J. Patrick, C. C. Chang and S. T. Vohra, "Long period gratings for structural bend sensing", Electronics Letters, **34**, pp. 1773-1775 (1998).

[118]. H. J. Patrick, C.C. Chang and S. T. Vohra, "*Long period gratings for structural bend sensing*", Electronics Letters, **34**, pp. 1773-1775 (1998).

[119]. R. Falciai, A.G. Mignani and A. Vannini, "*Long period gratings as solution concentration sensors*", Sensors and Actuators B, **74**, pp. 74-77 (2001).

[120]. H. J. Patrick, A. D. Kersey and F. Bucholtz, "*Analaysis of the long period fiber gratings to external index of refraction*", Journal of Lightwave Technology, **16**, pp. 1606-1642 (1998).

[121]. R. Hou, Z. Ghassemlooy, A. Hassan, C. Lu and K. P. Dowker, "*Modelling Of Long Period Fiber Grating Response To Refractive Index Higher Than That Of Cladding*", Measurement Science And Technology, **12**, pp. 1709- 1713 (2001).

[122]. C.C. Ye, S. W. James and R. P. Tatam, "*Long period fiber gratings for simultaneous temperature and bend sensing*", Optics Letters, **25**, pp. 1007-1009 (2000).

[123]. V. Bhatia, "*Properties and Sensing Applications of Long-Period Gratings*", Ph.D. Thesis, Virginia Polytechnic Institute and State University, Blacksburg, Virginia (1996).

[124]. T. Erdogan, "*Cladding-mode resonances in short and long period fiber grating filters*", Journal Optical Society of Americ A, **14**, pp. 1760–1773 (1997).

[125]. T. Erdogan, "Fiber grating spectra", Journal of Lightwave Technology, **15**, pp. 1277-1294 (1997).

[126]. C. Tsao, "*Optical fiber waveguide analysis*", Oxford University Press (1992).

[127]. R. J. Black, L. Gagnon, "*Optical Waveguide Modes: Polarization, Coupling and Symmetry*", Mcgrah-Hill (2010).

[128]. A. V. Brakel, "*Sensing characteristics of an optical fibre long-period grating michelson refractometer*", Ph.D. Thesis, Rand Afrikaans University (2004).

[129]. Z.J. Zhang and W.K. Shi. "*Eigen value and field equations of three-layered uniaxial fibers and their applications to the characteristics of long-period fiber gratings with applied axial strain*", Journal of the Optical Society of America A-Optics Image Science and Vision, **22**, pp. 2516- 2526 (2005).

[130]. X. Daxhelet and M. Kulishov, "*Theory and practice of long-period gratings: when a loss become a gain*", Optics Letters, **28**, pp. 686-688 (2003).

[131]. P. Lalanne, I. D. Villar, I. R. Mat´ıas and F. J. Arregui. "*Optimization of sensitivity in Long Period Fiber Gratings with overlay deposition*", Optics Express, **13**, pp. 56 – 69 (2005).

[132]. Y. Chung and U. C. Paek. "*Fabrication and performance characteristics of optical fiber gratings for sensing applications*", IEEE Transactions on Optical Fiber Sensors, **01**, pp. 36 – 42 (2002).

[133]. X. Shu, L. Zhang and I. Bennion, "*Sensitivity characteristics of long-period fiber gratings*", Journal of Lightwave Technology, **20**, pp. 255-266 (2002).

[134]. M. N. Ng and K. S. Chiang, "*Thermal effects on the transmission spectra of long period fiber gratings*", Optics Communication, **208**, pp.321–327 (2002).

[135]. X. Shu, T. Allsop, B. Gwandu, L. Zhang and I. Bennion, "*High-temperature sensitivity of log-period gratings in B-Ge codoped fiber*", IEEE Photonics Technology Letters, **13**, pp. 818-820 (2001).

[136]. J. Keith, S. Puckett and G.E. Pacey, "*Investigation of the fundamental behavior of long-period grating sensors*", Talanta, **61**, pp. 417-421, (2003).

[137]. X. Shu, T. Allsop, B. Gwandu, L. Zhang and I. Bennion, "*Room-temperature operation of widely tunable loss filter*", Electronics Letters, **37**, pp. 216–218 (2001).

[138]. T. W. MacDougall, S. Pilevar, C. W. Haggans and M. A. Jackson, "*Generalized expression for the growth of long period gratings*", IEEE Photonics Technology Letters, **10**, pp. 1449–1451 (1998).

[139]. G. Ghosh, M. Endo and T. Iwasaki, "*Temperature-dependent Sellmeier coefficients and chromatic dispersions for some optical fiber glasses*", Journal of Lightwave Technology, **12**, pp. 1338-1341 (1994).

[140]. T. Mizunami, T. Fukuda T and A. Hayash, "*Fabrication and characterization of long-period-grating temperature sensors using Ge–B-co-doped photosensitive fiber and single-mode fiber*", Measurement Science and Technology **15**, pp.1467–1473 (2004).

[141]. T. Yokouchi, Y. Suzaki, K. Nakagawa, M. Yamauchi, M. Kimura, Y. Mizutani , S. Kimura and S. Ejima, "*Thermal tuning of mechanically induced long-period fiber grating*", Applied Optics, **44**, pp. 5024–5028 (2005).

[142]. C.G. Atherton, A.L. Steele and J.E. Hoad, "'*Resonance conditions of long period gratings in temperature sensitive polymer ring optical fiber*", IEEE Photonics Technology Letters, **12**, pp. 65-67 (2000).

[143]. S. Khaliq, S. W. James and R. P. Tatam, "*Enhanced sensitivity fiber optic long period grating temperature sensor*", Measurement Science and Technology, **13**, pp. 792-795 (2002).

[144]. K. S. Chiang, Y. Liu, M. N. Ng and X. Dong, "*Analysis of etched long-period fiber grating and its response to external refractive index*", Electronics Letters, **36**, pp. 966-967 (2000).

[145]. A. A. Abramov, A. Hale, R.S. Windeler and T.A. Strasser, "*Widely tunable long period fiber gratings*", Electronics Letters, **35**, pp. 81- 82 (1999).

[146]. T. H. W. Johnstone, G. Stewart and B. Culshaw, "*Surface plasmon polaritons in thin metal films and their role in fiber optic polarizing devices*", IEEE Journal of Lightwave Technology, **8**, pp. 538 – 543 (1990).

[147]. T. Hiroshi and K. Urabe, "*Characterization of Long-period Grating Refractive Index Sensors and Their Applications*", Sensors, **9**, pp. 4559-4571 (2009).

[148]. B. H. Lee, Y. Liu, S. B. Lee, S. S. Choi and J. N. Jang, "*Displacements of the resonant peaks of a long period fiber grating induced by a change of ambient refractive index*", Optics Letters, **22**, pp. 1769- 1771 (1997).

[149]. X. Shu, X. Zhu, S. Jiang, W. Shi and D. Huang, "*High sensitivity of dual resonant peaks of long-period fiber grating to surrounding refractive index changes*", Electronics Letters, **35**, pp. 1580–1581 (1999).

[150]. A. Martínez Rios, D. Monzón Hernández, I. Torres Gomez, "*Highly sensitive cladding-etched arc-induced long-period fiber gratings for refractive index sensing*", Optics Communications, **283**, pp. 958-962 (2010).

[151]. Y. Koyamada, "*Numerical analysis of core-mode to radiation-mode coupling in long-period fiber gratings*", IEEE Photonics Technology Letters, **13**, pp. 308-310 (2001).

[152]. O. Duhem, J. Fraņois Henninot, M. Warenghem and M. Douay, "*Demonstration of long period-grating efficient couplings with an external medium of a refractive index higher than that of silica*", Applied Optics, **37**, pp. 7223-7228 (1998).

[153]. R. Hou, Z. Ghassemlooy, A. Hassan, C. Lu and K. P. Dowker, "*Modelling of long-period fiber grating response to refractive index higher than that of cladding*", Measurement Science and Technology, **12**, pp. 1709-1713 (2001).

[154]. D. B. Stegall and T. Erdogan, "*Leaky cladding mode propagation in long-period fiber grating devices*", IEEE Photonics Technology Letters, **11**, pp. 343-345 (1999).

[155]. P. Strop and A.T. Brunger, "*Refractive index-based determination of detergent concentration and its application to the study of membrane proteins*", Protein Science, **14**, pp. 2207-2211 (2005).

[156]. M. P. DeLisa, Z. Zhang, M. Shiloach, S. Pilevar, C. C. Davis, J. S. Sirkis and W. E. Bentley, "*Evanescent Wave Long-Period Fiber Bragg Grating as an Immobilized Antibody Biosensor*", Analytical Chemistry, **72**, pp. 2895–2900 (2000).

[157]. R. S. Nidhi, R. S. Kaler and P. Kapur, "*Theoretical and Experimental Study of Long-Period Grating refractive Index Sensor*", Fiber and Integrated Optics, **33**, pp. 37-46 (2014).

[158]. S. W. James, S. Korposh, S. W. Lee and R. P. Tatam, "*A long period grating-based chemical sensor insensitive to the influence of interfering parameters*", Optics Express, **22**, pp. 8012-8023 (2014).

[159]. S. M. Topliss, S. W. James, F. Davis, S. J. P. Higson and R. P. Tatam, "*Optical fiber long period grating based selective vapour sensing of volatile organic compounds*", Sensors and Actuators B , **143**, pp. 629–634 (2010).

[160]. A. Cusano, P. Pilla, L. Contessa, A. Iadicicco, S. Campopiano, A. Cutolo, M. Giordano and G. Guerra, "*High sensitivity optical chemosensor based on coated long-period gratings for sub-ppm chemical detection in water*", Applied Physics Letters, **87**, 234105 (2005).

[161]. I. M. Ishaq, A. Quintela, S.W. James, G.J. Ashwell R.P. Tatam, "*Modification of the refractive index response of long period gratings using thin film overlays*", Sensors and Actuators B, **114**, pp. 738–741 (2005) .

[162]. A. Cusano, A. Iadicicco, P. Pilla, L. Contessa, S. Campopiano, A. Cutolo and M. Giordano, "*Mode transition in high refractive index coated long period gratings*", Optics Express, **14**, pp. 19–34 (2006) .

[163]. N. D. Rees, S. W. James, R. P. Tatam and G. J. Ashwell, "*Optical fiber long-period gratings with Langmuir-Blodgett thin-film overlays*", Optics Letters, **27**, pp. 686–688 (2002).

[164]. M. Konstantaki, S. Pissadakis, S. Pispas, N. Madamopoulos and N. A. Vainos, "Optical fiber long-period grating humidity sensor with poly(ethylene oxide)/cobalt chloride coating", Applied Optics, **45**, pp. 4567–4571 (2006).

[165]. Y. Miao, K. Zhang, Y. Yuam, B Liu, H Zhang, Y Liu, and J. Yao, "*Agarose gel coated LPG based on two sensing mechanisms for relative humidity measurement*", Applied Optics, **52**, pp. 90-95 (2013).

[166]. S. Korposh, R. Selyanchyn, W. Yasukochi, S. W. Lee, S. W. James and R. P. Tatam, "*Optical fiber long period grating with a nanoporous coating formed from silica nanoparticles for ammonia sensing in water*", Materials Chemistry and Physics, **133**, pp.784–792 (2012).

[167]. M. Konstantaki, A. Klini, D. Anglos and S. Pissadakis, "An ethanol vapor detection probe based on a ZnO nanorod coated optical fiber long period grating," Optics Express, **20**, pp. 8472–8484 (2012).

[168]. A. Cusano, A. Iadicicco, P. Pilla, L. Contessa, S. Campopiano, A. Cutolo, M. Giordano and G. Guerra, "*Coated Long-Period Fiber Gratings as High-Sensitivity Optochemical Sensors*", IEEE J. Lightwave Technology, **24**, pp. 1776-1786 (2006).

[169]. V. Grubsky, A. Skorucak, D. S. Starodubov and J. Feinberg, "*Fabrication of long-period fiber gratings with no harmonics*", IEEE Photonics Technology Letters, **11**, pp. 87-89 (1999).

[170]. V. Grubsky, A. Skorucak, D. S. Starodubov and J. Feinberg, "*Fabrication of long-period fiber gratings with no harmonics*", IEEE Photonics Technology Letters, **11**, pp. 87-89 (1999).

[171]. E. M. Dianov, D. S. Starodubov, S. A. Vasiliev, A. A. Frolov and O. I. Medvedkov, "*Refractive index gratings written by near ultraviolet radiation*", Optics Letters, **22**, pp. 221–223 (1997).

[172]. K. O. Hill, B. Malo, K. A. Vineberg, F. Bilodeau, D. C. Johnson and I. Skinner, "*Efficient mode conversion in telecommunication fiber using externally written gratings*", Electronics Letters, **26**, pp. 1270-1272 (1990).

[173]. H. J. Patrick, C. G. Askins, R. W. McElhalon and E. J. Friebele, "*Amplitude mask patterned on an excimer laser mirror for high intensity writing of long period fiber gratings"*, Electronics Letters, **33**, pp. 1167-1168 (1997).

[174]. J. A. Rogers, R. J. Jackman, G. M. Whitesides, J. L. Wagener and A. M. Vengsarkar, "*Using microcontact printing to generate amplitude photomasks on the surfaces of optical fibers: A method for producing in-fiber gratings*", Applied Physics Letters, **70**, pp. 7-9 (1997).

[175]. A. P. Zhang, S. Gao, G. Yan and Y. Bai, "*Advances in Optical Fiber Bragg Grating Sensor Technologies*", Photonic Sensors, **2**, pp. 1–13 (2012).

[176]. B. J. Eggleton, P. S. Westbrook, R. S. Windeler, S. Spalter and T.A. Strasser, *"Grating resonances in air-silica microstructured optical fibers*", Optics Letters, **24**, pp. 1460-1462 (1999).

[177]. J. Albert, B. Malo, K. O. Hill, F. Bilodeau, D. C. Johnson and S. Theriault, "*Comparison of one-photon and two-photon effects in the photosensitivity of germaniumdoped silica optical fibers exposed to intense ArF excimer laser pulses*", Applied Physics Letters, **67**, pp. 3529-3531 (1995).

[178]. B. Malo, J. Albert, K. O. Hill, F. Bilodeau, D. C. Johnson and S. Thériault, "*Enhanced photosensitivity in lightly doped standard telecommunication fiber exposed to high fluence ArF excimer laser light*", Electronics Letters, **31**, pp. 879-880 (1995).

[179]. I. Bennion, J. A. R. Williams, L. Zhang, K. Sugden and N. J. Doran, "*UV written in-fiber Bragg gratings*", Optical and Quantum Electronics, **28**, pp. 93-135 (1996).

[180]. B. Guan, H. Tam, S. Ho, S. Liu and X. Dong, "*Growth of long-period gratings in H-2-loaded fiber after 193-nm UV inscription*", IEEE Photonics Technology Letters, **12**, pp. 642-644 (2000).

[181]. C.. Ye, S. James and R. Tatam, "*Simultaneous temperature and bend sensing with long-period fiber gratings*", Optics Letters, **25**, pp. 1007-1009 (2000).

[182]. P. J. Lemaire, R. M. Atkins, V. Mizrahi and W. A. Reed, "*High pressure $H_2$ loading as a technique for achieving ultrahigh UV photosensitivity and thermal sensitivity in $GeO_2$ doped optical fiber*", Electronics Letters, **29**, pp. 1191-1193 (1993).

[183]. D. D. Davis, T. K. Gaylord, E. N. Glytsis and S. C. Mettler, "*$CO_2$ laser-induced long-period fiber gratings: Spectral characteristics, cladding modes and polarization independence*", Electronics Letters, **34**, pp. 1416-1417 (1998).

[184]. D. D. Davis, T. K. Gaylord, E. N. Glytsis and S. C. Mettler, "*Very high-temperature stable $CO_2$ laser induced long period fiber gratings"*, Electronics Letters, **35**, pp. 740-742 (1999).

[185]. G. Rego, O. Okhotnikov, E. Dianov and V. Sulimov, "*High-temperature stability of long-period fiber gratings produced using an electric arc*", J. Lightwave Technology, **19**, pp. 1574-1579 (2001).

[186]. A. Malki, G. Humbert, Y. Ouerdane, A. Boukhenter and A. Boudrioua, "*Investigation of the writing mechanism of electric arc induced long period fiber gratings*", Applied Optics, **42**, pp. 3776–3779 (2003).

[187]. Y. Kondo, K. Nouchi, T. Mitsuyu, M. Watanabe, P. G. kazansky and K. Hirao, "*Fabrication of long-period fiber gratings by focused irradiation of infrared femtosecond laser pulses*", Optics Letters, **24**, pp. 646-648 (1999).

[188]. F. Hindle, E. Fertein, C. Przygodzki, F. Dürr, L. Paccou, R. Bocquet, P. Niay, G. Limberger and M. Douay, "*Inscription of long-period gratings in pure silica and germane silicate fiber cores by femtosecond laser irradiation*", IEEE Photonics Technology Letters, **16**, pp. 1861–1863 (2004).

[189]. Y. Jiang, C. Tang, J. Xu, "*Fabrication of long-period gratings with a mercury arc lamp*", Optics Communications, **283**, pp. 1311–1315 (2010).

[190]. M. Fujimaki, Y. Ohki, J. L. Brebner and S. Roorda, "*Fabrication of long-period optical fiber gratings by use of ion implantation*", Optics Letters, **25**, pp. 88-89 (2000).

[191]. M. Fujimaki, Y. Nishihara, Y. Ohki, J. L. Brebner and S. Roorda, "*Ion implantation induced densification in silica-based glass for fabrication of optical fibre gratings*", J. of Applied Physics, **88**, pp. 5534-5537 (2000).

[192]. V. I. Karpov, M. V. Grekov, E. M. Dianov, K. M. Golant, S. A. Vasiliev, O. I. Medvedkov and R. R. Khrapko, "*Mode field converters and long period gratings fabricated by thermo-diffusion in nitrogen-doped silica core fibers*", Proc. Optical Fiber Communication Conference and Exhibit, OFC '98, Technical Digest, pp. 279–280 ( 1998).

[193]. C. Narayanan, H. M. Presby and A. M. Vengsarkar, "*Band rejection fiber filter using periodic core deformation*", Electronics Letters, **33**, pp. 280-281 (1997).

[194]. M. Kim, D. Lee, B. I. Hong and H. Chung, "*Performance characteristics of long period fiber-gratings made from periodic tapers induced by electric arc discharge*", J. Korean Physical Society, **40**, pp. 369–373 (2002).

[195]. I. K. Hwang, S. H. Yun and B. Y. Kim, "*Long-period fiber gratings based on periodic microbends*", Optics Letters, **24**, pp. 1263-1265 (1999).

[196]. Y. Jiang, Q. Li, C. H. Lin, E. Lyons, I. Tomov and H. P. Lee, "*A novel strain induced thermally tuned long-period fiber grating fabricated on a periodic corrugated silicon fixture*", IEEE Photonics Technology Letters, **14**, pp. 941-943 (2002).

[197]. G. Kakarantzas, T. E. Dimmick, T. A. Birks, R. Le Roux and P. St. J. Russell, "*Miniature all-fiber devices based on $CO_2$ microstructuring of tapered fibers*", Optics Letters, **26**, pp. 1137-1139 (2001).

[198]. C. D. Poole, H. M. Presby and J. P. Meester, "*Two mode fiber spatialmode converter using periodic core deformation*", Electronics Letters, **30**, pp. 1437- 1438 (1994).

[199]. C. Y. Lin, G. W. Chern and L. A. Wang, "*Periodical corrugated structure for forming sampled fiber Bragg grating and long-period fiber grating with tunable coupling strength*", J. Lightwave Technology, **19**, pp. 1212- 1220 (2001).

[200]. S. Savin, M.J.F. Digonnet, G.S. Kino and HJ. Shaw, "*Tunable mechanically induced long period fiber gratings*", Optics Letters, **25**, pp. 710-712 (2000).

[201]. J. K. Bae, S. H. Kim, J. H. Kim, J. H. Bae, S. B. Lee and J. M. Jeong, "*Spectral shape tunable band-rejection filter using a long-period fiber grating with divided coil heaters*", IEEE Photonics Technology Letters, **15**, pp. 407-409 (2003).

[202]. T. Y. Tang, P. Y. Tseng, C. Y. Chiu, C. N. Lin, C. C. Yang, Y. W. Kiang and K. J. Ma, "*Long-period fiber grating effects induced by double-sided loading*", Optical Engineering, **42**, pp. 1910-1914 (2003).

[203]. Y. C. Jeong, B. C. Yang, B. H. Lee, H. S. Seo, S. S. Choi and K. W. Oh, "*Electrically controllable long period liquid crystal fiber gratings*", IEEE Photonics Technology Letters, **12**, pp. 519-521 (2000).

[204]. R. Faced, C. Alegria, M. N. Zervas and R. I. Laming, "*Acousto optic attenuation filters based on tapered optical fibers*", IEEE J. Selected Topics in Quantum Electronics, **5**, pp. 1278-1288 (1999).

[205]. A. Diez, T. A. Birks, W. H. Reeves, B. J. Mangan and P. St. J. Russell, "*Excitation of cladding modes in photonic crystal fibers by flexural acoustic waves*", Optics Letters, **25**, pp. 1499-1501 (2000).

[206]. G. Rego, R. Falate, J. L. Santos, H. M. Salgado, J. L. Fabris, S. L. Semjonov and E. M. Dianov, "*Arc induced long-period gratings in aluminosilicate glass fibers*", Optics Letters, **30**, pp. 2065- 2067 (2005).

[207]. G. Rego, A. F. Fernandez, A. Gusarov, B. Brichard, F. Berghmans, J. L. Santos and H.M. Salgado, "*Effect of ionizing radiation on the properties of arc induced long period fiber gratings*", Applied Optics, **44**, pp. 6258-6263 (2005).

[208]. S. Lee, R. Kumar, P. Kumar, P. Radhakrishnan, C. Vallabhan, and V. Nampoori. "*Long period gratings in multimode optical fibers: application in chemical sensing*" Optics Communications, **224**, pp. 237-241 (2003).

[209]. K.J. Han, Y.W. Lee, J. Kwon, S. Roh, J. Jung and B. Lee, "*Simultaneous measurement of strain and temperature incorporating a long-period fiber grating inscribed on a polarization maintaining fiber*", IEEE Photonics Technology Letters, **16**, pp. 2114-2116 (2004).

[210]. X. Chen, K. Zhou, L. Zhang and I. Bennion, "*Optical chemsensors utilizing long period fiber gratings UV Inscribed in D-Fiber with enhanced sensitivity through cladding etching*", IEEE Photonics Technology Letters, **16**, pp. 1352-1354 (2004).

[211]. T. J. Eom, S. J. Kim, T. Y. Kim, C. S. Park and B.H. Lee "*Optical pulse multiplication and temporal coding using true time delay achieved by long-period fiber gratings in dispersion compensating fiber*", Optics Express, **12**, pp. 6410-6420 (2004).

[212]. L. Dong, L. Reekie and J. Cruz, "*Long period gratings formed in depressed cladding fibers*", Electronics Letters, **33**, pp. 1897-1898 (1997).

[213]. G. Humbert, A. Malki, S. Fevrier, P. Roy, J. L. Auguste and J. M. Blondy, "*Long period grating filters fabricated with electric arc in dual concentric core fibers"*, Optics Communications, **225**, pp. 47-53 (2003).

[214]. H. L. An, B. Ashton and S. Fleming, "*Long period grating assisted optical add-drop filter based on mismatched twin-core photosensitive-cladding fiber*", Optics Letters, **29**, pp. 343-345 (2004).

[215]. G. Kakarantzas, T. Birks and P. Russell, "*Structural long-period gratings in photonic crystal fibers*", Optics Letters, **27**, pp. 1013-1015 (2002).

[216]. K. Morishita and Y. Miyake, "*Fabrication and resonance wavelengths of long period gratings written in a pure-silica photonic crystal fiber by the glass structure change*", Journal of Lightwave Technology, **22**, pp. 625-630 (2004).

[217]. V. Rastogi and K. Chiang "*Long-period gratings in planar optical waveguides*", Applied Optics, **41**, pp. 6351-6355 (2002).

[218]. B. Malo, J. Albert, K. O. Hill, F. Bilodeau and D. C. Johnson, "*Effective index drift from molecular hydrogen diffusion in hydrogen-loaded optical fibers and its effect on Bragg grating fabrication*", Electronics Letters, **30**, pp. 442-444 (1994).

[219]. H. Patrick, S. L. Gilbert,A. Lidgard and M. D. Gallagher, "*Annealing of Bragg gratings in hydrogen-loaded optical fiber*", Journal of Applied Physics, **78**, pp. 2940-2945 (1995).

[220]. J. N. Jang, H. G. Kim, S. G. Shin, M. S. Kim, S. B. Lee and K. H. Kwack, " *Effects of hydrogen molecule diffusion on $LP_{0m}$ mode coupling of long period gratings*", Journal of Non Crystalline Solids, **259**, pp. 156-164 (1999).

[221]. D. L. Williams and R. P. Smith, "*Accelerated Lifetime Tests On UV Written Intra-core Gratings in Boron Germania Co doped Silica Fiber*", Electronics Letters, **31**, pp. 2120-2121 (1995).

[222]. S. Kannan, J. Z. Y. Guo and P. J. Lemaire, "*Thermal stability analysis of UV induced fiber Bragg gratings*", J. Lightwave Technology, **15**, pp. 1478-1483 (1997).

# Chapter 3

# Fabrication and Characterization of Long Period Gratings

*Abstract*

*This chapter discusses the characterization of an LPG to measurands such as temperature and changes in the RI of surrounding medium. We also investigate the temperature sensitivity of the Long Period Gratings (LPG) fabricated in SMF-28 fiber and B-Ge co doped photosensitive fiber. The difference in temperature sensitivity between the SMF-28 and B-Ge fiber is explained on the basis of the thermo-optic coefficients of the core and the cladding materials. The influence of grating period of LPG on refractive index sensitivity is experimentally investigated in the second part of this chapter. The response of the LPG to surrounding refractive indices greater than and less than that of cladding is studied by monitoring the wave length shift and amplitude changes of the attenuation bands.*

[1]. T.M. Libish *et al*., Optik, **124**, pp. 4345-4348 (2013).
[2]. T.M. Libish *et al*., Micro. &Opt. Tech. Lett., **54**, pp.2356-2360 (2012).
[3]. T.M. Libish *et al*., Optoelectronics Lett.; **8**, pp. 101-104 (2012).
[4]. T.M. Libish *et al*., Sens. & Trans. Jrnl, **129**, pp. 142-148 (2011).
[5]. T.M. Libish *et al*., J. Optoelec. & Adv. Mat., **13**, pp. 491-496 (2011).
[6]. T.M. Libish *et al*., Fiber Opt. & Photonics, pp. 1-3 (2012).

## 3.1 Introduction

In Chapter 2, the basic properties of long-period gratings were introduced. One can now summarise the long-period gratings as devices that couple light from the guided mode to discrete cladding modes and result in attenuation bands for which spectral locations are functions of the grating period and the differential effective index. Thus any variation in the effective indices of these modes or in the grating period serves to modulate the phase-matching wavelengths [1,2]. Chapter 3 presents and discusses the characterization of an LPG in the presence of measurands such as temperature and changes in the RI of its surrounding medium.

The influence of grating length and annealing on the transmission spectrum of long period grating is investigated by monitoring the wavelength shift and the intensity variation in the loss peaks. It is important that the LPG is annealed, before use as a sensor, so that its transmission spectrum is stable. Then the effect of temperature on the transmission spectrum of LPGs written in hydrogen loaded standard single mode fiber and B-Ge co doped fiber is experimentally studied. The results obtained show that the LPG written in B-Ge doped fiber will show more sensitivity than the LPG written in SMF-28 fiber under identical temperature ranges. It has also been shown that LPGs in a B–Ge co-doped fiber have opposite sign of temperature dependence compared to those in a standard single mode fiber. The negative sensitivity of an LPG in a photosensitive B–Ge co-doped fiber is due to the negative thermo optic coefficient of the boron dopant.

In this chapter, the influence of grating period of Long Period Grating (LPG) on refractive index sensitivity is also experimentally investigated. Three LPGs with grating periods 400 μm, 415 μm and 550 μm are used to carry out the experimental study. The fundamental principle of analysis is the sensitive dependence of the resonance peaks of an LPG on the changes in the refractive

index of the medium surrounding the cladding surface of the grating. The response of the LPG to refractive indices greater than and less than that of cladding is studied by monitoring the wave length shift and amplitude changes of the attenuation bands. It is shown that for a given fiber the wavelength shifts are strong functions of the grating period and the order of the corresponding cladding mode.

## 3.2 LPG fabrication

LPGs can be produced in various types of fibers, from standard telecommunication fibers to micro structured ones [3,4]. We first discuss the spectral variation of the transmitted output of an LPG during the fabrication process and then the impact of annealing and temperature variations on the attenuation bands of LPGs. The LPGs used in our experiments were fabricated using a 248 nm KrF excimer laser source, employing point-by-point writing method [5]. A great advantage of the point-by-point method is that it is a highly flexible technique, since the grating periodicity and length can be individually adjusted to meet the desired LPG specifications and corresponding spectral characteristics. The duty cycle of grating period was ~ 50%. The LPGs were fabricated in three different types of fibers.

1) The standard single-mode fiber SMF-28e (Core RI: 1.46145, Cladding RI: 1.456).

2) B-Ge co-doped photosensitive fiber manufactured in CGCRI, Kolkota (Core RI: 1.463, Cladding RI: 1.456).

3) B-Ge co-doped photosensitive fiber supplied by Newport Corporation, USA (Core RI: 1.450, Cladding RI: 1.446).

As the core material of SMF-28e fiber is not sensitive enough to UV light to modulate the refractive index of the fiber core to the extent required for LPG inscription, prior photosensitization techniques are required. To enhance the

photosensitivity, the fibers were hydrogen loaded at 100°C and 1500 psi of pressure for 24 hours before the LPG fabrication. The fiber coating was removed just before exposure to the UV laser light.

Figure 3.1 shows the transmission spectra of two LPGs, i.e.LPG-1 and LPG-2, with grating periods of 550 μm and 415 μm, respectively with air as the surrounding medium. These LPGs were written into the cores of SMF-28 fiber. Attenuation bands in the range of 1200– 1700 nm related to the cladding modes of both the LPGs have been investigated. For LPG-1, power coupling to cladding modes $LP_{02}$, $LP_{03}$ and $LP_{04}$ are seen to occur at 1451,1497,1588 nm respectively. LPG-2 exhibited five resonance bands at 1254($LP_{02}$), 1284($LP_{03}$), 1333($LP_{04}$), 1423($LP_{05}$), 1610($LP_{06}$) nm respectively. When the grating period became shorter, the resonant loss peaks of the low order cladding modes appeared spectrally closer to each other and also collectively moved to the blue wavelength side. The simulations made (using Optigrating software by Optiwave) for these two LPGs are also shown in Fig. 3.2.

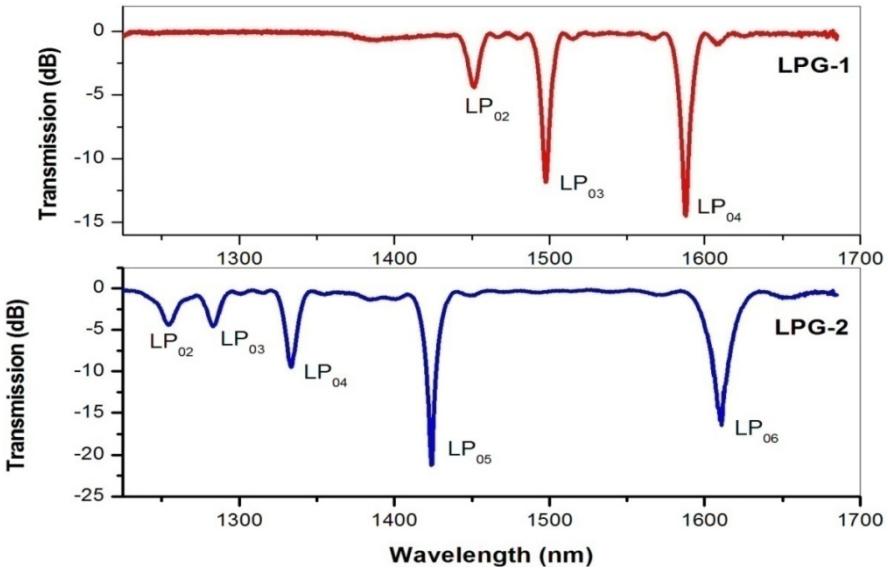


***Figure 3.1:*** *Transmission spectra of LPG-1 with a grating period of 550 μm and LPG-2 with a grating period of 415 μm (SMF-28 fiber).*

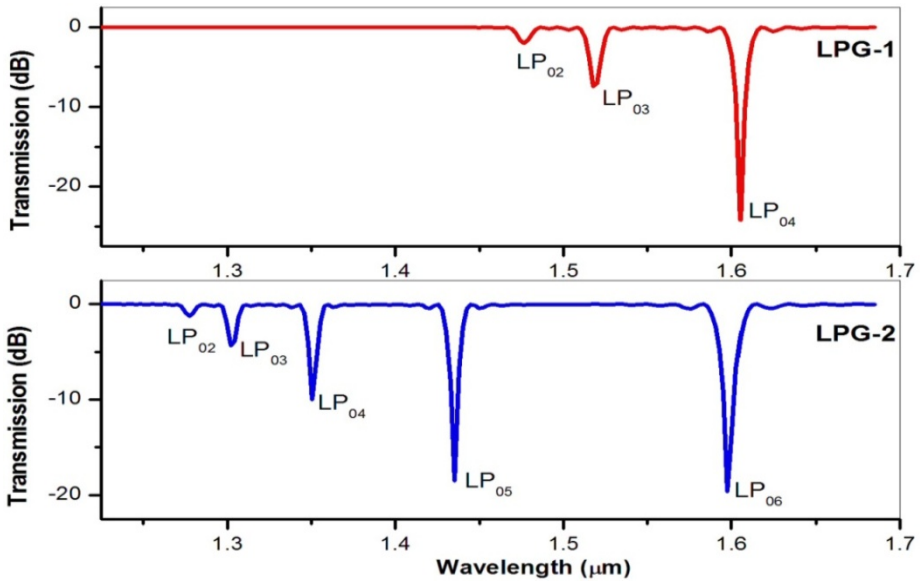


***Figure 3.2:*** *Simulated transmission spectra of LPG-1 with a grating period of 550* μm and *LPG-2 with a grating period of 415* μm *(SMF-28 fiber).*

## 3.3 The role of grating length on transmission spectra of long period gratings

During LPG fabrication, the transmission spectrum was recorded with an optical spectrum analyzer ([Yokogawa] AQ 6319). Figure 3.3 shows the transmission spectra of the LPG with grating period of 415 μm and various grating period numbers of 21, 36, 46 and 56. The appearance of attenuation dips in the transmission spectrum was first observed after the 21$^{st}$ period of the grating was created. Five loss peaks were detected in the wavelength range of 1240–1625 nm. They exhibited a slow initial growth rate followed by a progressively increasing growth rate. It can also be seen that, with an increase in the number of the grating period, the attenuation dip increases, and the 3 dB bandwidth of the transmission spectrum decreases. The increase in attenuation dip with increasing grating length is attributed to the increase in the power coupling to different cladding modes [Eq.2.31] [6,7]. After the writing of the 56$^{th}$ period, the power coupling to different

cladding modes $LP_{02}$, $LP_{03}$, $LP_{04}$, $LP_{05}$ and $LP_{06}$ were seen to occur at 1247.60, 1278.32, 1331.19, 1425.41, 1613.84 nm respectively. The maximum attenuation dip, corresponding to the $LP_{06}$ cladding mode observed is about 31.21 dB.

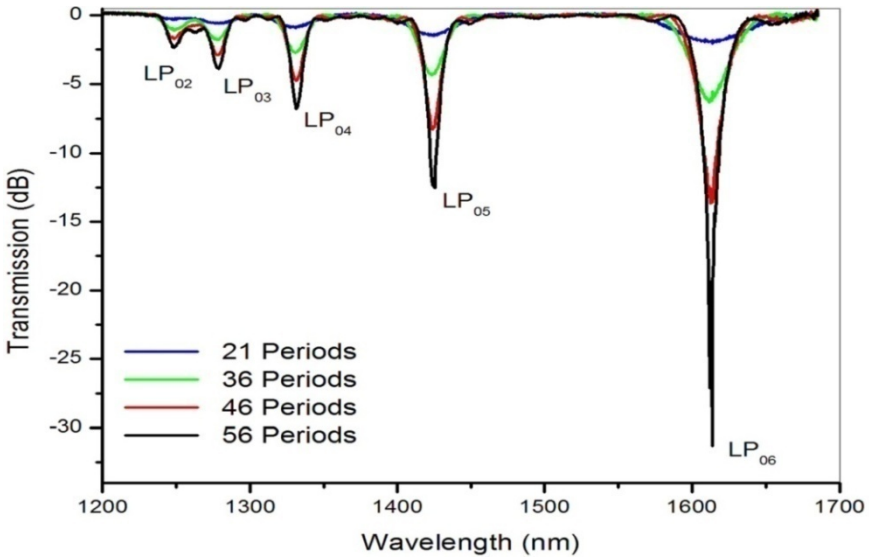


***Figure 3.3:*** *Evolution of normalized transmission spectra of LPG with a grating period of 415 μm in a standard single mode fiber (SMF 28e).*

## 3.4 The effect of annealing on the transmission spectrum of LPG

In the case of LPGs fabricated using hydrogen loaded fibers, the amount of hydrogen present in an optical fiber will be far in surplus of that required to achieve a given refractive index change [8,9]. The unused hydrogen remaining in the fiber can significantly influence spectral properties of the grating. The residual hydrogen slowly diffuses out of the fiber and changes the effective index of propagation of guided optical modes, resulting in a shift of the grating resonance wavelength and also causes a change in strength of the LPG attenuation bands [10]. So annealing of the fabricated LPGs was performed in an oven to stabilize the grating spectrum [11]. It serves well to remove the residual molecular hydrogen and

certain UV induced defects. Appropriate annealing conditions will depend on the fiber type, the expected operating temperature as well as on the required stability of the grating device.

During annealing, the LPGs were positioned in a temperature controlled oven (ASP, 500C Fiber Oven) as shown in Fig. 3.4. A white-light source ([Yokogawa] AQ 4305) was used as the signal source and the transmission spectra of the LPGs were interrogated with an optical spectrum analyzer (OSA) ([Yokogawa] AQ 6319). To avoid the effect of strain and bending, the LPGs were stretched and then fixed in the fiber oven. All readings were taken with air as the surrounding medium.

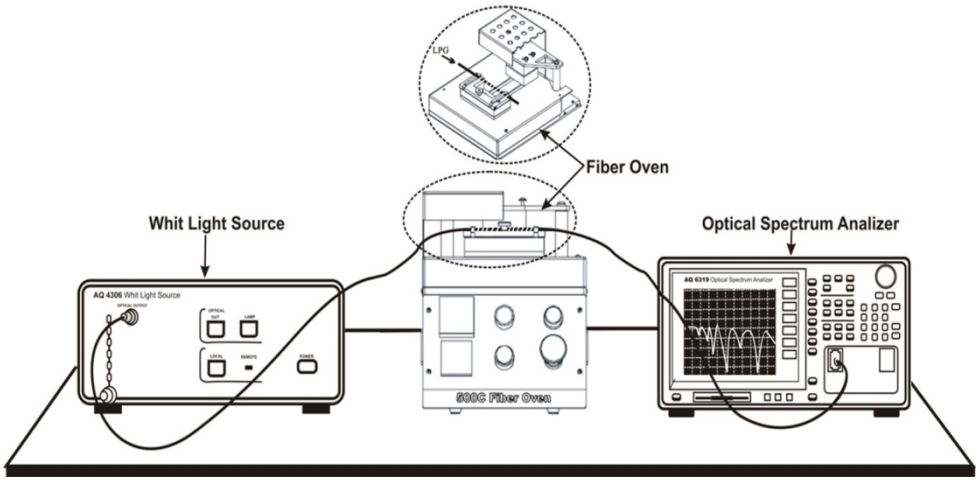


***Figure 3.4:*** *Experimental setup.*

Figure 3.5 shows the changes of the transmission characteristics of an LPG with a grating period of 550 μm during two cycles of annealing. Before annealing, the power coupled to cladding modes $LP_{02}$, $LP_{03}$ and $LP_{04}$ were seen to occur at 1453.60, 1500.44, 1591.33 nm respectively (Fig. 3.5.a). It can also be seen that the amount of power coupled to the $LP_{03}$ mode is more than that to $LP_{04}$ mode. This over coupling is mainly due to the presence of unused hydrogen in the fiber after LPG

fabrication. After first annealing (Temperature: 175°C, Time: 6 hrs), the resonance wavelengths shifted towards shorter wavelengths by 0.20, 0.71 and 0.79 nm. The peak loss of the $LP_{03}$ cladding mode decreased from 14.15 to 13.16 dB, and that of the $LP_{04}$ cladding mode increased from 11.39 to 11.77 dB (Fig.3.5.b). During annealing, the hydrogen in the cladding diffuses out first, and then that in the core follows. This temporal difference induces changes in the initial wavelengths of the fabricated LPGs. The overall shift during the annealing process is a function of the annealing temperature, residual concentrations of molecular hydrogen and on the annealing time.

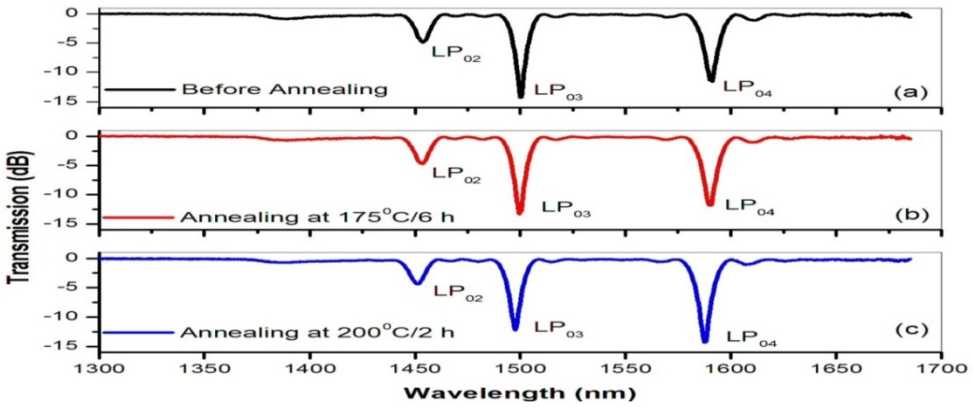


***Figure 3.5:*** *Transmission characteristics of LPG with a grating period of 550 μm (a) before annealing (b) after annealing at 175°C for 6hrs. (c) after annealing at 200°C for 2hrs.*

When the fiber is further annealed (Temperature: 200°C, Time: 2 hrs), almost all hydrogen molecules in both the cladding and the core diffuse out of the fiber. This out-diffusion again decreases the refractive indices of both the cladding and the core. As a result the resonance wavelengths shifted towards shorter wavelengths by 2.75, 2.68 and 3.73 nm from the initial position, and the final resonance wavelengths were 1450.85, 1497.76 and 1587.60 nm, respectively, for attenuation peaks $LP_{02}$, $LP_{03}$ and $LP_{04}$. It can also be observed from Fig. 3.5.c that

at the end of second annealing, $LP_{04}$ was associated with more power than $LP_{03}$. The peak loss of the $LP_{03}$ cladding mode decreased from 13.16 to 12.0 dB, and that of the $LP_{04}$ cladding mode increased from 11.77 to 14.39 dB. We reduced the duration of second annealing because; hydrogen diffuses faster with increase in temperature.

## 3.5 The effect of temperature variations on the transmission spectrum of LPG

To study the response of the LPG with temperature variations, we used the same experimental set-up as shown in Fig. 3.4. The grating period of LPG selected for this study was 415 μm and we properly annealed the LPG (SMF-28 fiber) before starting the experiments. The initial spectrum was recorded at the room temperature (25◦C) using the optical spectrum analyzer. The LPG was then heated from 50°C to 100°C in steps of 10°C using the temperature controller of fiber oven. During this process, the transmission spectra were recorded using the optical spectrum analyzer. After each step increase of the temperature, sufficient time was given so that the oven shows a stable reading at the desired temperature. All readings were taken with air as the surrounding medium. Figures 3.6 and 3.7 show the wavelength shifts experienced by the different cladding modes of LPG with temperature changes. We observed a spectral shift to longer wavelengths (red shift) with increasing temperature and the wavelength shift of the peaks were linear as shown in Fig. 3.8. The $LP_{02}$, $LP_{03}$, $LP_{04}$, $LP_{05}$ and $LP_{06}$ cladding modes experienced red shifts of 3.58, 2.39, 3.58, 2.78, 4.37 nm respectively when the temperature was enhanced up to 100°C. It can be seen that different resonant peaks have different temperature sensitivities and the highest order cladding mode $LP_{06}$ was most sensitive to external temperature changes with a sensitivity of about 0.06 nm/ °C. The lower order cladding mode $LP_{02}$ displayed a sensitivity of about 0.05 nm/ °C. These results show that the lower order bands can also be as sensitive to temperature changes as higher order bands.

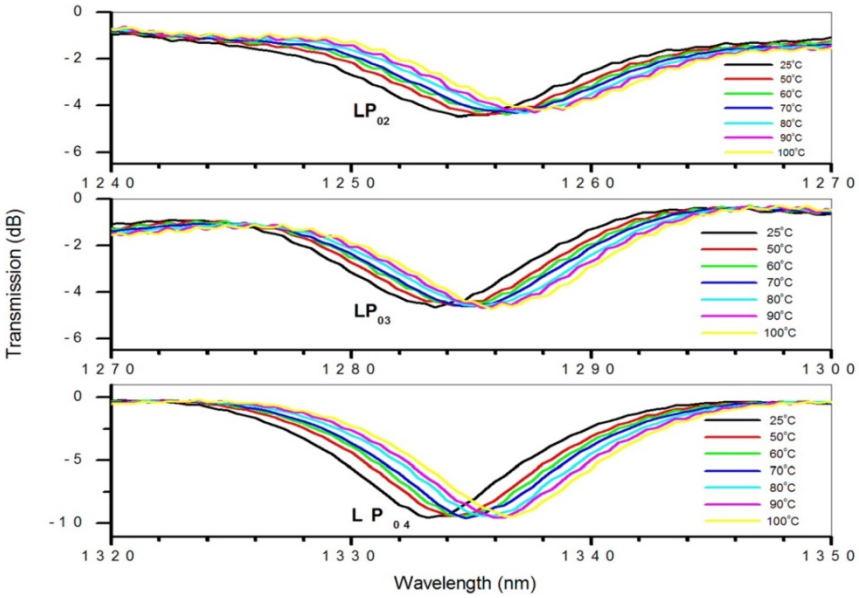


***Figure 3.6:*** *Evolution of the peak wavelengths of $LP_{02}$, $LP_{03}$ and $LP_{04}$ cladding modes of LPG (SMF-28 fiber) as a function of temperature.*

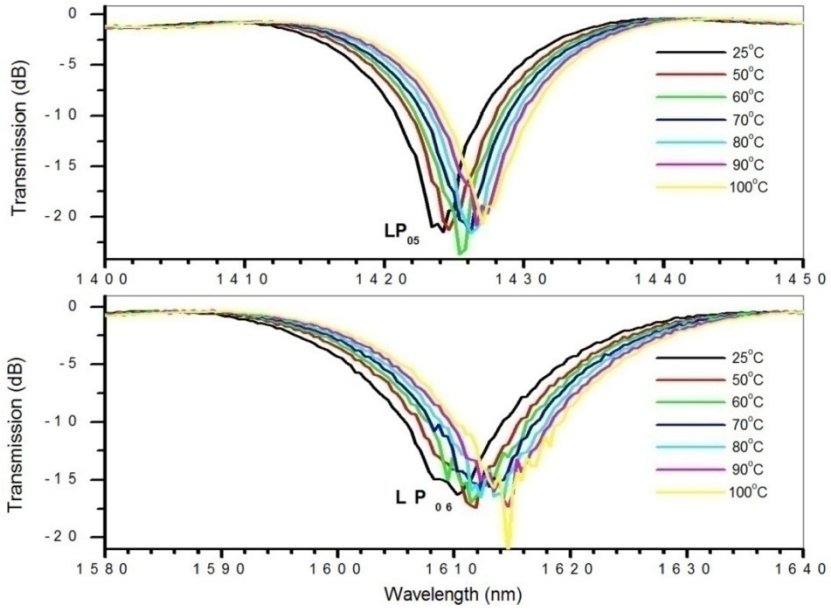


***Figure 3.7:*** *Evolution of the peak wavelengths of $LP_{05}$ and $LP_{06}$ cladding modes of LPG (SMF-28 fiber) as a function of temperature.*

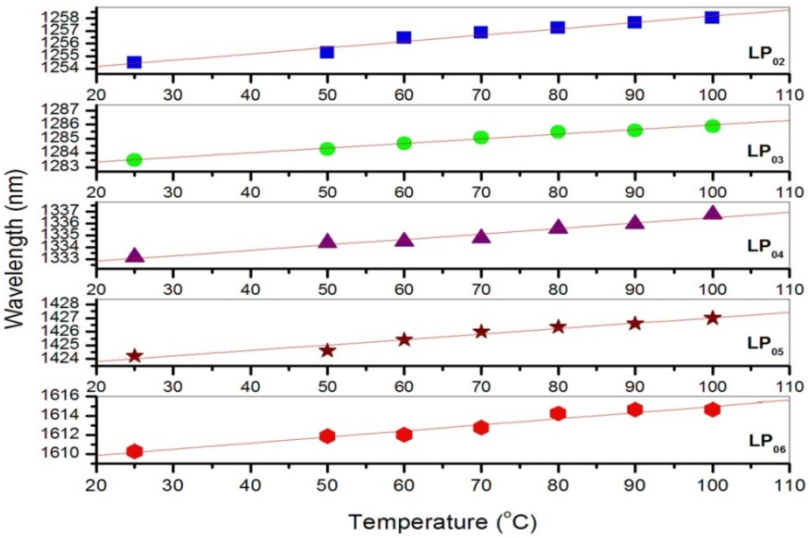


***Figure 3.8:*** *Temperature induced positive wavelength shifts of $LP_{02}$, $LP_{03}$, $LP_{04}$, $LP_{05}$ and $LP_{06}$ attenuation bands of LPG written in SMF-28 fiber.*

## 3.6 Thermal response of LPGs written in $H_2$ loaded SMF-28 and B-Ge co doped photosensitive fiber

The sensitivity of LPGs to temperature is influenced by the grating period [12], the order of the cladding mode to which coupling takes place [12,13] and by the composition of the optical fiber [14,15]. Shu *et al*. [14] derived an equation for the temperature sensitivity of the resonance wavelengths of LPGs and is explained in chapter 2 (Eq. 2.34).

An LPG with grating period of 435 μm was written in a photosensitive B-Ge co-doped fiber (F-SBG-15, Newport). This LPG was also heated from 50°C to 100°C in steps of 10°C using the temperature controller of fiber oven. The spectral shift of the LPG with increase in temperature is shown in Fig. 3.9 and 3.10. In this case the $LP_{04}$, $LP_{05}$ and $LP_{06}$ cladding modes experienced blue shifts of 3.30, 3.30, 5.44 nm respectively and $LP_{06}$ mode showed a sensitivity of about 0.07 nm/ °C. The difference in temperature sensitivity between the SMF-28 and B-Ge fibers can be explained on the basis of the thermo-optic coefficients of the core and the

cladding materials [2,14,16,17]. The presence of boron alters the temperature dependence of the refractive index. The difference in thermo-optic coefficients for the B/Ge fiber is higher than that of $SiO_2$, so that the sensitivity is also higher.

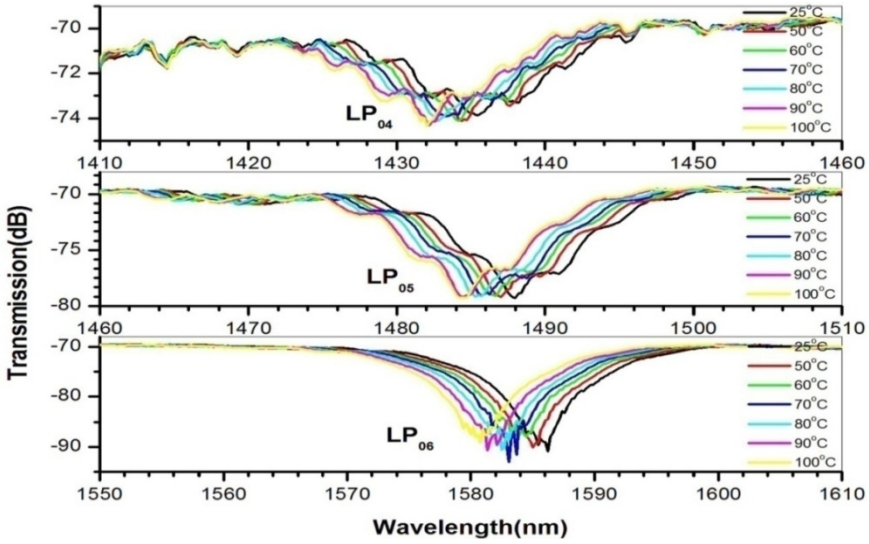


***Figure 3.9:*** *Evolution of the peak wavelengths of $LP_{04}$, $LP_{05}$ and $LP_{06}$ cladding modes of* B-Ge co-doped fiber *LPG as a function of temperature.*

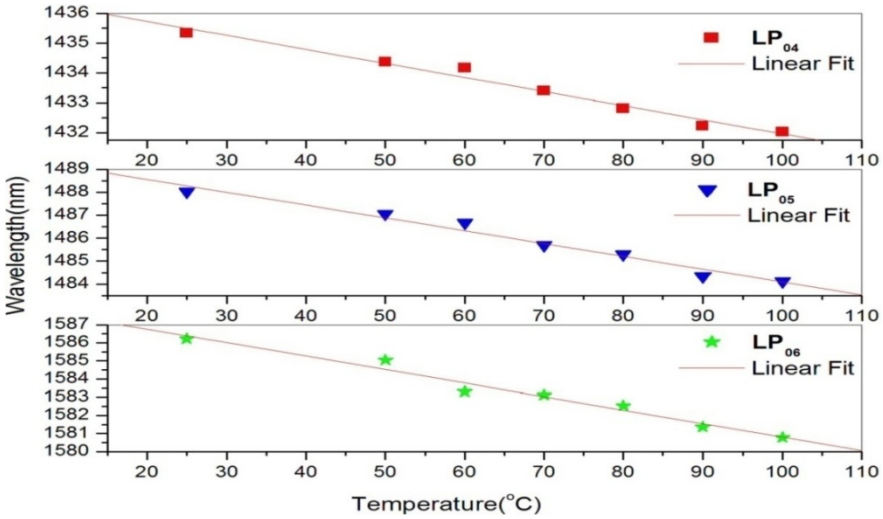


***Figure 3.10:*** *Temperature induced negetive wavelength shifts of $LP_{04}$, $LP_{05}$ and $LP_{06}$ attenuation bands of LPG written in B-Ge doped photosensitive fiber.*

The direction of attenuation band shift with temperature depends on the relative magnitudes of the core and cladding thermo-optic coefficients [14,18]. The thermo optic coefficient of the core depends on the concentration of the dopants in silica. $GeO_2$ has a larger thermo optic coefficient than that of $SiO_2$, whereas $B_2O_3$ has a negative thermo optic coefficient. In the case of standard fiber, the core contains $SiO_2$ and $GeO_2$ and the cladding contains only $SiO_2$. So the thermo optic coefficient of the core will be higher than that of the cladding ($\xi_{co} n_{co}^{eff} > \xi_{cl} n_{cl,m}^{eff}$). As a result when the temperature increases, these fibers will show a wavelength shift towards longer wavelengths [14,19]. On the other hand, the boron co-doped fibers will show a wavelength shift towards shorter wavelengths due to the negative thermo optic coefficient of the boron dopant ($\xi_{co} n_{co}^{eff} < \xi_{cl} n_{cl,m}^{eff}$ and $\Gamma < 0$) [14,18,20]. Thus, it is to be expected that the thermal responses of LPFGs produced in different fiber types will exhibit different trends.

## 3.7 Sensitivity of the LPG to Ambient Refractive Index Changes

LPG with grating length of 21 mm and grating period of 420 μm was selected for the experimental testing. The LPG was written in a B-Ge co-doped photosensitive fiber fabricated in CGCRI using a 248 nm KrF excimer laser source and employing point-by-point writing method. There was no protective coating in the grating section, so that the external RI could easily affect the effective refractive index of the cladding modes. The experimental set up to study the sample refractive index performance is shown in Fig. 3.11. A white-light source ([Yokogawa] AQ 4305) was used as the light source and the transmission spectrum of the LPG was interrogated with an optical spectrum analyzer ([Yokogawa] AQ 6319). The LPG sensor head was fixed in a specially designed glass cell with provision for filling the sample and draining it out when desired. The fiber containing the LPG element was connected to the light source on one side and to the OSA on the other side.

Drastic changes in performance of the LPG were noted when there were changes in external characteristics like strain, temperature and bending. To avoid the effect of strain and bending, a glass cell holder was designed and the fiber was placed stretched and bonded with epoxy at both the end points of the cell so that the grating section was kept at the centre of the cell. For precise measurement, the experimental setup and sample solution temperature were maintained at 25.0 ± 0.5 °C. The resonance wavelength shift and amplitude changes of the LPG attenuation dip were measured with the fiber section containing the LPG immersed in samples of different refractive indices.

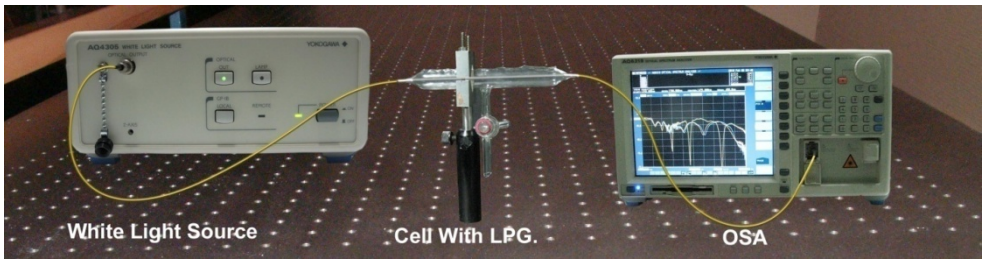


***Figure 3.11:*** *Experimental setup.*

Sensor responded to RI changes as soon as samples were introduced to the glass cell. But, to get a stabilized output, all readings were taken one minute after the LPG was immersed in the solution. An Abbe refractometer was employed to measure the sample refractive indices, just after the sample was drained out from the glass cell. The initial spectrum of the LPG in air (Fig.3.12) was used as reference spectrum for all the sample analysis. The use of this reference spectrum serves two purposes: 1) to remove any trace of each sample between two different measurements 2) to assure that the LPG attenuation dip returns to the original wavelength after each sample measurement. At the end of each sample measurement, the grating was cleaned with isopropyl alcohol repeatedly, followed by drying properly, so that the original transmission spectrum of LPG was obtained. The drying of the LPG was done using a hair dryer.

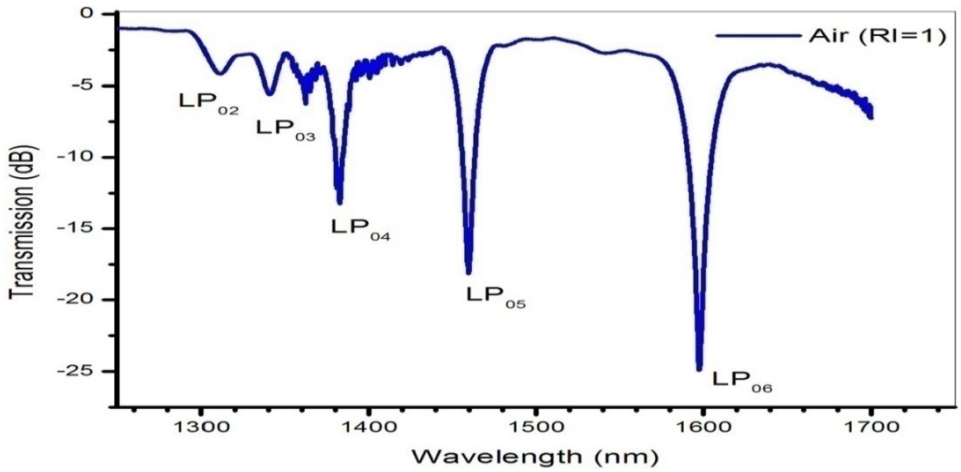


***Figure 3.12:*** *Transmission spectrum of LPG with a periodicity of 420* μm *in air.*

The changes of the LPG transmission spectrum with the changes in the RI of the external medium are shown in Fig. 3.13. Attenuation bands in the range of 1250– 1700 nm related to the cladding modes $LP_{02}$, $LP_{03}$, $LP_{04}$, $LP_{05}$ and $LP_{06}$ have been investigated. When we changed the SRI from 1 to 1.4540, the principal effect was a blue shift of these attenuation bands, as discussed in the theory section of chapter 2. Each mode exhibited maximum wavelength shift when the SRI came close to the RI of cladding. The higher order cladding modes, $LP_{05}$ and $LP_{06}$ exhibited longer displacements compared to lower order modes. The $LP_{06}$ mode was most sensitive to the surrounding refractive index changes and exhibited a blue shift of approximately 128nm. This shift is comparatively higher compared to reported values [21-23].

When the value of the ambient refractive index matches with that of the cladding (1.4560), the cladding layer acts as an infinitely extended medium and thus supports no discrete cladding modes. In this case, a broadband radiation mode coupling occurs with no distinct attenuation bands [24]. To be precise, at an external RI equal to that of the cladding, rejection bands disappear, and the transmission spectrum gets flattened, as shown in Fig.3.14. With an ambient index

higher than that of the cladding, the resonance peaks reappeared at a wavelength slightly longer than that measured in air and the strength of the attenuation peaks increased with increasing SRI. As shown in figures 3.15 and 3.16 an abrupt change in the spectral characteristics was observed from SRI 1.4560 to 1.4580. Figure 3.16 shows the wavelength shift of the $LP_{06}$ resonance band with external medium refractive index changes in the range 1 to 1.6. These measurements were carried out using liquids of known refractive indices.

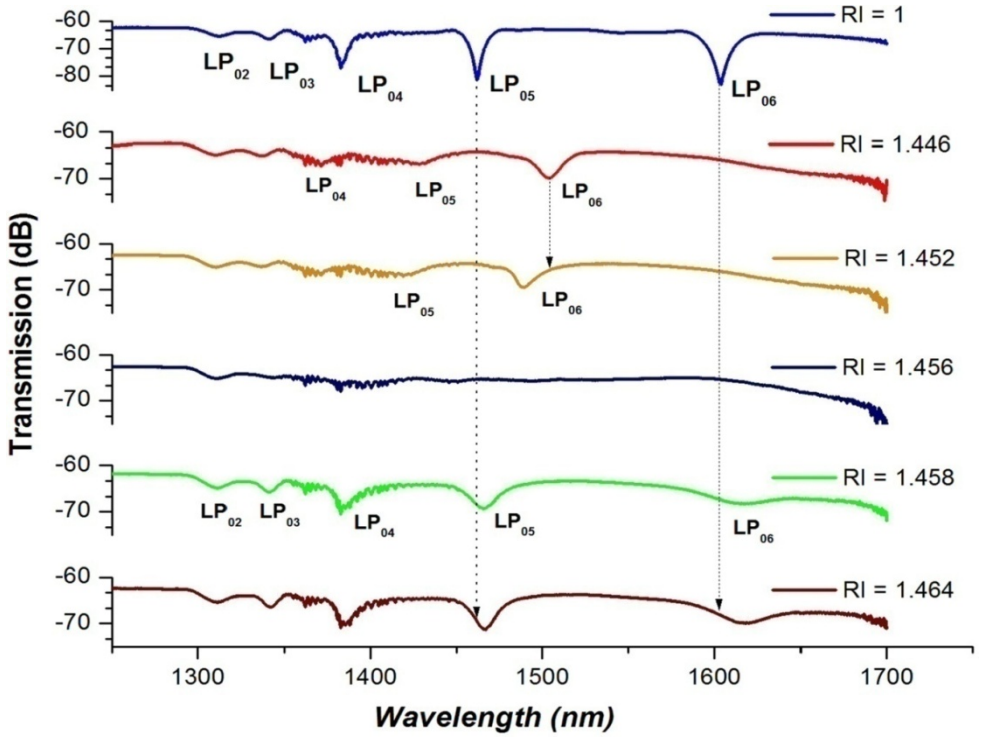


***Figure 3.13:*** *Progression of transmission spectra of the LPG for increasing external refractive indices.*

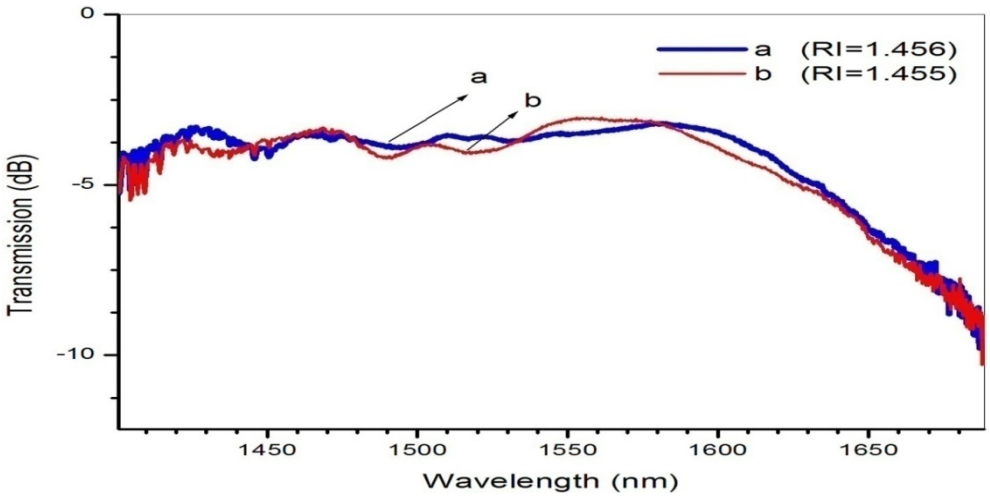


***Figure 3.14:*** *Transmission spectrum of LPG with* $n_{sur} \cong n_{clad}$

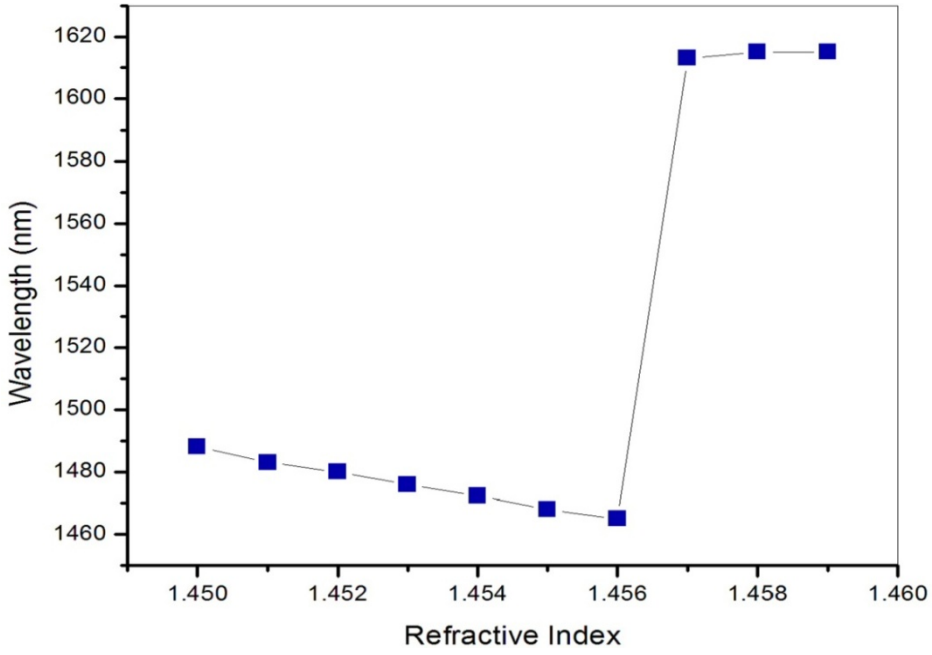


***Figure 3.15:*** *Plot of the wavelength shift versus the SRI near the cladding RI for the* $LP_{06}$ *mode of LPG.*

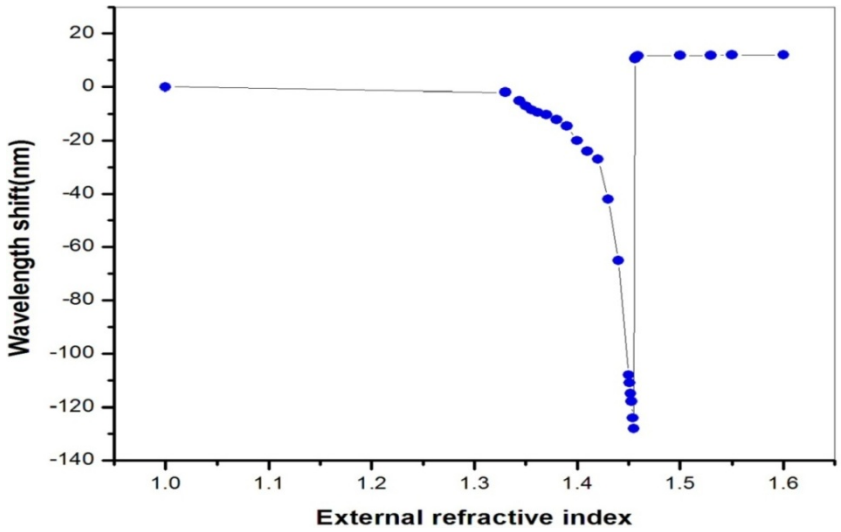


***Figure 3.16:*** *Wavelength shift of $LP_{06}$ mode for SRI ranging from 1.000 to 1.600.*

## 3.8 The Effect of Grating Period on Refractive Index Sensitivity of Long Period Gratings

In this section, the influence of grating period of LPG on refractive index sensitivity is experimentally investigated. Figures 3.17 and 3.18 show the transmission spectra of three LPGs, i.e.LPG-1,LPG-2 and LPG-3, with grating periods of 550 μm, 415 μm and 400 μm, respectively with air as the surrounding medium. These LPGs were written in standard single-mode fiber (SMF-28e, Corning). Attenuation bands in the range of 1200– 1700 nm related to the cladding modes of these three LPGs have been investigated. For LPG-1, power coupling to cladding modes $LP_{02}$, $LP_{03}$ and $LP_{04}$ are seen to occur at 1451,1497,1588 nm respectively. LPG-2 exhibited five resonance bands at 1254($LP_{02}$), 1284($LP_{03}$), 1333($LP_{04}$), 1423($LP_{05}$), 1610($LP_{06}$) nm respectively. LPG-3 also exhibited five resonance bands at 1222($LP_{02}$), 1249($LP_{03}$), 1294($LP_{04}$), 1375($LP_{05}$), 1534($LP_{06}$) nm respectively. When the grating period became shorter, the resonant loss peaks of the low order cladding modes appeared spectrally closer to each other and also collectively moved to the blue wavelength side [21].

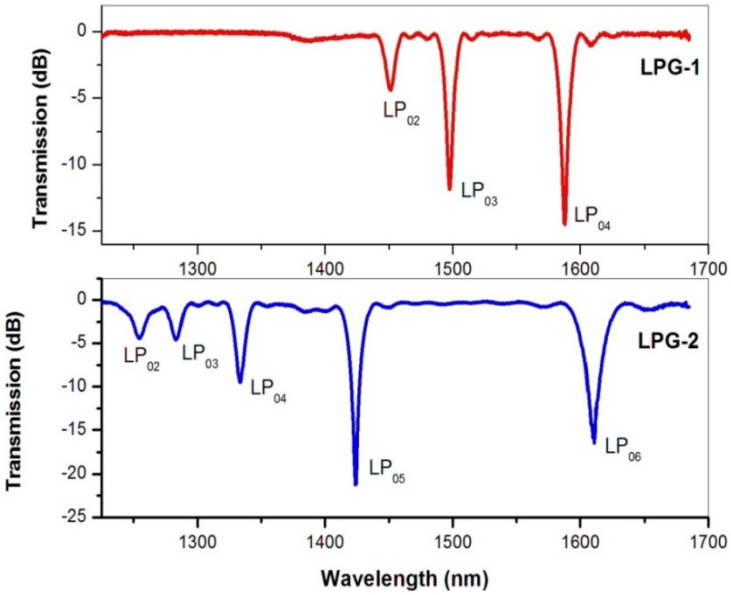


***Figure 3.17:*** *Transmission spectra of LPG-1 with a grating period of 550* μm and *LPG-2 with a grating period of 415* μm.

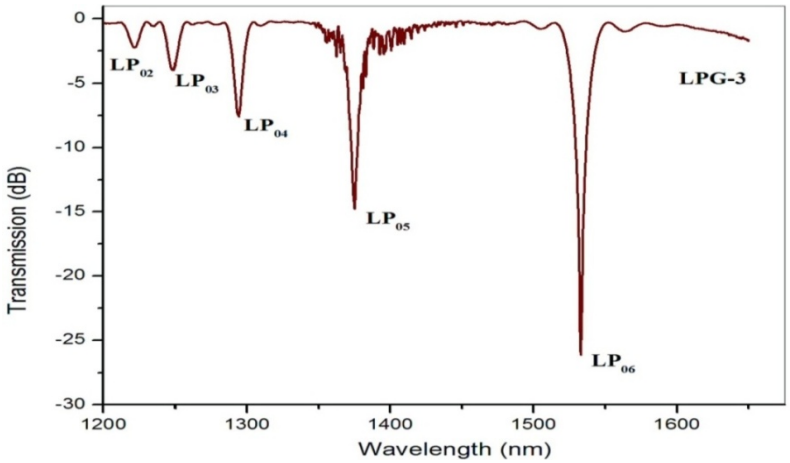


***Figure 3.18:*** *Transmission spectra of LPG-3 with a grating period of 400* μm.

### 3.8.1 Sensitivity of the LPG to Ambient Refractive Index Changes Lower than the Cladding Refractive Index.

The changes of the LPG transmission spectra with the changes in the RI of the external medium are shown in Figures 3.19, 3.20 and 3.21. When we changed

the SRI from 1 to 1.454, a shift of the resonance bands towards the shorter wavelength (blue shift) side can be seen, as discussed in the theory [12,14,21,22]. We found that highest order attenuation bands exhibited high sensitivity and longer displacements compared to lower order cladding modes. This wavelength shift occurs because of increasing SRI which in turn increases $n_{eff,m}^{cl}$, particularly for the higher order cladding modes which extend further into the external medium [23,25]. As the grating period decreases, the number of higher order modes increases leading to better sensitivity. For LPG-1 the highest order cladding mode is $LP_{04}$ and for LPG-2 and LPG-3 the highest order cladding mode is $LP_{06}$. The highest RI sensitivity of LPGs is observed when the external medium index is close to that of the cladding. Figures 3.22, 3.23 and 3.24 show the wavelength shifts experienced by resonances of the highest observed cladding modes for each LPG, when the external refractive index changes. For LPG-1, $LP_{04}$ exhibited a total blue shift of approximately 21.20 nm when the SRI was gradually changed from 1 to 1.45. For LPG-2 and LPG-3 the highest order cladding mode, $LP_{06}$ exhibited a total blue shift of approximately 102.30 nm and 127 nm respectively in the same RI range.

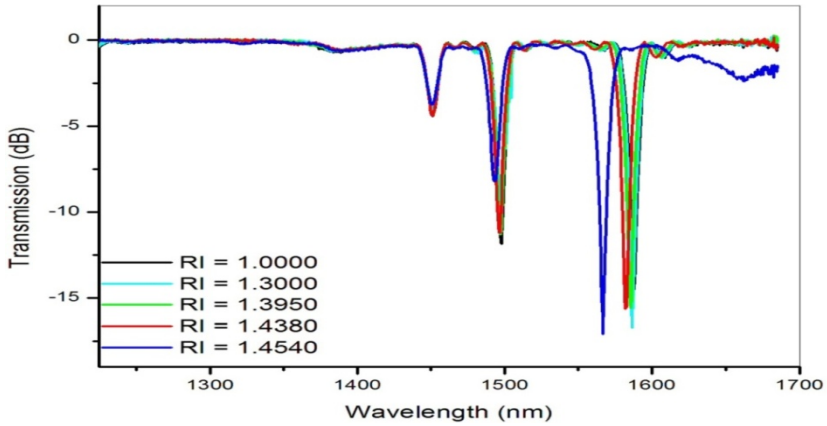


***Figure 3.19:*** *Transmission spectrum of LPG-1 with a periodicity of* 550 μm *for different ambient refractive indices, lower than that of fiber cladding.*

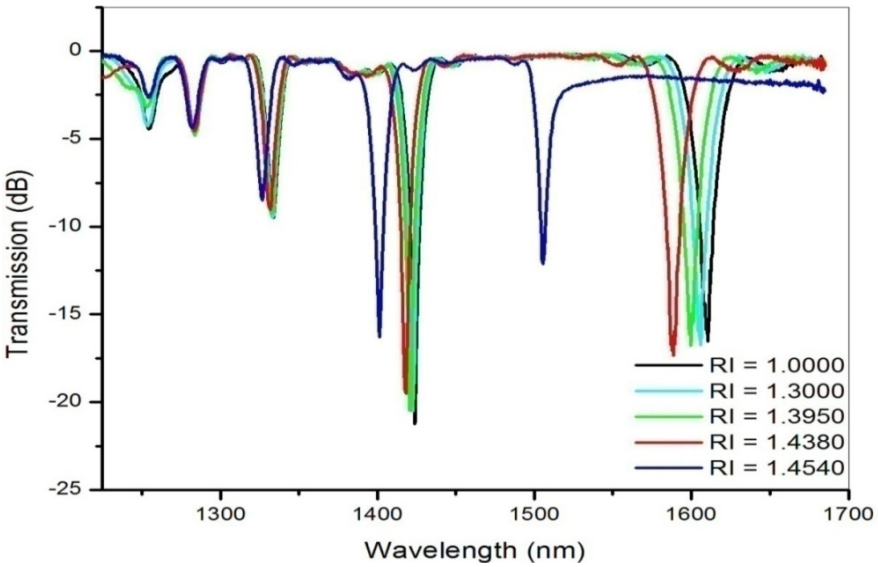


***Figure 3.20:*** *Transmission spectrum of LPG-2 with a periodicity of 415* μm *for different ambient refractive indices, lower than that of fiber cladding.*

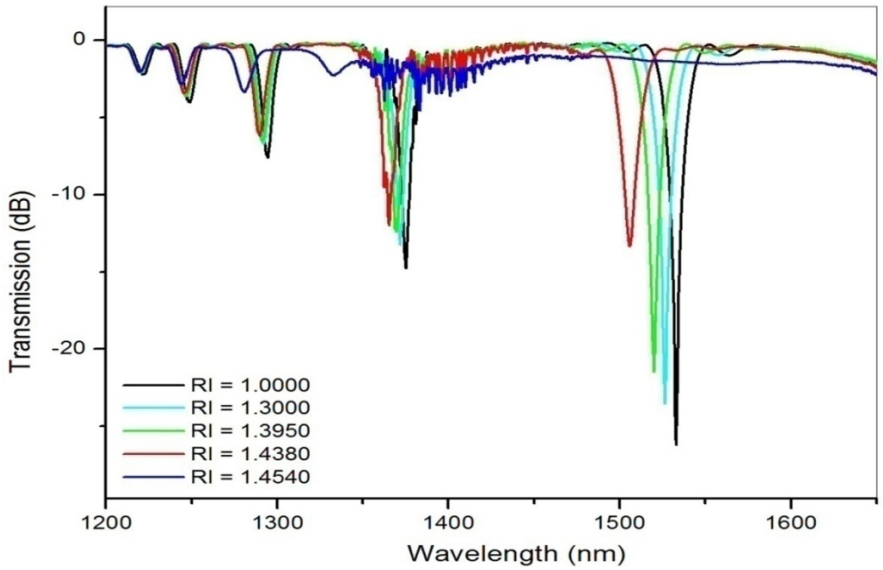


***Figure 3.21:*** *Transmission spectrum of LPG-3 with a periodicity of 400 μm for different ambient refractive indices, lower than that of fiber cladding.*

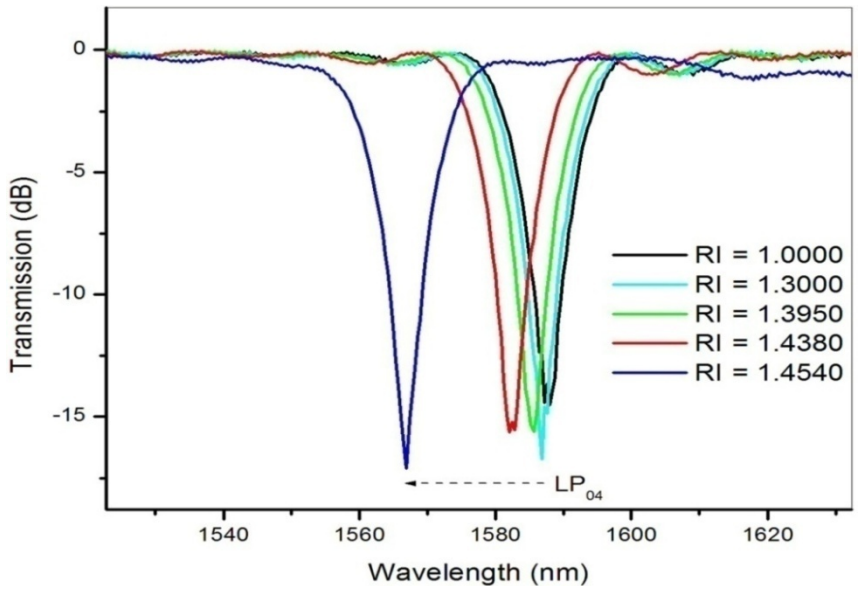


***Figure 3.22:*** *Transmission spectra of highest* order cladding mode (*$LP_{04}$*) of *LPG-1 for different ambient refractive indices, lower than that of fiber cladding.*

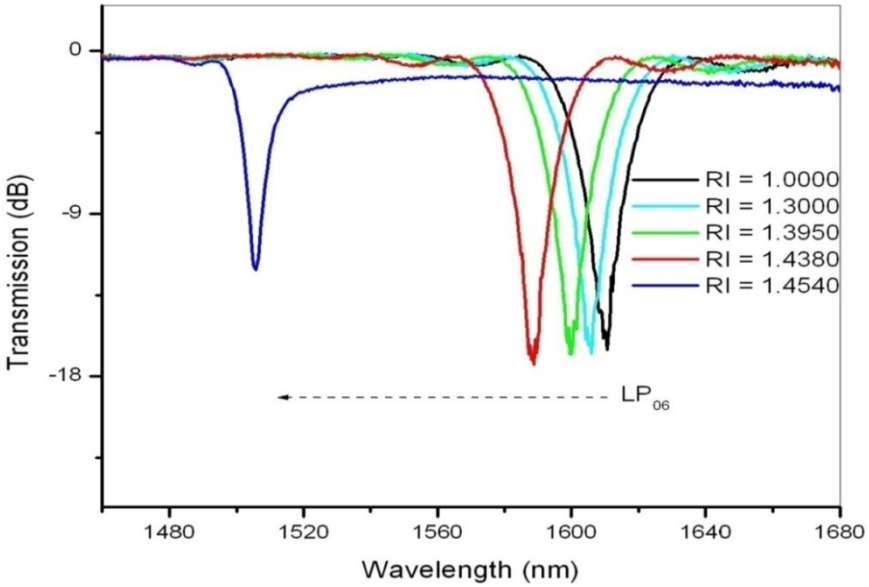


***Figure 3.23:*** *Transmission spectra of highest* order cladding mode (*$LP_{06}$*) of *LPG-2 for different ambient refractive indices, lower than that of fiber cladding.*

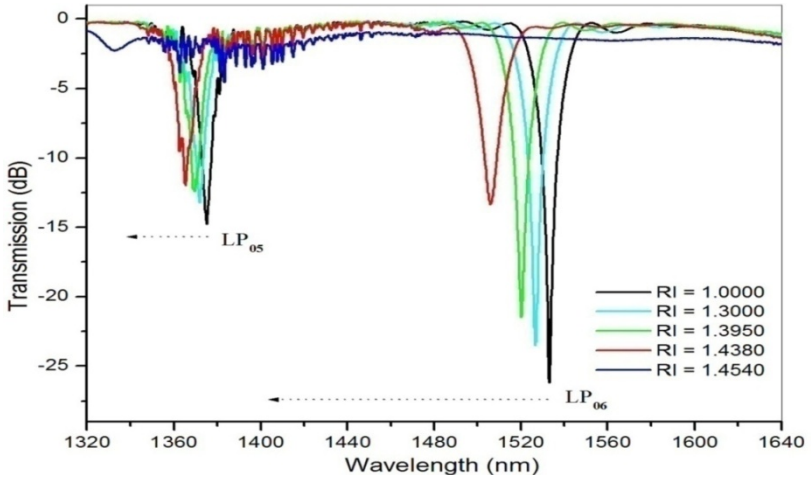


***Figure 3.24:*** *Transmission spectra of highest* order cladding modes (*$LP_{06}$ and $LP_{05}$)* of *LPG-3 for different ambient refractive indices, lower than that of fiber cladding.*

Table 3.1 shows the wavelength shift of the highest order modes of the LPGs with reference to air as the surrounding medium.

***Table 3.1:*** *Wavelength shift (blue shift) of the different modes of the LPGs with respect to air (RI=1) as the surrounding medium.*

| **Sample RI** | **$LP_{06}$ of LPG-3(nm)** | **$LP_{06}$ of LPG-2(nm)** | **$LP_{04}$ of LPG-1(nm)** |
|---|---|---|---|
| 1.3000 | 6.66 | 4.78 | 1.19 |
| 1.3950 | 13.11 | 10.75 | 2.38 |
| 1.4380 | 27.40 | 21.87 | 5.97 |
| 1.4540 | 127.00 | 102.30 | 21.07 |
| **Sample RI** | **$LP_{05}$ of LPG-3(nm)** | **$LP_{05}$ of LPG-2(nm)** | **$LP_{03}$ of LPG-1(nm)** |
| 1.3000 | 3.33 | 1.2 | 0.80 |
| 1.3950 | 5.68 | 2.8 | 0.95 |
| 1.4380 | 9.78 | 5.56 | 1.2 |
| 1.4540 | 52.21 | 22.65 | 4.77 |
| **Sample RI** | **$LP_{04}$ of LPG-3(nm)** | **$LP_{04}$ of LPG-2(nm)** | **$LP_{02}$ of LPG-1(nm)** |
| 1.3000 | 2.54 | 0.39 | 0.01 |
| 1.3950 | 3.2 | 1.59 | 0.03 |
| 1.4380 | 4.69 | 1.98 | 0.04 |
| 1.4540 | 13.5 | 7.15 | 1.2 |

The measured wavelength shifts varied by approximately six times depending on grating period, with the highest order band in the LPG-3 shifting 127 nm while that in LPG-1 by only 21.07 nm. The results obtained show that the shorter period LPG-3 was found to be more sensitive than the longer period LPG-1, when the RI of the surrounding medium was lower than the RI of the cladding of the fiber. It is also verified that the sensitivity of the highest order mode is very high compared to lower order modes. The wavelength shift experienced by the highest order attenuation bands of the LPGs are shown in Fig. 3.25.

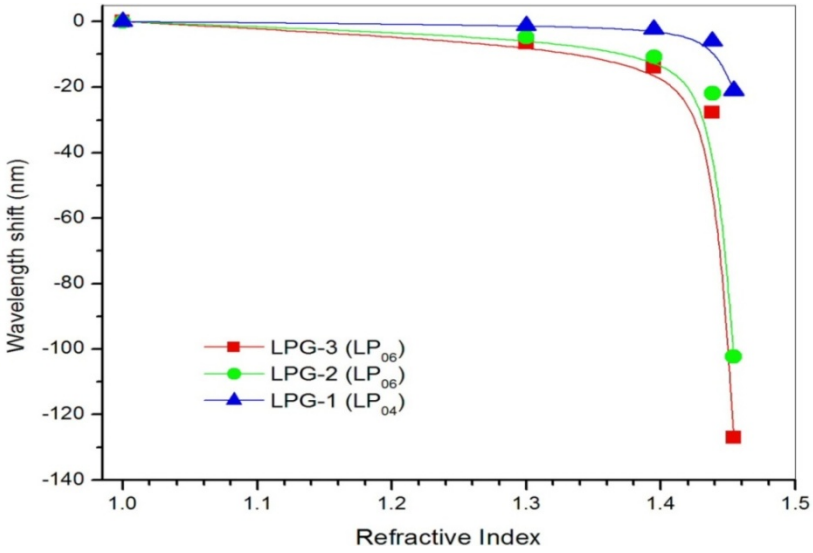


***Figure 3.25:*** *Peak shift of the major attenuation bands in the transmission spectrum of LPG-1 (550 μm), LPG-2 (415 μm) and LPG-3 (400 μm) as a function of the refractive index of the external medium.*

### 3.8.2 Sensitivity of the LPG to ambient refractive indices higher than the cladding refractive index.

When the ambient index is higher than that of the cladding (1.456), the resonance peaks of all the LPGs reappeared at a wavelength slightly longer than that measured in air and the strength of the attenuation peaks increased with increasing SRI (Figures 3.26 ,3.27 and 3.28).

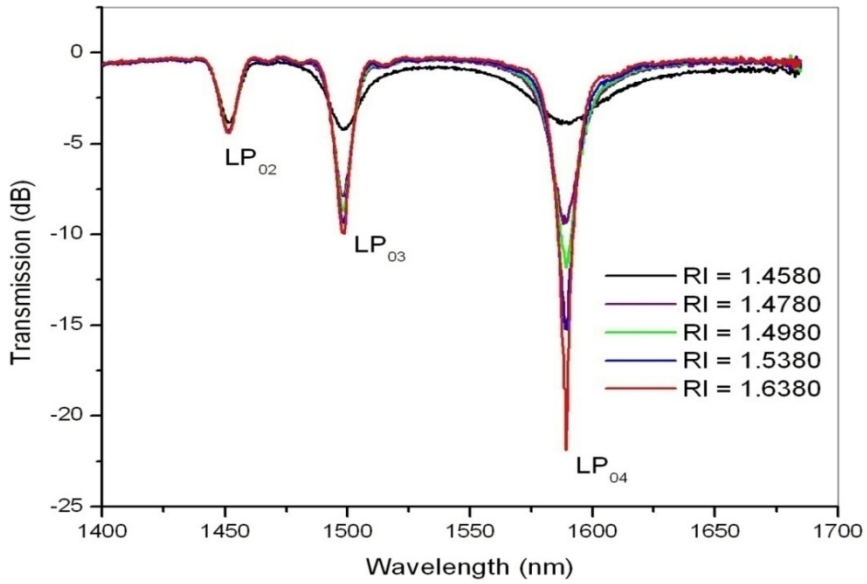


***Figure 3.26:*** *Transmission spectrum of the LPG-1 with a periodicity of 550* μm *for different ambient refractive indices, higher than that of fiber cladding.*

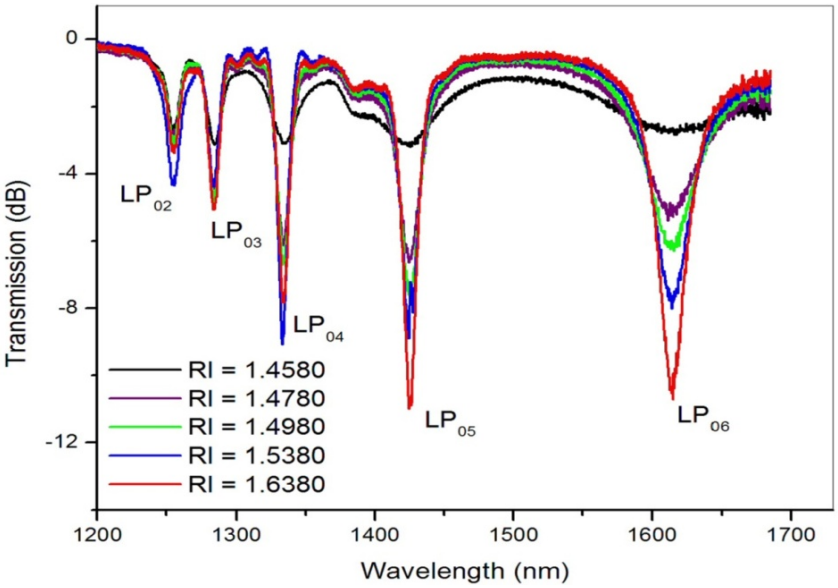


***Figure 3.27:*** *Transmission spectrum of the LPG-2 with a periodicity of* 415 μm *for different ambient refractive indices, higher than that of fiber cladding.*

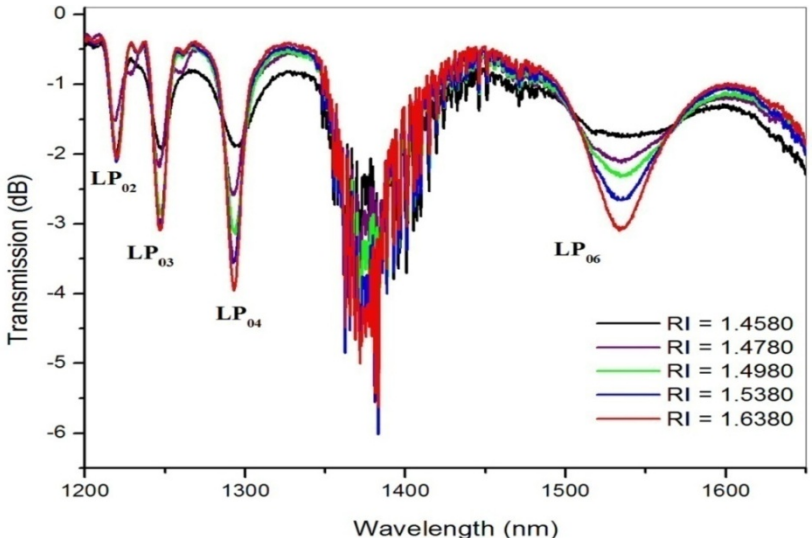


***Figure 3.28:*** *Transmission spectrum of the LPG-3 with a periodicity of* 400 μm *for different ambient refractive indices, higher than that of fiber cladding.*

Progression of transmission spectra of the highest order cladding modes of LPGs, corresponding to the external refractive index changes are shown in figures 3.29, 3.30 and 3.31. Measurement of the transmitted signal intensity in a chosen spectral interval was used for our analysis since all the used samples were with refractive indices higher than the refractive index of the fiber cladding. The LPGs exhibited negligible wavelength shift in this case [26-28]. So no analysis was conducted for the wavelength shift. However there is a change in the transmission intensity with external RI changes which has been utilized for sensitivity measurements. The transmission dip changes experienced by the highest order cladding modes of LPGs, corresponding to the external refractive index changes are shown in Fig. 3.32. The depth of the attenuation peak steadily increased with increase in refractive index of the surrounding medium, owing to larger Fresnel reflection coefficients that yield improved reflection at the cladding boundary [24, 28]. An intensity change of 17.81 dB was obtained for the $LP_{04}$ mode of LPG-1, in the refractive index range 1.4580 to 1.6380, which

corresponds to an average resolution of 1.01 x $10^{-2}$ $dB^{-1}$. In the case of LPG-2, an intensity change of 7.81 dB was obtained for the $LP_{06}$ mode in the same refractive index range, which corresponds to an average resolution of 2.30 x $10^{-2}$ $dB^{-1}$. In the case of LPG-3, for the same refractive index range, an intensity change of 1.32 dB was obtained for $LP_{06}$ mode which corresponds to an average resolution of 13.63 x $10^{-2}$ $dB^{-1}$. The results obtained show that the longer period LPG-1 (550 μm) was found to be more sensitive than the shorter period LPG-2 (415 μm ) and LPG-3 (400 μm), when the RI of the surrounding medium was higher than the RI of the cladding of the fiber.

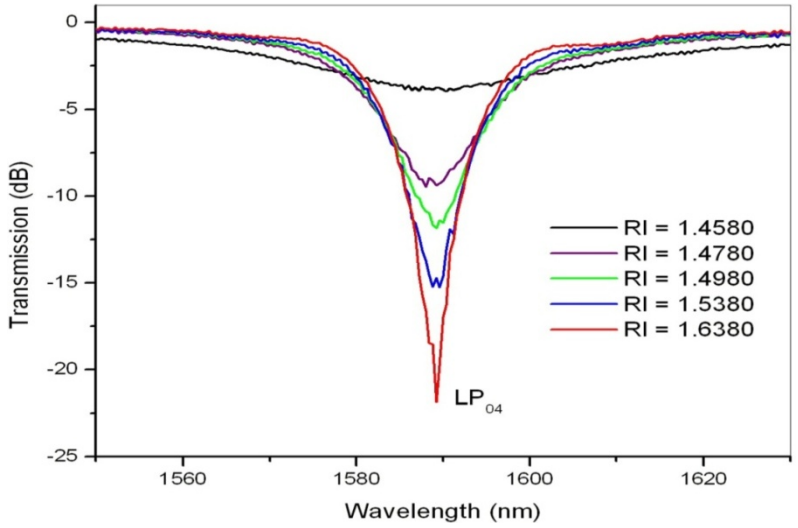


***Figure 3.29:*** *Progression of transmission spectra of* $LP_{04}$ mode of *LPG-1 for increasing external refractive indices higher than that of cladding index.*

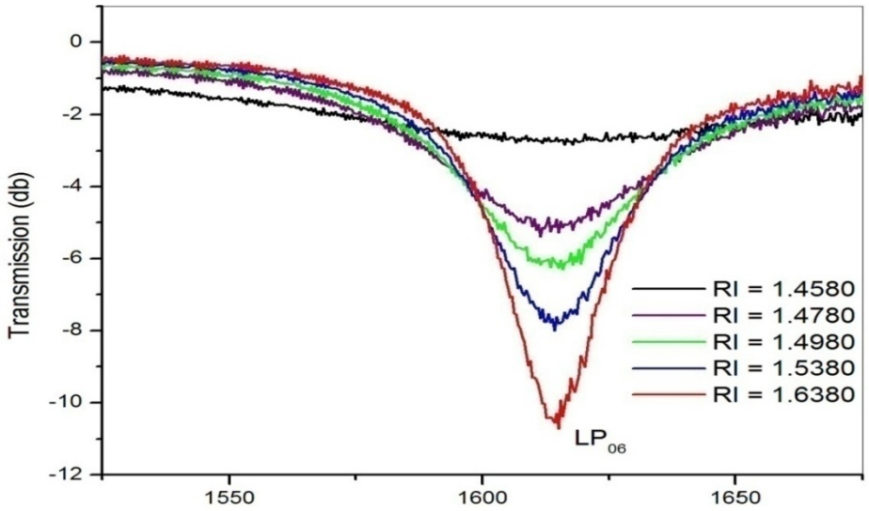


***Figure 3.30:*** *Progression of transmission spectra of* $LP_{06}$ mode of *LPG-2 for increasing external refractive indices higher than that of cladding index.*

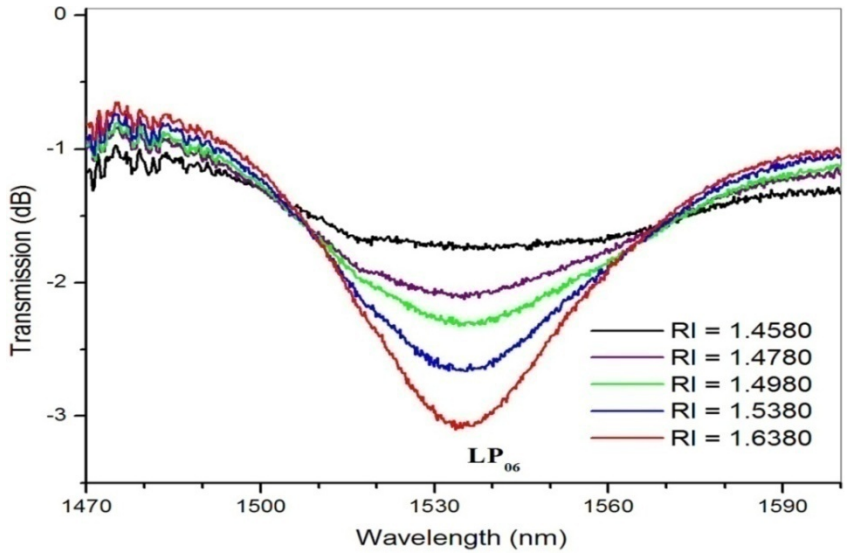


***Figure 3.31:*** *Progression of transmission spectra of* $LP_{06}$ mode of *LPG-3 for increasing external refractive indices higher than that of cladding index.*

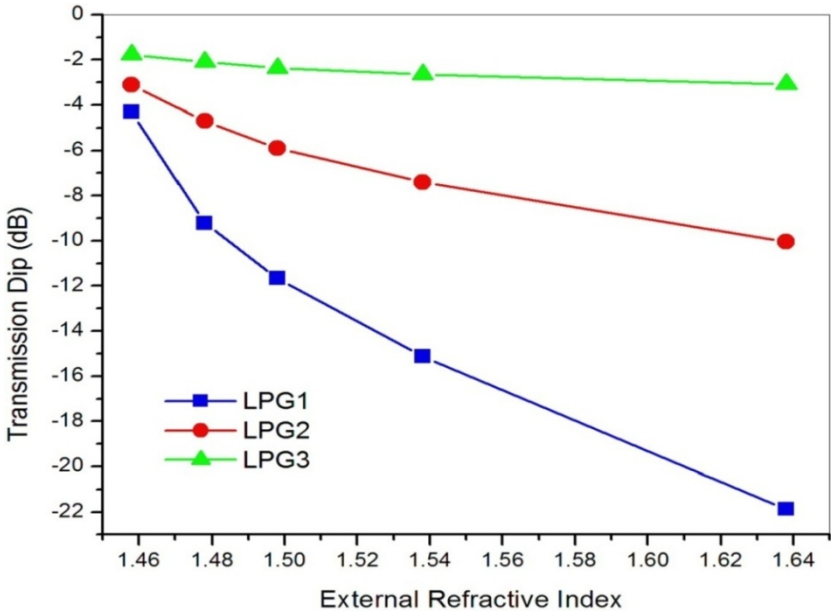


***Figure 3.32:*** *Transmission spectral intensity changes of the highest order cladding modes of* LPG-1 (550 μm), LPG-2 (415 μm) and LPG-3 (400 μm) *in response to external medium refractive index.*

## 3.9 Demonstration of LPG as a chemical sensor

Here a glucose concentration sensor is demonstrated by exploiting the sensitivity of LPGs to the concentration of the solution under test. Glucose, which is a basic necessity of many organisms, is a complicated molecule having the ability to adapt several different structures. All forms of glucose are colorless and is soluble in water. The glucose concentration measurement is of great interest in a variety of applications, including pharmaceutical, biomedical research, food processing and industrial chemistry.

A RI variation occurs with change in glucose concentration levels. Such changes cause corresponding shifts in the resonance wavelength and change in depth (amplitude) of the loss bands in the LPG transmission spectrum [29-32]. Glucose levels can be detected by analyzing these spectral changes.

### 3.9.1 Experimental Setup

LPG with grating length of 21 mm and grating period of 420 μm was selected for the experimental investigation and we used the same experimental set up as shown in Fig. 3.11. Experiments were carried out using glucose samples with concentrations of 5, 10, 15, 20, 25 and 30 g per 100 ml of distilled water. The weighing of the glucose was done using an electronic balance (BEL M120 A) with a precision of ± 0.1 mg. Sensor responded to RI changes as soon as samples were introduced in the glass cell. But, to get a stabilized output, all readings were taken one minute after the LPG was immersed in the solution. An Abbe refractometer was employed to measure the sample refractive indices, just after the sample was drained out from the glass cell. The refractive indices of the samples varied from 1.3376 to 1.3661. The initial spectrum of the LPG in air was used as reference spectrum for all the sample analysis. At the end of each sample measurement, the sensor element was cleaned with isopropyl alcohol repeatedly, followed by drying properly, so that the original transmission spectrum of LPG was obtained.

### 3.9.2 Results and discussion

The dependence of the sensor sensitivity on glucose concentration levels in terms of the LPG resonance wavelength shift has been analyzed while the samples, obtained by mixing glucose with distilled water in different proportions, were in contact with the grating. For the grating used in our studies the strongest attenuation peak ($LP_{06}$) in air, is located at 1602 nm. Figure 3.33 shows the changes in the wavelength and amplitude corresponding to this major attenuation dip, with increasing concentration of glucose. The refractive indices of the mixture of different samples used in this experiment were less than the refractive index of the cladding. For RI values lower than that of the cladding, LPG sensitivity to increasing external index of refraction is evident as a blue shift in the central wavelength of the attenuation band in the grating's transmission spectrum.

The LPG exhibited a total blue shift of approximately 5.7 nm when the surrounding medium was gradually changed from pure distilled water to 100 ml of distilled water containing 30 gram of glucose. This spectral shift of 5.7 nm was obtained in the refractive index range 1.3376 to 1.3661, which corresponds to an average resolution of 5 x $10^{-3}$ $nm^{-1}$. Apart from the wavelength shift with the changes in refractive index of the external medium, there was a reduction in the peak intensity of the resonance band with increasing glucose concentration. The sensitivity of the LPG, when used as a sensor for various weight percentage of glucose in distilled water is shown in Fig.3.34. The LPG sensor sensitivity was around 0.19 nm/wt.% of glucose in the measurement range. In this case, the LPG showed low sensitivity because the value of SRI was very much lower than the cladding index of the fiber (1.456).

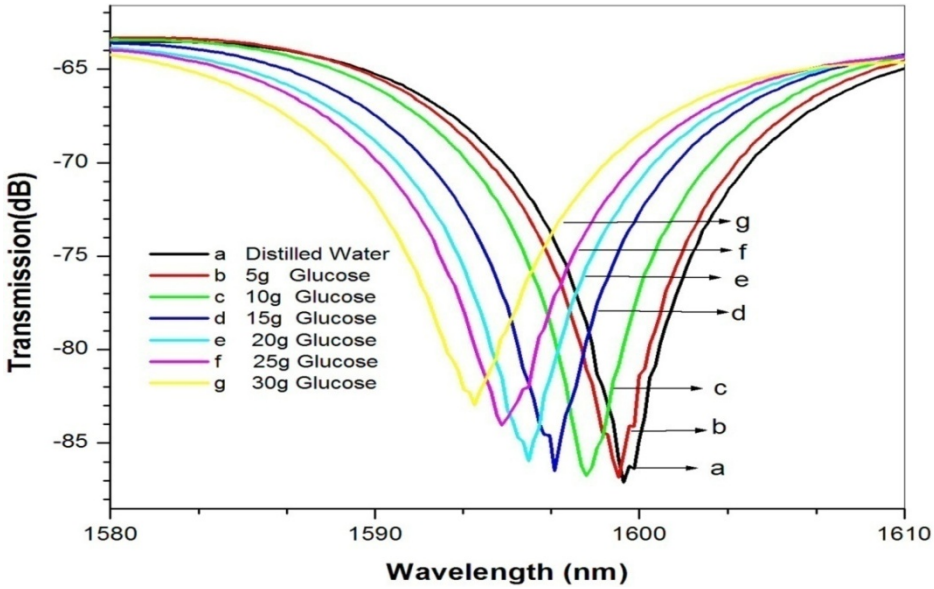


***Figure 3.33:*** *Transmission spectra of the LPG with a grating period of* 420 μm *for various concentrations of glucose in distilled water.*

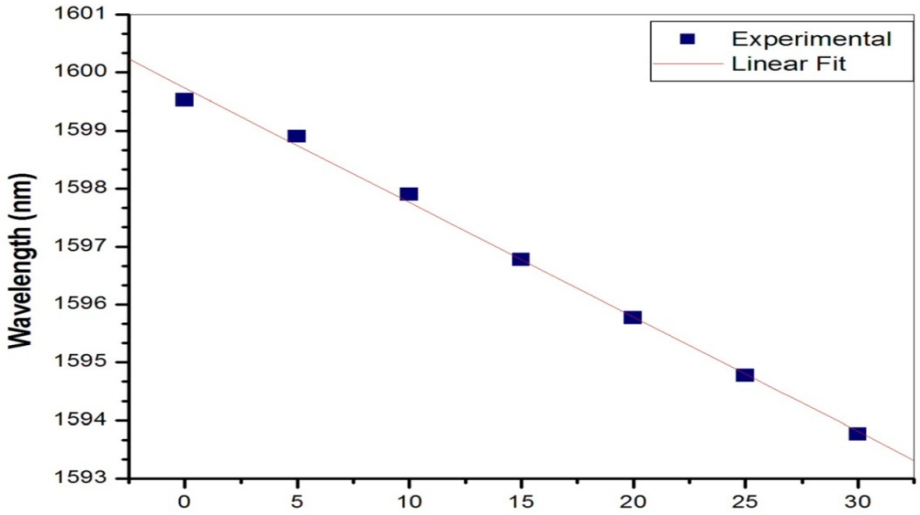


***Figure 3.34:*** *Peak positions of the $LP_{06}$ resonance band in the LPG transmission spectra as a function of increasing glucose concentration in distilled water.*

## 3.10 Conclusions

A series of experiments have been performed to characterize the response of the LPGs transmission spectrum for monitoring the variations in temperature and RI. Such characterization experiments are important in order to forecast the behaviour of the LPG's transmission spectrum to the measurands when the LPG is utilised for sensing applications.

We first studied the effect of grating length and annealing on the transmission spectrum of LPG written in hydrogen loaded standard single mode fiber. The analyses were made in terms of wavelength shift and transmission band intensity variations. We observed that the annealing of the LPG after their fabrication is a very essential process for stabilizing the grating spectrum and for obtaining good quality LPG for sensing applications. We also investigated the temperature sensitivity of the LPG fabricated in SMF-28 fiber and B-Ge co doped

photosensitive fiber. The difference in temperature sensitivity between the SMF-28 and B-Ge fiber is explained on the basis of the thermo-optic coefficients of the core and the cladding materials. The results obtained show that different resonant peaks have different temperature sensitivities and lower order attenuation bands of the LPG can also exhibit good temperature sensitivity as higher-order bands. Since we used standard telecommunication fiber for LPG fabrication, the sensing system can be easily implemented with the existing fiber networks for remote sensing applications.

The changes in wavelength and attenuation of an LPG resonance band with external refractive index were also investigated. For external index higher than that of the cladding index, the wavelength sensitivity was low as compared to the case when the external RI is lower than that of the cladding. The effect of grating period on the behavior of an LPG, relative to the variation of the refractive index of the external medium was also studied. The results obtained show that the shorter period LPG was found to be more sensitive than the longer period LPG, when the RI of the surrounding medium was lower than the RI of the cladding of the fiber. But the longer period LPG showed more sensitivity, when the RI of the surrounding medium was higher than that of the cladding of the fiber. The measurement system may be used to detect chemical or biological changes in the surrounding media. The simplicity and high sensitivity of the sensor make it worthy for food industry applications, pharmaceutical, chemical and biomedical sensing applications.

In the final part of this chapter we presented an LPG based chemical sensing system for the concentration measurement of glucose in distilled water. The performance of the sensor has been tested by monitoring the wave length shift and amplitude changes of the attenuation bands of the LPG in response to variation of glucose concentration levels.

## References


[1]. V. Bhatia and A. M. Vengsarkar, "*Optical fiber long period gratings sensors*", Optics Letters, **21**, pp. 692 – 694 (1996).

[2]. S.W. James and R.P. Tatam, "*Optical fiber long-period grating sensors: characteristics and applications*", Measurement Science and Technology, **14**, pp. 49-61 (2003).

[3]. Y. Chung and U. C. Paek. "*Fabrication and performance characteristics of optical fiber gratings for sensing applications*", IEEE Transactions on Optical Fiber Sensors, **1**, pp. 36 – 42 (2002).

[4]. B. J. Eggleton, P. S. Westbrook, R. S. Windeler, S. Spalter and T.A. Strasser, *"Grating resonances in air-silica microstructured optical fibers*", Optics Letters, **24**, pp. 1460-1462 (1999).

[5]. E. M. Dianov, D. S. Starodubov, S. A. Vasiliev, A. A. Frolov and O. I. Medvedkov, "*Refractive index gratings written by near ultraviolet radiation*", Optics Leters, **22**, pp. 221–223 (1997).

[6]. T. W. MacDougall, S. Pilevar, C. W. Haggans and M. A. Jackson, "*Generalized expression for the growth of long period gratings*", IEEE Photonics Technology Letters, **10**, pp. 1449–1451 (1998).

[7]. V. Bhatia, "*Properties and Sensing Applications of Long-Period Gratings*", Ph.D. Thesis, Virginia Polytechnic Institute and State University, Blacksburg, Virginia (1996).

[8]. A. M. Vengsarkar, P. J. Lemaire, J. B. Judkins, V. Bhatia, T. Erdogan and J. E. Sipe, "*Long-period fiber gratings as band-rejection filters*", Journal of Lightwave Technology, **14**, pp. 58-65 (1996).

[9]. H. Patrick, S. L. Gilbert, A. Lidgard and M. D. Gallagher, "*Annealing of Bragg gratings in hydrogen-loaded optical fiber*", Journal of Applied Physics, **78**, pp. 2940–2945 (1995).

[10]. J. N. Jang, H. G. Kim, S. G. Shin, M. S. Kim, S. B. Lee and K. H. Kwack, "*Effects of hydrogen molecule diffusion on $LP_{0m}$ mode coupling of long period gratings*", Journal of Non Crystalline Solids, **259**, pp. 156-164 (1999).

[11]. D. L. Williams and R. P. Smith, "*Accelerated Lifetime Tests On UV Written Intra core Gratings in Boron Germania Co doped Silica Fiber*", Electronics Letters, **31**, pp. 2120-2121 (1995).

[12]. V. Bhatia, "*Applications of long-period gratings to single and multi-parameter sensing*", Optics Express, **4**, pp. 457-466 (1999).

[13]. M. N. Ng and K. S. Chiang, "*Thermal effects on the transmission spectra of long period fiber gratings*", Optics Communications, **208**, pp.321–327 (2002).

[14]. X. W. Shu, L. Zhang and I. Bennion, "*Sensitivity characteristics of long-period fiber gratings*", Journal of Lightwave Technology, **20**, pp. 255-266 (2002).

[15]. X. W. Shu, T. Allsop, B. Gwandu, L. Zhang and I. Bennion, "*High-temperature sensitivity of log-period gratings in B-Ge codoped fiber*", IEEE Photonics Technology Letters, **13**, pp. 818-820 (2001).

[16]. P. J. Lemaire, R. M. Atkins, V. Mizrahiu and W. A. Reed, "*High pressure $H_2$ loading as a technique for achieving ultra high UV photosensitivity and thermal sensitivity in $GeO_2$ doped optical fibers*", Electronics Letters, **29**, pp. 1191–1194 (1993).

[17]. D. L. Williams, B. J. Ainslie, J. R. Armitage, R. Kashyap and R. Campbell, "*Enhanced UV photosensitivity in boron co doped germane silicate fibers*", Electronics Letters, **29**, pp. 45–52 (1993).

[18]. T. Mizunami, T. Fukuda and A. Hayashi, "*Fabrication and characterization of long period-grating temperature sensors using Ge–B co-doped photosensitive fiber and single mode fiber*", Measurement Science and Technology, **15**, pp. 1467–1473 (2004).

[19]. G. Ghosh, M. Endo and T. Iwasaki, "*Temperature-dependent Sellmeier coefficients and chromatic dispersions for some optical fiber glasses*", Journal of Lightwave Technology, **12**, pp. 1338-1341 (1994).

[20]. T. Yokouchi, Y. Suzaki, K. Nakagawa, M. Yamauchi, M. Kimura, Y. Mizutani , S. Kimura and S. Ejima "*Thermal tuning of mechanically induced long-period fiber grating*", Applied Optics, **44**, pp. 5024–5028 (2005).

[21]. H. J. Patrick, A. D. Kersey and F. Bucholtz, "*Analaysis of the long period fiber gratings to external index of refraction*", Journal of Lightwave Technology, **16**, pp. 1606-1642 (1998).

[22]. T. Hiroshi and K. Urabe, "*Characterization of Long-period Grating Refractive Index Sensors and Their Applications*", Sensors, **9**, pp. 4559-4571 (2009).

[23]. B. H. Lee, Y. Liu, S. B. Lee, S. S. Choi and J. N. Jang, "*Displacements of the resonant peaks of a long period fiber grating induced by a change of ambient refractive index*", Optics Letters, **22**, pp. 1769- 1771 (1997).

[24]. Y. Koyamada, "*Numerical analysis of core-mode to radiation-mode coupling in long-period fiber gratings*", IEEE Photonics Technology Letters, **13**, pp. 308-310 (2001).

[25]. X. Shu, X. Zhu, S. Jiang, W. Shi and D. Huang, "*High sensitivity of dual resonant peaks of long-period fiber grating to surrounding refractive index changes*", Electronics Letters, **35**, pp. 1580–1581 (1999).

[26]. R. Hou, Z. Ghassemlooy, A. Hassan, C. Lu and K. P. Dowker, "*Modelling Of Long Period Fiber Grating Response To Refractive Index Higher Than That Of Cladding*", Measurement Science And Technology, **12**, pp. 1709- 1713 (2001).

[27]. O. Duhem, J. Fraņois Henninot, M. Warenghem and M. Douay, "*Demonstration of long period-grating efficient couplings with an external medium of a refractive index higher than that of silica*", Applied Optics, **37**, pp. 7223-7228 (1998).

[28]. D. B. Stegall and T. Erdogan, "*Leaky cladding mode propagation in long-period fiber grating devices*", IEEE Photonics Technology Letters, **11**, pp. 343-345 (1999).

[29]. R. S. Nidhi, R. S. Kaler and P. Kapur, "*Theoretical and Experimental Study of Long-Period Grating refractive Index Sensor*", Fiber and Integrated Optics, **33**, pp. 37-46 (2014).

[30]. S. W. James, S. Korposh, S. W. Lee and R. P. Tatam, "*A long period grating-based chemical sensor insensitive to the influence of interfering parameters*", Optics Express, **22**, pp. 8012-8023 (2014).

[31]. S. M. Topliss, S. W. James, F. Davis, S. J. P. Higson and R. P. Tatam, "*Optical fiber long period grating based selective vapour sensing of volatile organic compounds*", Sensors and Actuators B: Chemical, **143**, pp. 629–634 (2010).

[32]. R. Falciai, A.G. Mignani and A. Vannini, "*Long period gratings as solution concentration sensors*", Sensors and Actuators B: chemical, **74**, pp. 74-77 (2001).

Chapter 4

# Fiber Optic Sensor for the Measurement of Adulteration in Edible Oils

*Abstract*

*A fiber optic sensing system for the adulteration detection of coconut oil and olive oil by less expensive paraffin oil is presented. The fundamental principle of detection is the sensitive dependence of the resonance peaks of a Long Period Grating (LPG) on the changes in the refractive index of the environmental medium, surrounding the cladding surface of the grating.*

*The performance of the sensor has been tested by monitoring the wavelength and amplitude changes of the attenuation bands of the LPG in response to variation of adulteration levels. The developed sensor is user-friendly, reusable and allows instantaneous measurement of the amount of adulteration without involving any reagents.*

[1]. T. M. Libish *et al*., Laser Physics, 23 (4), pp. 045112 (2013).

[2]. T. M. Libish *et al*., Sensors & Transducers Journal, 114(3), pp. 102-111 (2010).

## 4.1 Introduction and motivation

A food article is branded adulterated if any inferior or cheaper substance has substituted wholly or its part in a genuine food article, downgrading the quality of the product. Adulteration of edible oil - blending cheaper oil with premium oil - has always been a profitable business for unscrupulous players. Analysis of the quality of edible oils is of paramount importance in most of the countries. Ensuring the authenticity of the food that we consume has intensified exponentially over the years in every country. Authenticity is a very important quality criterion, especially for edible oils as they are much frequently subjected to rampant adulteration. Higher the price of premium oil, greater is the propensity to adulterate it with low priced oil. The unethical and filthy practice of edible oil adulteration results in the formation of harmful substances in the human organism. The most common adulteration is addition of paraffin oil to expensive edible oils like coconut oil and adulterate virgin olive oil with sunflower oil.

Adulteration of coconut oil with paraffin oil is a common malpractice in South East Asian countries. The much acclaimed properties of coconut oil include its fragrance, taste and presence of medium chain fatty acids, antioxidants, vitamins etc. It is also acknowledged for its good digestibility. Besides cooking purposes, coconut oil is also used widely for medical and industrial purposes in Asian countries. The common adulterants used in coconut oil are liquid Paraffin, Palm oil, palm kernel oil etc. Addition of liquid paraffin is extremely hazardous to human health as it can ultimately lead to several health problems such as liver disorders or even cancer. Up to 20 percent of paraffin oil can be easily mixed with coconut oil and there will not be any notable difference in the smell or colour of coconut oil.

Olive oil is popular edible oil mainly produced and consumed in Mediterranean countries. Although more expensive than other oils, virgin olive oil has many health

benefits. It is important oil that is high in nutritional value due to its high content of antioxidants and monounsaturated fatty acids. Studies have also found that consumption of olive oil can lower the risk of coronary heart disease by reducing bad cholesterol- Low-density lipoprotein (LDL) while raising the good cholesterol- High-density lipoprotein (HDL). It is a common practice today to adulterate virgin olive oil with sunflower oil for financial gain. Sunflower oil is used as the usual adulterant due to its close resemblance to virgin olive oil composition. Adulteration of virgin olive oil with other edible oils also may cause serious health problems.

Different analytical techniques are employed in legitimacy testing of edible oils. Among them are chromatographic methods [1,2], differential scanning calorimetry [3], fourier transform infrared spectroscopy [4], photopyroelectric detection [5] etc. These techniques have the disadvantage that they are expensive, time consuming, require considerable analytical skill and produce hazardous chemical waste. Due to increased public concern and legal requirements, the need for more reliable, rapid and less expensive monitoring and quality checking of edible oil is growing continuously. Fiber-optic sensors offer very attractive solutions in this respect due to their intrinsic merits such as high sensitivity, small size, immunity to electromagnetic interference, high performance, fast response etc. [6]. In 2005, M. Sheeba *et al*. had reported a fiber optic intensity based evanescent wave sensor for the detection of adulterant traces in coconut oil using an unclad plastic fiber [7]. The main limitation of this evanescent wave sensor is that the cladding and small portion of the core has to be removed manually. This will reduce the mechanical stability of the fiber. In order to avoid this limitation, we are proposing a new LPG based sensor for the detection of adulteration in coconut oil which provides improved sensitivity and robustness.

Unlike FBG, LPG couples light from the fundamental core mode to other forward-propagating cladding modes, produces a discrete set of attenuation bands

in the transmission spectrum of the optical fiber [8-10]. The resonance wavelength of LPGs is a strong function of external perturbations like strain, temperature and surrounding refractive index (SRI) [11-14]. Presence of these external perturbations affects the coupling strength between the core and cladding modes, which could lead to both amplitude and wavelength shift of the attenuation bands in the LPG transmission spectrum. Measurement of these spectral parameters in response to environment, surrounding the grating region, is the basis of sensing with LPGs [15,16]. LPG can be used as an ambient index sensor or a chemical concentration indicator with high stability and reliability [17-20]. With respect to chemical sensing, the resonant wavelength shift and amplitude change of the LPG attenuation bands with the SRI is certainly the most interesting. The RI sensing is very important for biological, chemical and biochemical applications as a number of substances can be detected through the measurements of refractive index.

At present, the refractive index sensing based on the LPG is an extraordinarily important subject in the biochemical sensing area which attracts significant research interest. Here an edible oil adulteration measurement sensor is being demonstrated by exploitation of the sensitivity of LPGs to the concentration of the solution under test. When the edible oils are subjected to adulteration, a change in its original refractive index occurs. Such changes cause corresponding shifts in the resonance wavelength and change in depth (amplitude) of the loss bands in the LPG. Adulteration levels can be measured by analyzing these spectral changes. A complete experimental analysis, on the use of an LPG for adulteration detection in coconut oil and virgin olive oil is being presented. The device performance is analyzed in terms of its sensitivity and resolution. This LPG based sensor possesses the advantages of requirement of small volumes of sample for analysis and provides the response in real time.

## 4.2 Theory of operation

The LPG operates by coupling the fundamental core mode (i.e. the $LP_{01}$ mode) to co-propagating cladding modes ($LP_{0m}$ mode with m =2, 3, 4. . .) in the fiber. This coupling yields rejection bands around specific wavelengths (resonant wavelengths) in the transmission spectrum of the LPG [21,22]. The wavelength at which the guided mode couples to the cladding modes can be obtained through the phase-matching equation [23,24]:

$$\lambda_m = \left[n_{eff}^{co} - n_{eff,m}^{cl}\right]\Lambda \quad \text{.....(4.1)}$$

where $\lambda_m$ is the resonance wavelength corresponding to coupling to the $m^{th}$ cladding mode, $\Lambda$ is the grating period, $n_{eff}^{co}$ is the effective index of the fundamental core mode ($LP_{01}$), $n_{eff,m}^{cl}$ is the effective index of the $m^{th}$ order cladding mode ($LP_{0m}$).

The strength of transmission of the attenuation bands [10] can be written as

$$T_m = 1 - \sin^2(k_m L) \quad \text{.....(4.2)}$$

where L is the length of LPG and $k_m$ is the coupling coefficient for $m^{th}$ cladding mode. Therefore, the coupled power % depends on L and $k_m$. The parameter $k_m$ however depends on the specific cladding mode and also on the amplitude of refractive index modulation ($\Delta n_{co}$) induced in the fiber core. Changes that occur in the refractive index of the surrounding medium will affect the cladding effective refractive indices and, as a direct consequence, attenuation dips experience both changes in its amplitude ($T_m$) and shifts in the resonance wavelengths ($\lambda_m$). These spectral changes can be used to measure the external medium refractive index and allows the LPG to be used as a sensor device to determine the concentration of a specific substance in a binary mixture.

The shift of the centre wavelength of the attenuation peaks can occur towards longer or shorter wavelengths based on the SRI. The refractive index sensitivity of the LPG arises from the dependence of the effective index of the cladding mode ($n_{eff,m}^{cl}$) on the refractive index of the surrounding material. The effect of refractive index of the surrounding medium on the resonant wavelength is expressed by [8,22]:

$$\frac{d\lambda_m}{dn_{sur}} = \frac{d\lambda_m}{dn_{eff,m}^{cl}}\left[\frac{dn_{eff,m}^{cl}}{dn_{sur}}\right] \quad \text{.....(4.3)}$$

where $n_{sur}$ is the refractive index of the surrounding material. For each cladding mode, the term $\left[\frac{dn_{eff,m}^{cl}}{dn_{sur}}\right]$ is distinct and hence an LPG is expected to have a strong dependence on the order of the coupled cladding mode. Higher order cladding modes tend to show greater sensitivity to changes in external refractive index because these modes extend further out into the area exterior to the fiber [10,24].

The spectral change of LPG sensors can be characterized in terms of external RI as follows. If the SRI is lower than the refractive index of the cladding ($n_{sur} < n_{cl}$), mode guidance can be explained using total internal reflection. In this case, typically strong resonance peaks are observed and the attenuation dips shift towards shorter wavelengths (blue shift) when the external medium refractive index increases up to the fiber cladding refractive index[13,14]. The closer the refractive index of the external medium to that of the cladding, the higher the grating sensitivity and leads to larger wavelength shift. When the value of the ambient refractive index matches with that of the cladding, the cladding layer acts as an infinitely extended medium and thus supports no discrete cladding modes. In this case, a broadband radiation mode coupling occurs with no distinct attenuation bands [25]. In short, when the external RI becomes equal to the RI of the cladding, rejection bands disappear, and the transmission spectrum gets flattened. Once the

SRI is higher than the refractive index of the cladding ($n_{sur} > n_{clad}$), the cladding modes no longer experience total internal reflection and Fresnel reflection can be used to explain the mode structure[26]. Whatever may be the value of the external refractive index, a part of the energy is reflected at the interface of the cladding and the external medium. The ratio of the energy reflected will be determined by the Fresnel coefficients. In this case the resonance peaks reappear at slightly longer wavelengths (red shift) compared to those measured with air as the surrounding medium [27]. The depth of each attenuation peak steadily increases with increase in refractive index of the surrounding medium, owing to larger Fresnel reflection coefficients that yield improved reflection at the cladding boundary [28]. So, chemical concentration changes can also be measured by studying the amplitude changes in the LPG attenuation dips.

## 4.3 Experimental setup

In our experiments, a broadband white light source ([Yokogawa] AQ 4305) was used as the light source and the transmission spectrum of the LPG was monitored with an optical spectrum analyzer (OSA) ([Yokogawa] AQ 6319). The LPG sensor head was fixed in a specially designed glass cell with provision for filling the sample and draining it out when desired. We used an LPG with grating length of 21 mm and grating period of 420 μm. The LPG was fabricated at CGCRI using a 248 nm KrF excimer laser source employing point-by-point writing method [10]. The hydrogen loaded photosensitive fiber used has a cladding diameter of 125 micron and a numerical aperture of 0.14. The core and the cladding refractive indices were 1.463 and 1.4563, respectively. There was no protective coating in the grating section, so that the external RI could easily affect the effective refractive index of the cladding modes. The fiber containing the LPG element was connected to the light source on one side and to the OSA on the other side (Fig.4.1). The spectra were recorded on the OSA in the wavelength range 1250–1700 nm.

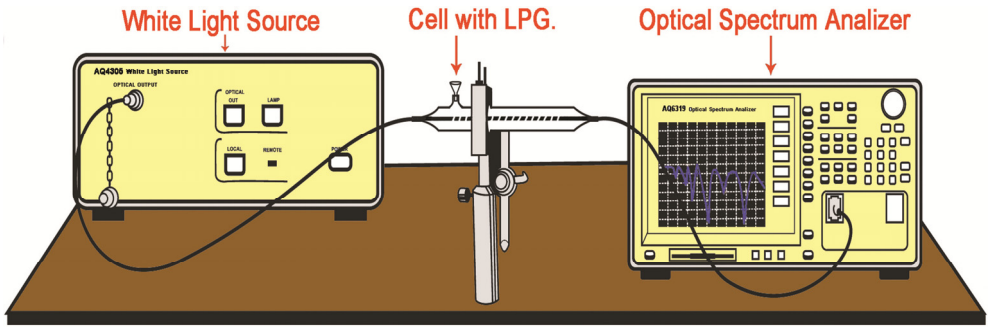


***Figure 4.1:*** *Experimental setup.*

Drastic changes in performance of the LPG had been noted when there were variations in external characteristics like temperature, bending and strain. To avoid the effect of strain and bending, a special glass cell holder was designed and the fiber was placed stretched and bonded with epoxy at both the end points of the cell such that the grating section was kept at the centre of the cell. For precise measurement, the experimental setup and sample solution temperature were maintained at 25.0 ± 0.5 °C. The resonance wavelength of the LPG dip was measured with the fiber section containing the LPG immersed in samples obtained by mixing paraffin oil and pure coconut oil in different proportions.

Sensor responded to RI changes as soon as samples were introduced to the glass cell. But, to get a stabilized output, all readings were taken one minute after the LPG was immersed in the solution. An Abbe refractometer was employed to measure the sample refractive indices, just after the sample was drained out from the glass cell. The initial spectrum of the LPG in air (Fig.4.2) is used as reference spectrum for all the sample analysis. The use of this reference spectrum serves two purposes: 1) to remove any trace of each adulterated sample between two different measurements and 2) to assure that the LPG attenuation dip returns to the original wavelength after each sample measurement. At the end of each sample measurement, the grating was cleaned with isopropyl alcohol repeatedly, followed by drying

properly, so that the original transmission spectrum of LPG was obtained. The changes in the refractive index of the surrounding medium were obtained by increasing the paraffin oil concentration in pure edible oil samples. The refractive indices of pure coconut oil and paraffin oil were found to be 1.450 and 1.454 respectively.

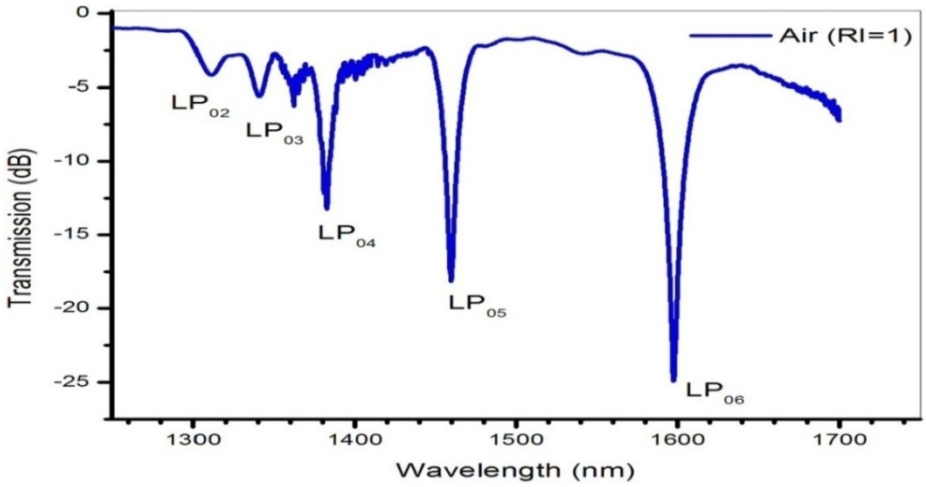


***Figure 4.2:*** *Transmission spectrum of LPG with* $n_{sur} = 1$.

## 4.4 Results & discussion

### 4.4.1 Coconut oil adulteration measurement

The dependence of the sensor sensitivity on adulteration in terms of the LPG resonance wavelength shift has been analyzed, while the samples obtained by mixing of paraffin oil and pure coconut oil in different proportions were in contact with the grating. For the grating used in these studies the strongest attenuation peak in air, is located at 1602 nm. Figure 4.3 shows the changes in the wavelength and amplitude corresponding to main attenuation dips ($LP_{05}$ and $LP_{06}$) with increasing concentration of paraffin oil in the mixture with pure coconut oil. The highest order attenuation band ($LP_{06}$) was most sensitive to the surrounding refractive index changes and is shown in Fig. 4.4.

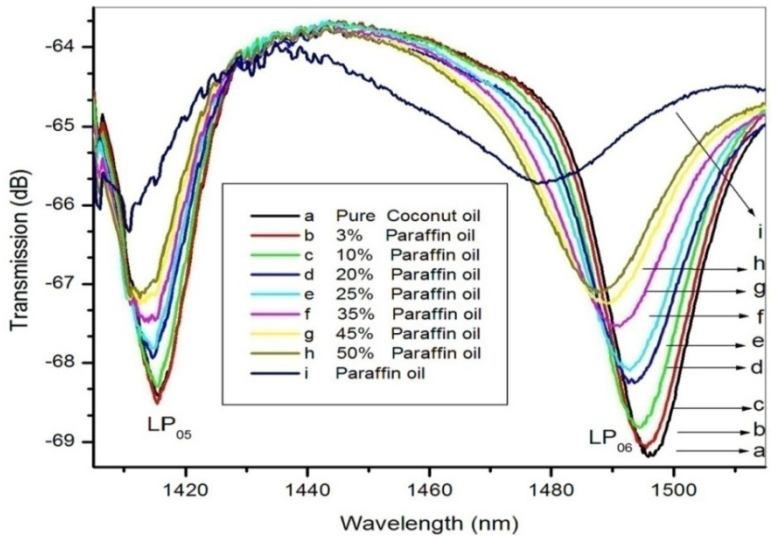


***Figure 4.3:*** *Transmission spectra of the LPG surrounded by a mixture of paraffin oil and pure coconut oil in different proportions.*

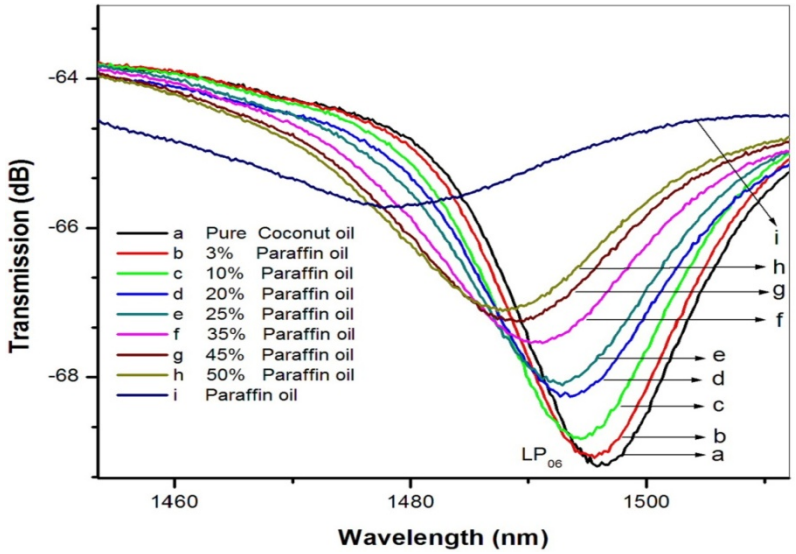


***Figure 4.4****: Wavelength shift of the $LP_{06}$ mode of the LPG surrounded by a mixture of paraffin oil and pure coconut oil in different proportions.*

The refractive indices produced by different oil samples used in the experiments were less than the cladding refractive index of the LPG. If the refractive

index of the surrounding medium is lower than that of the cladding, the fiber supports bounded cladding modes that are maintained by total internal reflection at the surrounding cladding interface. In this case, the surrounding refractive index sensitivity arises from the evanescent wave interaction between the cladding modes and the external medium. This interaction will lead to a strong modification of the central wavelength of the attenuation bands of LPG. For RI values lower than that of the cladding, LPG sensitivity to increasing external index of refraction is evident as a blue shift in the central wavelength of the attenuation band in the grating's transmission spectrum. The LPG exhibited a total blue shift of approximately 15 nm when the surrounding medium was gradually changed from pure coconut oil to pure paraffin oil sample. For all the adulterated oil sample analyses, the wavelength shifts were measured relative to that of the LPG immersed in the pure coconut oil sample used as a reference fluid. Apart from the wavelength shift with the changes in refractive index of the external medium, LPG also produced a reduction in the peak intensity of the resonance band as reported earlier [18,20].

Figure 4.5 shows the sensitivity of the LPG when used as a sensor for various volume percentage of paraffin oil in coconut oil. It can be seen from the results that the sensor is useful to determine paraffin oil concentration even upto 3% by volume with a good linear sensitivity between 3 % and 50 %. This region is very useful because most of the adulteration and malpractices using paraffin oil are within this range. Repeatability was found to be poor below 3 % adulteration. A spectral shift of 15 nm was obtained in the refractive index range 1.450 to 1.454, which corresponds to an average resolution of $2.66 \times 10^{-4}$ $nm^{-1}$.

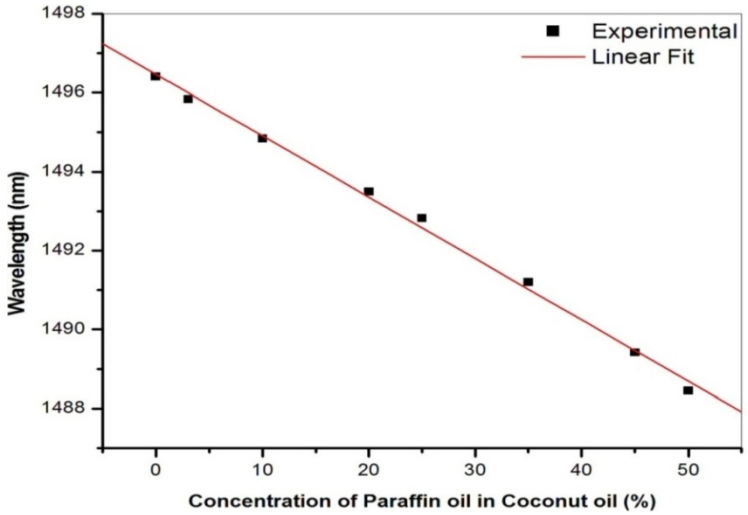


***Figure 4.5:*** *Peak positions of the highest order resonance band in the LPG transmission spectra as a function of Paraffin oil proportion.*

### 4.4.2 Virgin olive oil adulteration measurement

Measurement of the transmitted signal intensity in a chosen spectral interval was used for olive oil adulteration analysis since all the used samples were with refractive indices higher than the refractive index of the fiber cladding. When the LPG was immersed in pure olive oil sample, the transmission spectrum indicated that the attenuation bands were red shifted compared with those in air**.** The refractive indices of the binary mixture samples used in the experiments were increased, when we increased the sunflower oil concentration from 0 to 30%. The refractive indices of pure olive oil and adulterated oil samples used in the experiments were varied from 1.4635 to 1.4670. Under these conditions, the sensor exhibited a low sensitivity for measurements in the wavelength domain. So no analysis was conducted for the wavelength shift. The most pronounced effect was the change in the LPG transmission intensity. For intensity measurements the $LP_{06}$ mode exhibited noticeable amplitude changes and minimal wavelength shifts. So we selected the attenuation dip near 1600 nm for adulteration analysis. As can

be seen from Fig. 4.6, when the adulteration level was increased, there was a very small shift in wavelength and a detectable increase in the intensity of the transmission dip. In short, the depth of each attenuation peak steadily increased when we increased the adulteration level up to 30% sunflower oil in pure olive oil sample.

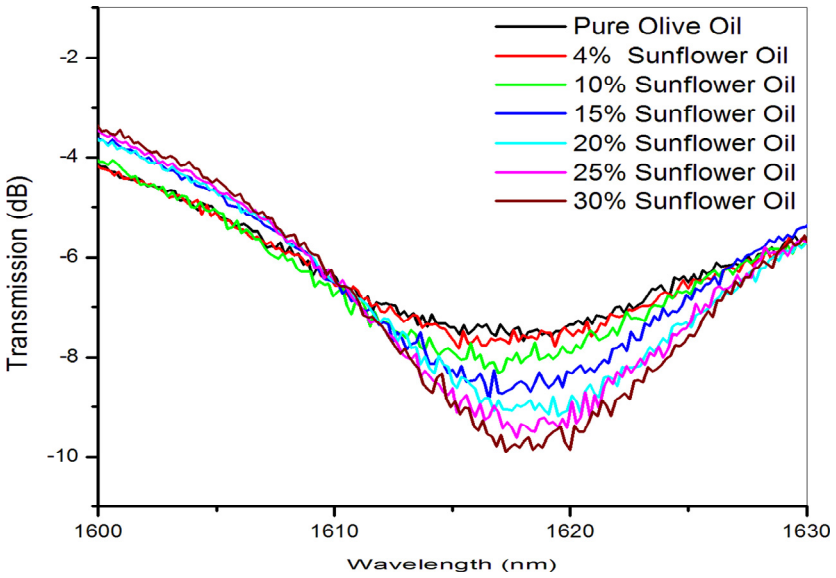


***Figure 4.6:*** *Transmission spectra of the LPG surrounded by a mixture of sunflower oil and pure olive oil in different proportions.*

Figure 4.7 shows the sensitivity of the LPG when used as a sensor for various volume percentage of sunflower oil in olive oil. It can be seen from the results that the sensor is useful to determine sunflower oil concentration even upto 4% by volume with a good linear sensitivity between 4 % and 30 %. This region is very useful because most of the adulteration and malpractices using sunflower oil are within this range. Repeatability was found to be poor below 4 % adulteration. An intensity change of 2.18 dB was obtained in the refractive index range 1.4635 to 1.4670**,** which corresponds to an average resolution of 1.61 x $10^{-3}$ $dB^{-1}$. The

LPG sensor sensitivity was around 0.07 dB/vol% of sunflower oil in the measurement range.

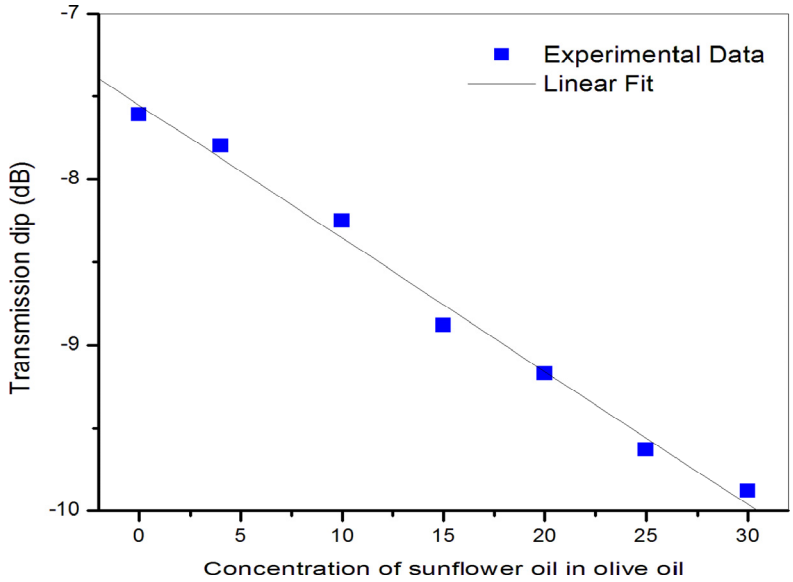


***Figure 4.7:*** *Transmission spectral intensity changes in the $LP_{06}$ resonance band of the LPG as a function of sunflower oil proportion in olive oil.*

## 4.5 Conclusions

Resonance wave length shift and amplitude changes of the attenuation bands of the LPG have been monitored to demonstrate an edible oil adulteration measurement sensor. Detection limit of adulteration was found to be 3% for coconut oil- paraffin oil binary mixture and 4 % for olive oil- sunflower oil binary mixture. The LPG sensor sensitivity was around 0.15 nm/vol% of paraffin oil in the measurement range. The advantages of this type of grating sensor are their simple fabrication, very easy implementation for measurement, easy interrogation and the fact that it does not involve the use of solvents or toxic chemicals. The developed sensor is user-friendly, reusable and allows instantaneous determination of the percentage concentration of adulterant in an olive oil sample without

involving any chemical analysis. The newly developed sensor also showed good reversibility and repeatability. The measurement system may be used to detect chemical or biological changes in the surrounding media. The simplicity and high sensitivity of the sensor make it worthy for food industry applications, pharmaceutical, chemical and biomedical sensing applications.

This method enables quantitative measurement of adulterant to a level of 3% adulteration with a wide dynamic range. The selectivity of this LPG based sensor can be improved by the identification and application of suitable coating materials which selectively react to a specific type of adulterant.

## References

[1]. F. Guimet, J. Ferre and R. Boque, "*Rapid detection of olive-pomace oil adulteration in extra virgin olive oils from the protected denomination of origin Siurana using excitation emission fluorescence spectroscopy and three-way methods of analysis*", Analytica Chimica Acta, **544**, pp. 143–152 (2005).

[2]. G. P. Blanch, M. D. Mar Caja, M. L. Ruiz, Castillo and M. Herraiz, "*Comparison of different methods for the evaluation of the authenticity of olive oil and hazelnut oil*", Journal of Agricultural and Food Chemistry, **46**, pp. 3153–3157 (1998).

[3]. M. Marina, Y. B. Cheman, S.A.H. Nazimah and I. Amin, "*Monitoring the adulteration of virgin coconut oil by selected vegetable oils using differential scanning calorimetry*", Journal of Food Lipids, **16**, pp. 50-61 (2009).

[4]. M. A. Manaf, Y. B. Che man , N. S. Abdul Hamid, A. Ismail and S. Zainul abidin, "*Analysis of adulteration of virgin coconut oil by palm kernel oil using fourier transform infrared spectroscopy*", Journal of Food Lipids, **14**, pp. 111-121 (2007).

[5]. M. Streza, D. Dadarlat, C. Socaciu, C. Bele, F. Dulf and V. Simon, "*Photopyroelectric Detection of Vegetable Oils Adulteration*", Food Biophysics, **4**, pp. 147-150 (2009).

[6]. Eric Udd and William B. Spillman, "*Fiber Optic Sensors: An Introduction for Engineers and Scientists*", John Wiley & Sons (2011).

[7]. M. Sheeba, M. Rajesh, C. P. G. Vallabhan, V. P. N. Nampoori and P. Radhakrishnan, "*Fibre optic sensor for the detection of adulterant traces in coconut oil*", Measurement Science and Technology, **16**, pp. 2247–2250 (2005).

[8]. V. Bhatia and A. M. Vengsarkar, "*Optical fiber long period gratings sensors*", Optics Letters, **21**, pp. 692 – 694 (1996).

[9]. J. Keith, S. Puckett and G.E. Pacey, "*Investigation of the fundamental behavior of long-period grating sensors*", Talanta, **61**, pp. 417-421(2003).

[10]. S.W. James and R.P. Tatam, "*Optical fiber long-period grating sensors: characteristics and applications*", Measurement Science and Technology, **14**, pp. 49-61 (2003).

[11]. T. Mizunami , T. Fukuda and A. Hayashi, "*Fabrication and characterization of long period-grating temperature sensors using Ge–B co-doped photosensitive fiber and single-mode fiber*", Measurement Science and Technology, **15**, pp. 1467–1473 (2004).

[12]. Y. Liu, L. Zhang and I. Bennion, "*Fiber optic load sensors with high transverse strain sensitivity based on long-period gratings in B/Ge co-doped fiber*", Electronics Letters, **35**, pp. 661-662 (1999).

[13]. B. H. Lee, Y. Liu, S. B. Lee, S. S. Choi and J. N. Jang, "*Displacements of the resonant peaks of a long period fiber grating induced by a change of ambient refractive index*", Optics Letters, **22**, pp. 1769- 1771 (1997).

[14]. T. Hiroshi and K. Urabe, "*Characterization of Long-period Grating Refractive Index Sensors and Their Applications*", Sensors, **9**, pp. 4559-4571 (2009).

[15]. R. S. Nidhi, R. S. Kaler and P. Kapur, "*Theoretical and Experimental Study of Long-Period Grating refractive Index Sensor*", Fiber and Integrated Optics, **33**, pp. 37-46 (2014).

[16]. H. J. Patrick, A. D. Kersey and F. Bucholtz, "Analysis of the response of long period fiber gratings to external index of refraction", J. Lightwave Technology, **16**, pp. 1606–1612 (1998).

[17]. J. H. Chong, P. Shum, H. Haryono, A. Yohana, M.K. Rao, Chao Lu and Yinian Zhu, "*Measurements of refractive index sensitivity using long-period grating refractometer*", Optics Communications, **229**, pp. 65–69 (2004).

[18]. R. Falciai, A.G. Mignani and A. Vannini, "*Long period gratings as solution concentration sensors*", Sensors and Actuators B, **74**, pp. 74-77 (2001).

[19]. R. Falate, R. C. Kamikawachi, M. Müller, H. J. Kalinowski and J. L. Fabris, "*Fiber optic sensors for hydrocarbon detection*", Sensors and Actuators B, **105**, pp. 430–436 (2005).

[20]. S. M. Topliss, S. W. James, F. Davis, S. J. P. Higson and R. P. Tatam, "*Optical fiber long period grating based selective vapour sensing of volatile organic compounds*", Senors and Actuators B, **143**, pp. 629–634 (2010).

[21]. A. M. Vengsarkar, P. J. Lemaire, J. B. Judkins, V. Bhatia, T. Erdogan and J. E. Sipe, "*Long-period fiber gratings as band-rejection filters*", J. Lightwave Technology, **14**, pp. 58-65 (1996).

[22]. V. Bhatia, "*Applications of long-period gratings to single and multi-parameter sensing*", Optics Express, **4**, pp. 457-466 (1999).

[23]. T. W. MacDougall, S. Pilevar, C. W. Haggans and M. A. Jackson, "*Generalized expression for the growth of long period gratings*", IEEE Photonics Technology Letters, **10**, pp. 1449–1451 (1998).

[24]. X. W. Shu, L. Zhang and I. Bennion, "*Sensitivity characteristics of long-period fiber gratings*", Journal of Lightwave Technology, **20**, pp. 255-266 (2002).

[25]. Y. Koyamada, "*Numerical analysis of core-mode to radiation-mode coupling in long-period fiber gratings*", IEEE Photonics Technology Letters, **13**, pp. 308-310 (2001).

[26]. O. Duhem, J. Fraṇois Henninot, M. Warenghem and M. Douay, "*Demonstration of long period-grating efficient couplings with an external medium of a refractive index higher than that of silica*", Applied Optics, **37**, pp. 7223-7228 (1998).

[27]. D. B. Stegall and T. Erdogan, "*Leaky cladding mode propagation in long-period fiber grating devices*", IEEE Photonics Technology Letters, **11**, pp. 343-345 (1999).

[28]. R. Hou, Z. Ghassemlooy, A. Hassan, C. Lu and K. P. Dowker, "*Modelling of long-period fiber grating response to refractive index higher than that of cladding*", Measurement Science and Technology, **12**, pp. 1709-1713 (2001).

# Chapter 5

# Fabrication of Etched FBGs and Refractive Index Sensing

*Abstract*

*The fabrication method and characterization of FBGs used in the present studies are outlined in this chapter. It also summarizes the details of RI sensing based on etched FBGs. FBGs have been extensively used as temperature and strain sensors. However, FBGs are intrinsically insensitive to surrounding refractive index of the medium since the light coupling takes place only between well-bound core modes, which are shielded from the influence of the surrounding refractive index by the fiber cladding. To make the FBG sensitive to changes in the surrounding refractive index, the cladding thickness around the grating region must be reduced. The resultant FBG is often termed as an etched, thinned or reduced cladding FBG. A reliable and stable method of etching of FBGs using a special mount and the spectral response of FBGs during etching process is discussed. The experimental verification of the RI sensitivity of the FBGs is given in the final part of the chapter.*

## 5.1 Introduction

Fiber Bragg grating (FBG) sensors are one of the most exciting developments in the field of optical fiber sensors in recent years. FBGs make promising candidates as sensors because of their significant sensing advantages, the most important of which is that the information on a measurand is encoded in the reflected or transmitted wavelength from the grating. Thus problems associated with source power fluctuations, bending losses and reflection losses are eliminated. It has been shown that a fiber Bragg grating (FBG) can also be used as a refractive index sensor by partially removing the cladding region around the grating to make the FBG sensitive to changes in the surrounding refractive index [1-3]. Subsequently, this research was utilized to study fiber sensors based on etched FBGs for a variety of chemicals [4-6]. Refractive index (RI) is a basic optical property of materials and its accurate measurement is of great importance in many applications. Today, it is of large importance to monitor biological, physical and chemical parameters in industrial processes, medical treatment, oil and gas, food, pharmaceutical, and biotechnology, where a large number of physical, biological or chemical features have to be measured.

In the initial part of this chapter, the theory of etched FBG and the set up used for fabricating different types of gratings used in this thesis is explained. Although the propagation of light is different in LPG and FBG, the physical structure of both is almost the same. The only difference is in the period of the gratings. Therefore most of the fabrication methods used for the fabrication of LPGs and FBGs are the same. But due to some geometrical and optical limitations, there are some specific methods which are most commonly adopted for fabricating LPG or FBG. We used phase mask method for fabricating FBGs and point by point method for fabricating LPGs.

## 5.2 Refractive index sensing using FBGs

A standard fiber Bragg grating consists of a refractive index modulation in the core of an optical fiber that acts to couple the fundamental forward propagating mode to the contra-propagating core mode. The principle of operation of an FBG sensor is based on the shift of the Bragg wavelength when it is under the influence of a measurand. Compared with conventional fibre-optic sensors, FBG sensors have a number of distinguishing advantages such as high sensitivity, high spatial resolution, immunity to electromagnetic interference (EMI), fast response, compatibility with fiber optical networks, multiplexing and distributed sensing capabilities. Over the last two decades, FBGs have been utilized as optical sensors to measure a wide range of physical parameters including temperature, strain, pressure, loading etc [7-9]. Since the light coupling takes place between well-bound core modes that are screened from the influence of the surrounding-medium refractive index (SRI) by a thick cladding layer, normal FBGs are intrinsically insensitive to SRI. So normal FBGs cannot be used as chemical sensor. For this reason, long-period fiber gratings (LPFGs) are generally used for chemical sensing applications, where the light coupling between the core and the cladding modes exist, accompanying an optical interaction between the cladding and an external medium [10-13]. However, the broad transmission spectrum and the multiple resonance peaks are the major disadvantages of the LPG based measurement system. To resolve these problems, several types of modified FBG chemical sensors have been proposed, which enable the optical core mode to interfere with the SRI variation. To use the FBG as an effective refractometric sensor element, the cladding radius around the grating region must be reduced, allowing the effective refractive index of the fiber core to be significantly affected by the refractive index of external medium [14, 15]. As a consequence, shifts are expected in the Bragg wavelength combined with a modulation of the reflected amplitude. A

very simple method to reduce the cladding can be the uniform chemical etching of the Bragg grating section of the fiber using hydrofluoric acid (HF).

At present, refractive index sensing based on the etched FBG is an extraordinarily important subject in the bio-chemical sensing area which attracts significant research interest. The sensitivity of the sensor depends upon the change in the effective index for the core mode, which is related to the change in the refractive index of the biological or chemical solution under test. To date, a number of SRI sensors have been realized using etched FBG structures to measure concentrations of some chemicals or bio samples [16–25].

## 5.3 Etched or thinned or reduced cladding FBGs

To make the FBG sensitive to changes in the surrounding refractive index, the cladding radius around the grating region must be reduced. The resultant FBG is often termed as an etched or thinned or reduced cladding FBG. The structure is schematically shown in Fig. 5.1. Uniform etched FBGs were first demonstrated by Asseh *et al*. [1] in 1998.

For bio sensing and chemical sensing applications, the sensitivity and selectivity of FBGs can be improved by applying suitable material coatings with high refractive indices along the thinned region. The basis of these FBG sensors relies on the use of a suitable measurand-specific material to induce a secondary effect, to which the etched FBG is susceptible. i.e. The interaction of the specific target molecule with the coating changes the film refractive index and thus causes a Bragg wavelength shift and a variation in the grating reflectivity. Therefore concentration measurement of bio-chemical samples can be done by analyzing the spectral changes in FBG transmission or reflection spectrum.

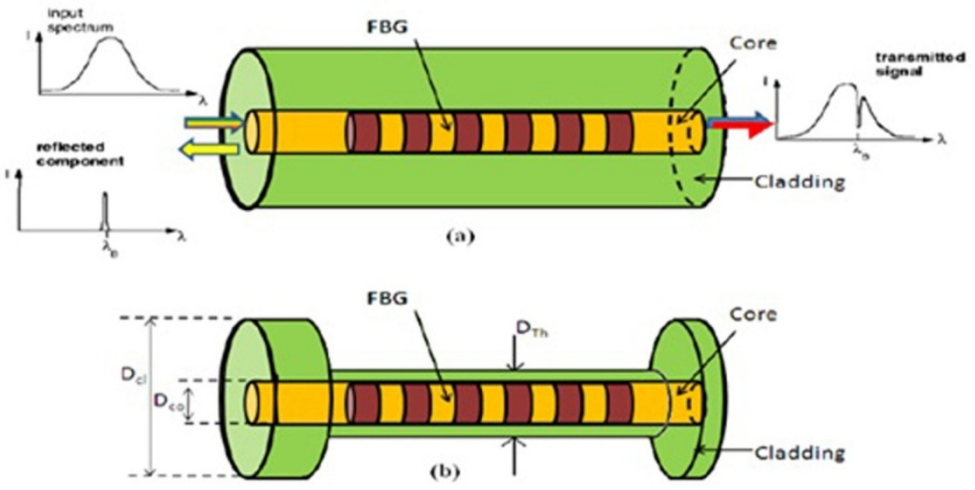


***Figure 5.1:*** *Schematic diagram of FBG (a) Standard FBG (b) Thinned FBG.*

If the fiber cladding layer is partially or fully removed symmetrically along the grating region using chemical etching, the effective refractive index $n_{eff}$ is significantly affected by the external RI [26]. As a consequence a shift in the Bragg wavelength combined with a modulation of the reflected amplitude is expected as the surrounding refractive index changes[5]. Unlike the common use of FBG sensors for temperature and strain measurements, in this case, only the refractive index is affected by measurand changes while the grating pitch remain practically unaffected. The strong dependence of the effective refractive index on the surrounding refractive index of the medium, recommends the use of a thinned FBG as highly sensitive fiber refractive index sensor [2, 5, 27-30]. If the refractive index of the external media is higher than that of silica, the modes are leaky, because there is no total internal reflection at the silica–external boundary. However, for field modes to exist, it is sufficient to provide an external refractive index smaller than the silica refractive index. An etched FBG will show maximum Bragg wavelength shift when the surrounding index is close to the core refractive index.

In a variety of chemical and biological applications, refractive index sensing is very important since a number of substances can be detected through measurement of the refractive index. The refractive index changes with the concentration of bio-chemical solution variation, and this refractive index changing energizes the core effective index changing, which could make the Bragg wavelength shift [3,19-24]. The Bragg wavelength changes could be detected with an optical spectrum analyzer. The variation in bio-chemical solution concentration is calculated by analyzing the relation between shifts of Bragg wavelength with change in concentration of chemical or biological sample.

### 5.3.1 Etched and coated FBG for sensing applications

The etched FBGs can be made to detect extremely low concentration of biochemical target molecules with high sensitivity by applying suitable material coatings of high refractive index on their surface. These coatings selectively react with specific target molecules and result in a refractive index change and which will thereby affect the effective refractive index of the FBG to a great extent. We have discussed this in detail in chapter 6 of this thesis. The basic configuration of the sensor is shown in Fig.5.2. The presence of a specific target molecule is detected by analyzing the Bragg wavelength shift of the FBG reflection spectra. Therefore, FBGs are ideal candidates for biomolecular and chemical sensing applications, if properly complemented with suitable chemo-sensitive materials or biorecognition elements.

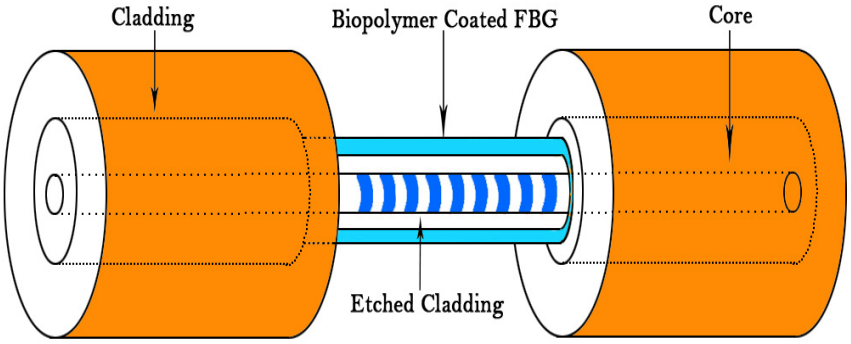


***Figure 5.2:*** *Structure of the biopolymer coated etched FBG sensor.*

The first fiber grating-based hydrogen sensor was reported by Sutapun *et al*. in 1999 [31]. Its sensing head was an etched 2–3 cm long fiber Bragg grating, coated with a 560 nm thick Pd film. In 2008, L. Ai, *et al*. presented a volatile-solvent gas fiber sensor based on polyaniline film coated on superstructure fiber Bragg gratings [32]. A first demonstration of biosensor concept based on etched FBG was reported by Chryssis *et al*. in 2005 [33]. The number of biosensing applications exploiting different designs of FBGs is rapidly growing and they are expected to become a key technology in the next few years [34-36].

## 5.4 Grating writing system used for FBG fabrication

FBGs used for the sensor experiments were written on the middle of stripped section of optical fibers using phase-mask writing method at Central Glass and Ceramic Research Institute (CGCRI), a unit lab of Council of Scientific and Industrial Research (CSIR), Kolkota, India. The grating writing system at CGCRI was designed and delivered by TeraXion, a technology leader in the development of advanced optical components for high speed communication networks. BraggStar 500, a pulsed KrF Excimer laser (Wavelength: 248nm, Pulse duration: 20ns, Energy per pulse: 18mJ, Maximum pulse repetition rate: 500Hz) is used as source.

The experimental setup for inscribing gratings is shown in Fig. 5.3. A shutter is used to cutoff the laser when not in use. The UV radiation is brought to the phase mask by multiple reflections and finally focusing using a cylindrical lens. The cylindrical lens and last mirror is kept in a precision motorized translational stage, by the movement of which the laser can be moved across the fiber. The fiber is mounted in another small translational stage so that the distance between fiber and phase mask can be controlled. The fiber aligned perfectly horizontal. The movement of the fiber and phase mask is monitored using a camera through the software.

Optical fiber of about 100cm length is used for writing each grating. To enhance the photosensitivity, the fibers were hydrogen loaded at 100$^{o}$C and 1500 psi of pressure for 24 hours before the grating fabrication. The residual molecular hydrogen which was not used in the photochemical reaction at the time of grating writing has been removed by annealing process. The jacket of the fiber is removed from the middle section, around 6-7cm, using a thermo mechanical stripper supplied by TeraXion. The stripped zone must be thoroughly cleaned using isopropyl alcohol (IPA). The ends of fiber are connected to source and Optical Spectrum Analyzer (OSA). A circulator switch is used in case of FBG to switch between transmission and reflection spectra. The fiber is mounted on the setup using magnetic fiber clamps. Horizontal and vertical alignments of the fiber are done to ensure the beam to fall vertically on the fiber. The online monitoring of the spectrum is done using a white light source (Yokogawa, AQ4305) and OSA (Ando, AQ6317B). The spectrum is also fed to the computer for monitoring thorough the controlling software. The whole system is kept inside a UV protective enclosure. UV protection goggles must be worn during the operation of laser. The grating fabrication setup used in CGCRI is shown in Fig. 5.4.

Different types of optical fibers are used to fabricate the gratings. The major fiber types are

1) CGCRI made photo sensitive fiber (RI-cladding: 1.4563, RI-core: 1.463, Diameter of core: 7.6 micron, Diameter of cladding: 125 micron).

2) Newport make Photo sensitive fiber, F-SBG-15 (RI-cladding: 1.446, RI-core: 1.45, Diameter of core: 8.3 micron, Diameter of cladding: 125 micron).

3) Standard telecommunication fiber, Corning SMF-28e after proper hydrogen loading (RI-cladding: 1.456, RI-core: 1.46145, Diameter of core: 8.28 micron, Diameter of cladding: 125 micron)

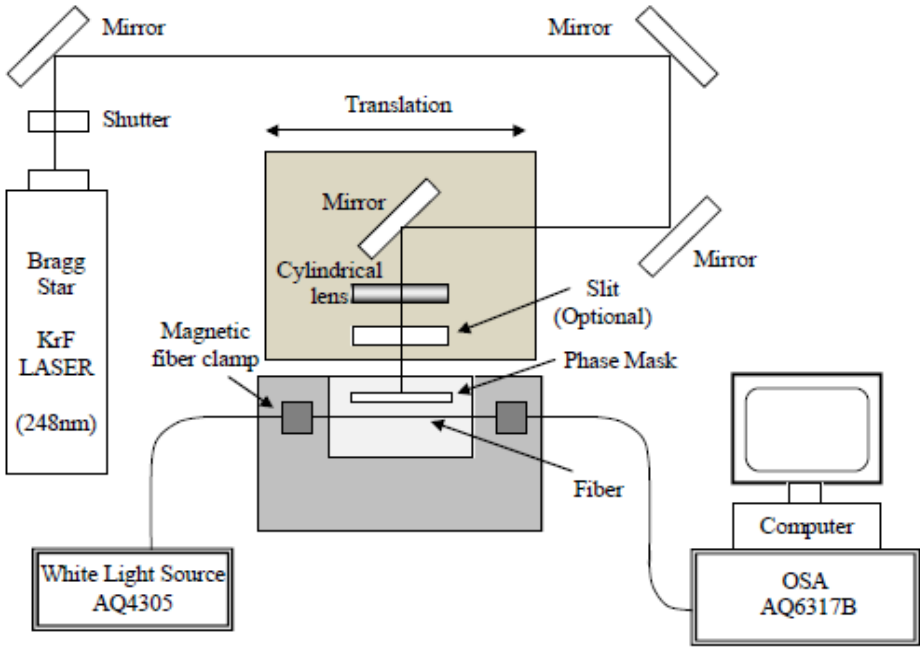


***Figure 5.3:*** *Simplified schematic diagram of the grating writing system at CSIR-CGCRI, Kolkota.*

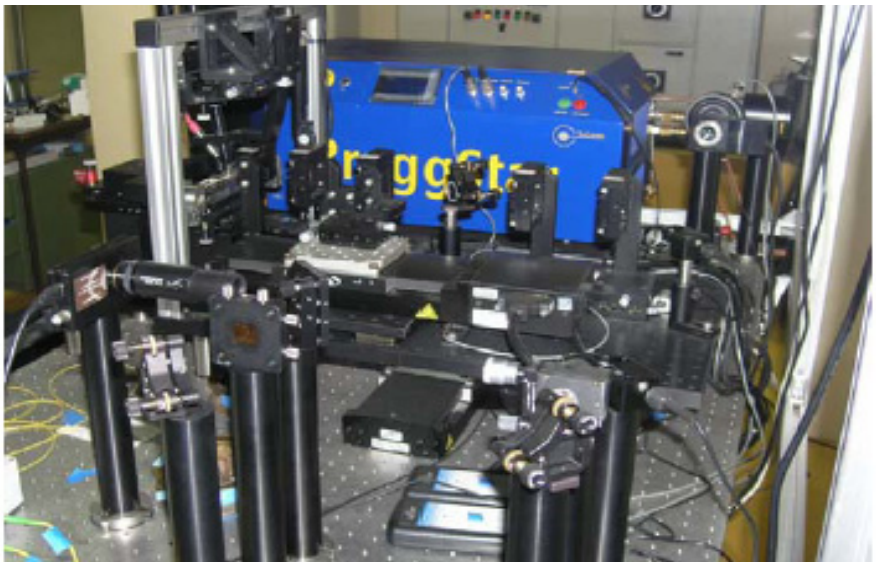

***Figure 5.4:*** *The grating fabrication setup used in CSIR- CGCRI, Kolkota.*

## 5.5 Strain measurement using FBG strain sensor system

Even though the following section on strain and temperature measurement does not relate to etched FBGs, they are included here to get a better understanding of the FBG performance. The basic operation of FBG strain sensor is based on the measurement of the peak wavelength shift induced by the applied strain [7]. The strain sensitivity of the Bragg wavelength arises from the change in period of the fiber, coupled with a change in the refractive index arising from the strain-optic effects. Strain measurements based on FBG is a rapidly developing technology which is driven by its performance accuracy and versatility and is being used for structural monitoring and smart structure applications [8].

### 5.5.1 Experimental setup

The experimental setup for the strain sensitivity of bare fiber Bragg grating system is shown in Fig. 5.5. It consists of a white light source ([Yokogawa] AQ 4305), an optical spectrum analyzer ([Yokogawa] AQ 6319), a coupler and a

cantilever load cell structure. The measurement using this system is made for FBG for a Bragg wavelength of 1564.23 nm. The FBG was fabricated in a CGCRI made photo sensitive fiber using phase mask.

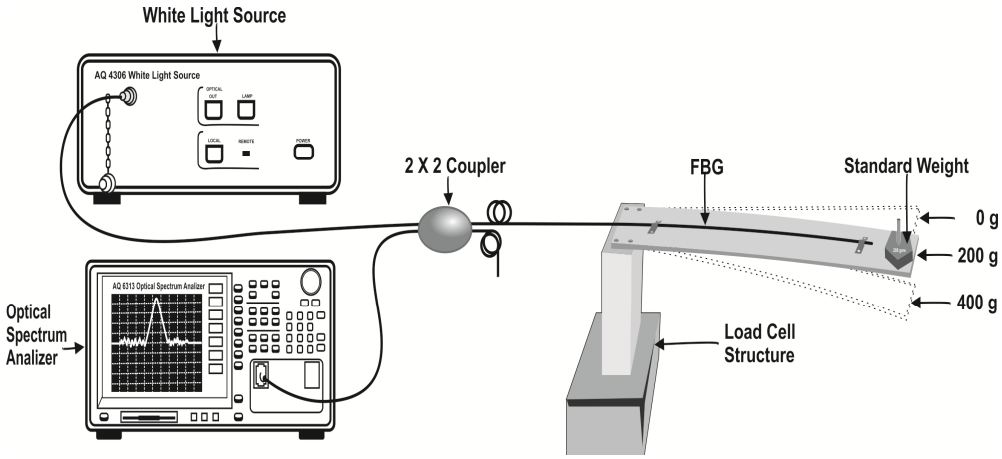


***Figure 5.5:*** *Experimental setup for the measurement of strain.*

The white light source is connected to one input of the coupler. The other input of the coupler is connected to the OSA for detecting the reflected Bragg signal. The FBG is then connected to one of the outputs of the coupler. The cantilever structure is made of spring steel of 4mm thick and 5cm width with a length of 20cm. The cantilever is bolted to a strong pillar with good base. The base is again bolted to a vibration free optical table. The fiber with the FBG is then bonded to the cantilever load cell structure using a fast setting epoxy. Provisions are made on the cantilever structure so that the standard weights are added at the same location to provide repeatability. Sufficient time is provided for settling the strain, to avoid loading transients.

### 5.5.2 The Effect of strain variations on the transmission spectrum of FBG

During the experiment, standard weights of 200gm were added to the cantilever load cell structure in successive steps and the corresponding reflected

spectra were recorded. Sensor responded to strain changes as soon as new weights were introduced to the cantilever load cell structure. But, to get a stabilized output, all readings were taken one minute after loading the set up. To avoid the effect of temperature and for precise measurement, the experimental setup was maintained at 24.0 ± 0.5 °C.

The initial spectrum of the FBG with no load is used as a reference spectrum. The reflection spectrum during loading of cantilever is shown in Fig. 5.6. The transmission spectra were also studied for verifying the obtained results and are shown in Fig. 5.7. In order to check the hysteresis of measurement, spectrums were analyzed during the loading and unloading of cantilever structure (Fig. 5.8).

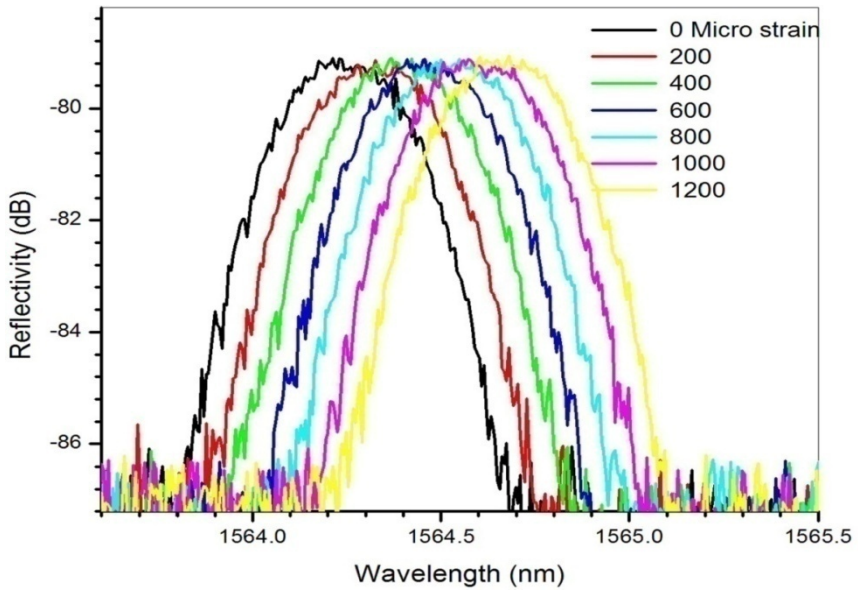


***Figure 5.6:*** *The reflection spectrum of normal FBG for different values of applied strain (During loading of cantilever structure).*

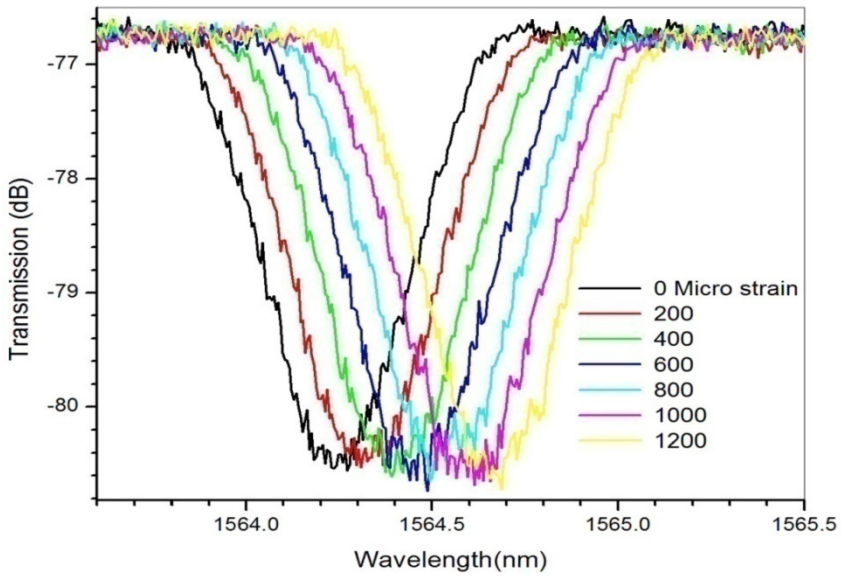


***Figure 5.7:*** *The transmission spectrum of FBG for different values of applied strain (During loading of cantilever structure).*

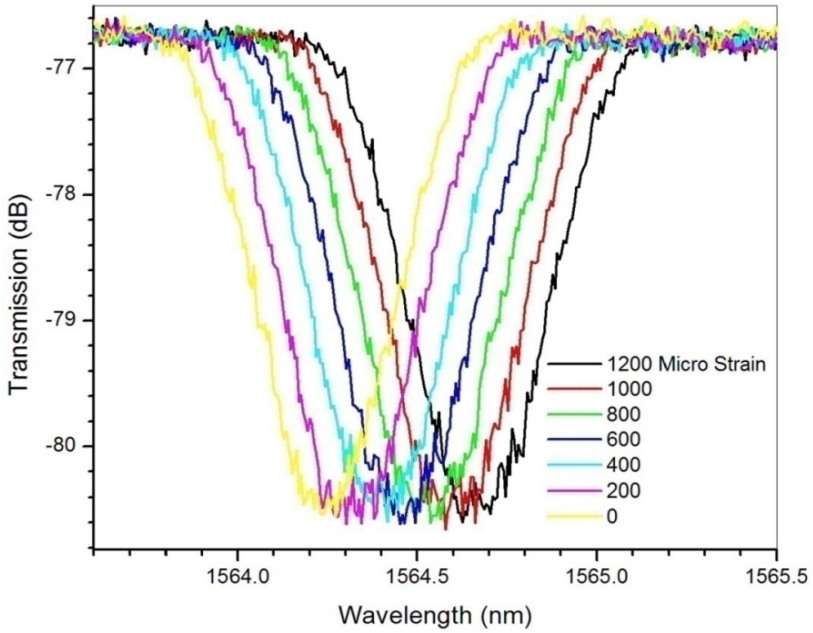


***Figure 5.8:*** *The transmission spectrum of FBG for different values of applied strain (During unloading of cantilever structure).*

The wavelength shift of the FBG with the changes in loading of the structure is shown in Fig. 5.9. The shift at the central wavelength was ranging from 1564.23 to 1564.70 nm for the loading from 0 to 1200g. The structure is loaded many times and checked the reflected spectrum to ensure the repeatability. Shift in wavelength was found linear and repeatable. Transmitted spectrum of the FBG was also measured. The observations were same during the loading and unloading of the structure. The traces were found coinciding, which shows that the hysteresis is negligible. The dependence of the red-shift of the resonance wavelength of the FBG on the applied strain was measured to be 0.39 Pico meter/ μstrain. The good linear relationship between the applied strain and Bragg wavelength has shown the potential of FBG for strain sensing applications.

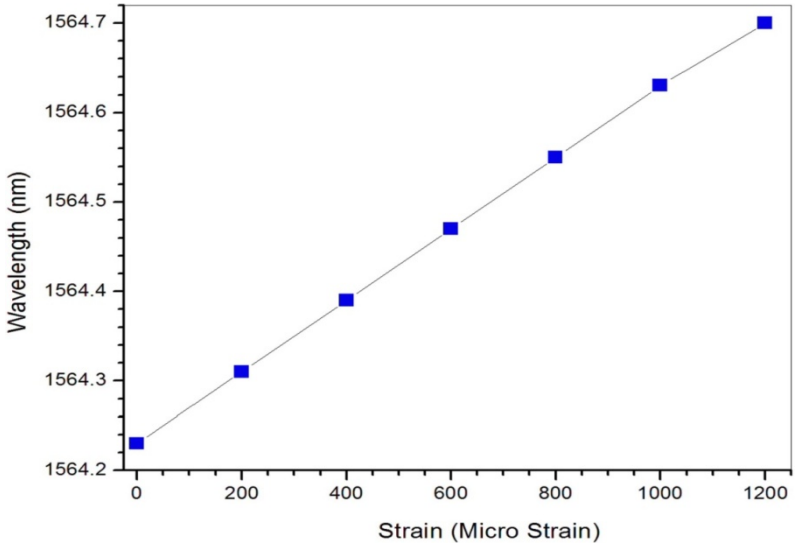


***Figure 5.9:*** *Wavelength Shift of FBG with the applied strain.*

## 5.6 FBG based temperature measurement

The temperature sensitivity of the Bragg wavelength arises from the change in period associated with the thermal expansion of the fiber, coupled with a change in the refractive index arising from the thermo-optic effect [7,9].

### 5.6.1 Experimental setup

The experimental set up for studying temperature sensitivity of unetched fiber Bragg grating system is shown in Fig.5.10. A white-light source ([Yokogawa] AQ 4305) was used as the signal source and the transmission spectra of the FBGs were interrogated with an optical spectrum analyzer (OSA) ([Yokogawa] AQ 6319). FBG central wavelength is 1564.23 nm with a grating length of 10mm. To avoid the effect of strain and bending, the FBG was stretched and then positioned inside a temperature controlled fiber oven. All readings were taken with air as the surrounding medium.

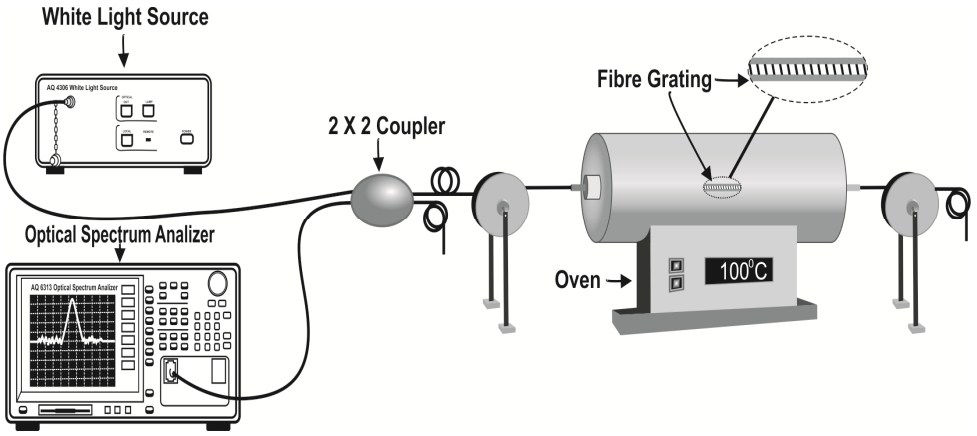


***Figure 5.10:*** *Experimental setup to study the temperature response of FBG.*

### 5.6.2 The Effect of temperature variations on the reflection spectrum of FBG

The FBG was heated from 30°C to 100°C in steps of 10°C using the temperature controller of fiber oven. The oven temperature rises up linearly with an accuracy of 0.1°C. During this process, the reflection spectra were recorded using the optical spectrum analyzer. The Bragg resonance wavelength shifts experienced by the FBG as a function of increasing temperature is shown in Fig. 5.11.

We observed a spectral shift to longer wavelengths (red shift) with increasing temperature and the wavelength shift of the peak was also linear as shown in Fig. 5.12.

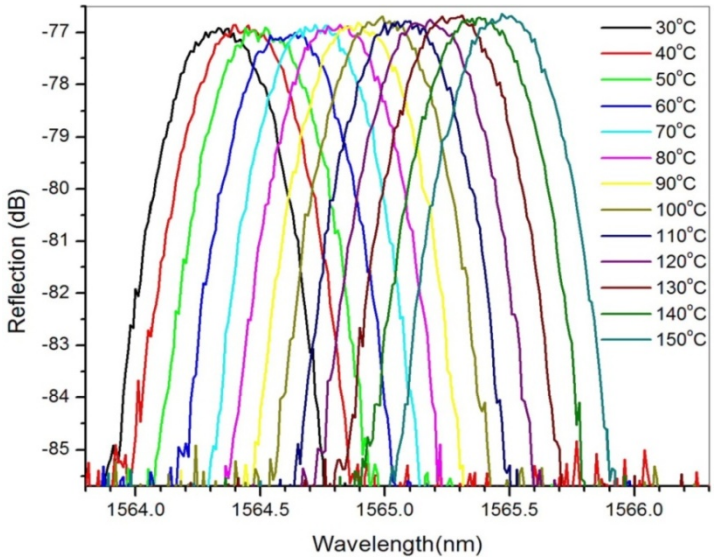


***Figure 5.11:*** *Reflection Spectra of the FBG as a function of increasing temperature.*

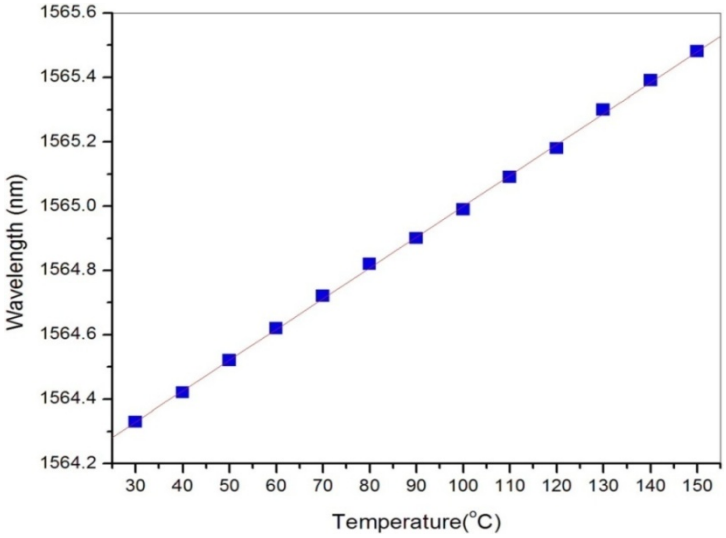


***Figure 5.12:*** *Plot of the Bragg Wavelength of the FBG, as a function of temperature.*

As evident from figures 5.11 and 5.12, the grating exhibited a linear variation in the shift of Bragg wavelength with temperature over a wide range. The dependence of the red-shift of the resonance wavelength of the FBG on the increasing temperature was measured to be 0.0095 nm/ °C. The good linear relationship between temperature and Bragg wavelength has shown the potential of using FBG for different temperature sensing applications.

## 5.7 Fabrication of etched FBGs

To make the FBGs sensitive to changes in the surrounding refractive index, the cladding radius around the grating region was reduced by wet chemical etching in a buffered hydrofluoric acid (HF 48%) solution. The experimental set-up used for monitoring the grating spectra during etching process is shown in Fig. 5.13. It comprises of a white light source, a directional 3dB coupler to collect the reflected spectrum from the sensor head and an optical spectrum analyzer for spectral measurements. For the etching purpose HF solution was taken in a special Teflon mount, which is non reactive to HF. The Teflon mount has an inlet and an outlet provision and the dimensions were suitably selected to facilitate the process of etching and sensor operation.

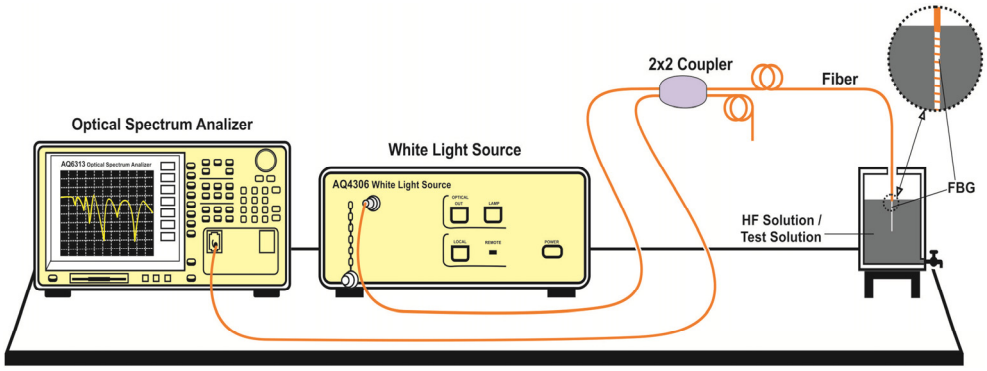


***Figure 5.13:*** *Experimental setup for FBG etching.*

### 5.7.1 The effect of etching on Bragg spectral response

The FBGs were individually chemically etched in HF solution and during the chemical etching process the Bragg wavelength shift relative to the initial Bragg wavelength was monitored in real time. During the process of etching, the room temperature was maintained at 25°C. Two 7 mm-length FBGs with very approximate Bragg wavelengths 1564.25 nm (FBG-1); 1534.81 nm (FBG-2) were selected for the experimental purpose. The FBG-1 was written in a CGCRI made photo sensitive fiber and FBG-2 in a Newport made Photo sensitive fiber, F-SBG-15.

The procedure of measuring the Bragg peak shift was as follows: The zero time was defined when the FBG was dipped into HF solution. At this zero time, the Bragg peak was recorded to serve as the reference. The shift in the Bragg wavelength was recorded with respect to etching time.

#### 5.7.1.1 Spectral shift of FBG-1 during etching process

The FBG-1 was chemically etched for a period of 35.42 minutes in 48% HF solution. Figure 5.14 shows the shift in the Bragg wavelength with respect to etching time of FBG-1. Monitoring the reflection spectra during etching revealed two distinct trends. For the first 32.24 minutes, the spectrum slowly moves towards longer wavelengths (Fig 5.15). The increase in Bragg wavelength $\lambda_B$ from A to B is due to generation of heat caused by chemical reaction of HF with silica glass. This increase in temperature reflects as the red shift in grating spectra. The change in strain during the thinning process also contributes to this initial red shift slightly [2,5,14]. The FBG-1 etching spectra showed a red shift of 0.51 nm in the region A to B. ie. From time t=0 to t=32.24 minutes.

After 32.25 minutes of etching, the Bragg wavelength shows an abrupt blue shift. i.e. from B towards C. In this region the optical mode begins to penetrate the cladding liquid interface and produces corresponding spectral changes. The blue shift in $\lambda_B$ can be attributed to the predominance of effective refractive index change caused by cladding diameter reduction over the effect due to temperature variation [2,14-16]. Figure 5.16 shows the relative peak reflectivity observed during the final stages of etching process. It can also be seen that the reflectivity of FBG decreases with etching in the final period (Fig 5.17). This effect can be explained by considering the change in numerical aperture between the unperturbed fiber and the etched region depending on the refractive indices of core, cladding and surrounding medium [5,17]. This feature is an indication that the fiber diameter approaches the fiber core diameter and, if the chemical etching is not interrupted, the FBG and the fiber can be destroyed.

To stop the etching process at the desired fiber diameter, the HF solution was removed and to restrict the etching activity the Teflon tube was filled with deionized water. A final shift of 0.17 nm in the Bragg wavelength has been measured between unperturbed and etched grating with air as external medium. Experimentally we also found that the sharpness of the reflection spectrum of FBG degrades after chemical etching. The spectrum of FBG-1 before etching and after partial etching of the cladding is depicted in Fig. 5.18**,** where a shift in the Bragg spectrum to lower wavelengths is observed due to lowering of the effective refractive index in the thinned region.

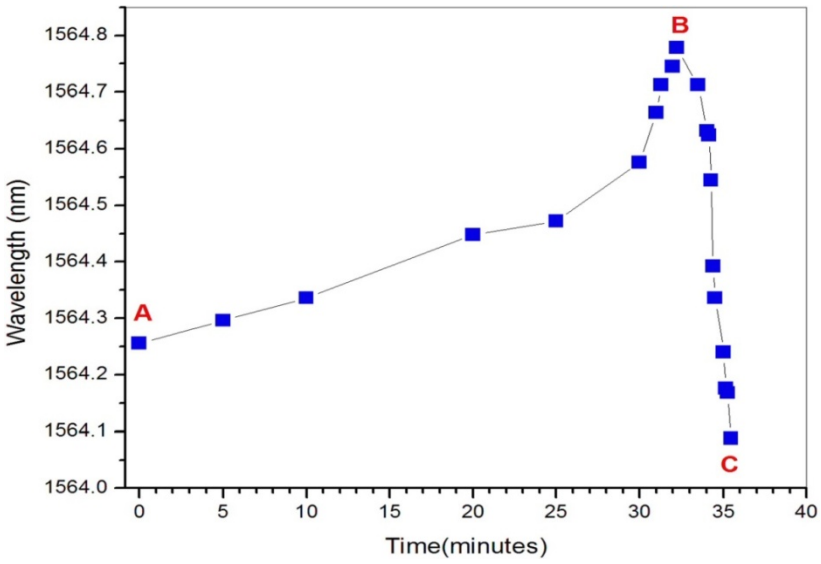


***Figure 5.14:*** *Bragg peak wavelength with time during HF etching process of FBG-1.*

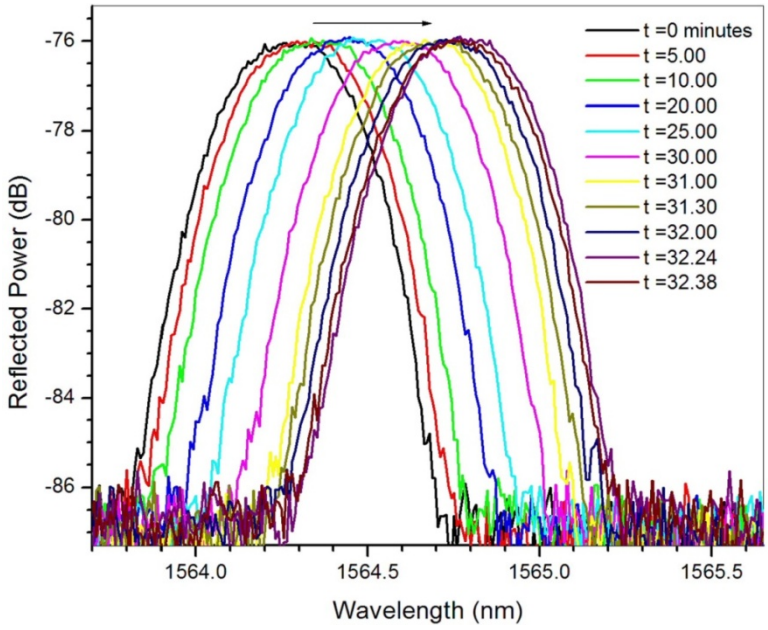


***Figure 5.15:*** *Bragg reflectivity versus wavelength shift (red shift) during the etching process of FBG-1.*

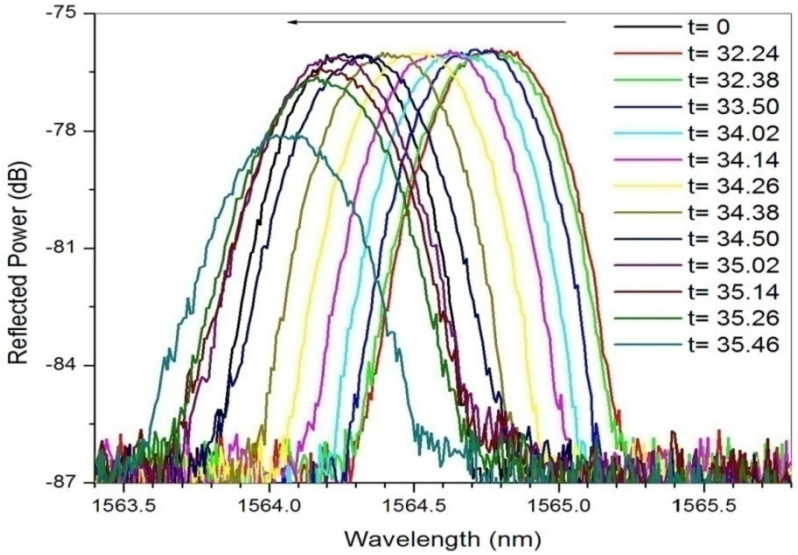


***Figure 5.16:*** *Bragg reflectivity versus wavelength (blue shift) for final stages of the etching* process.

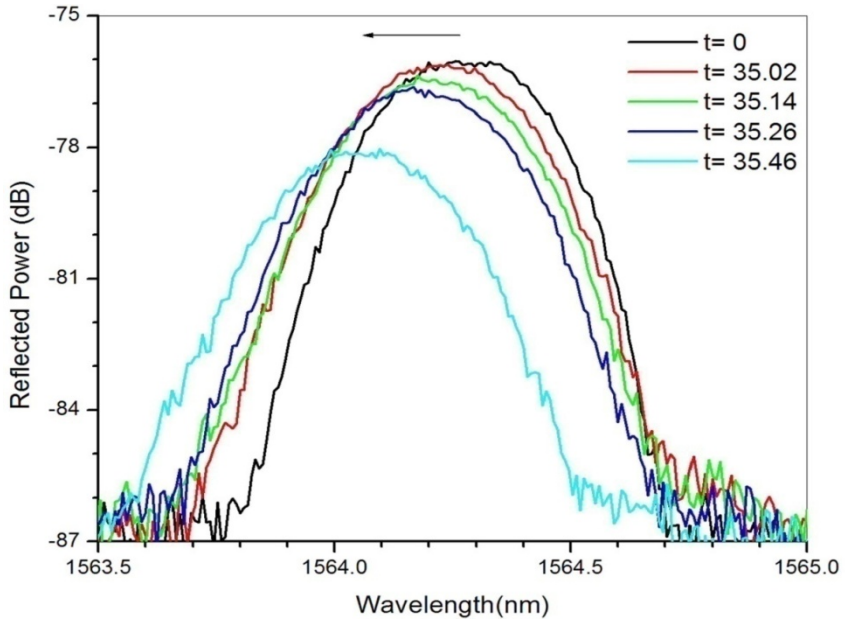


***Figure 5.17:*** *Bragg reflectivity versus wavelength (blue shift) for last minute of the etching process.*

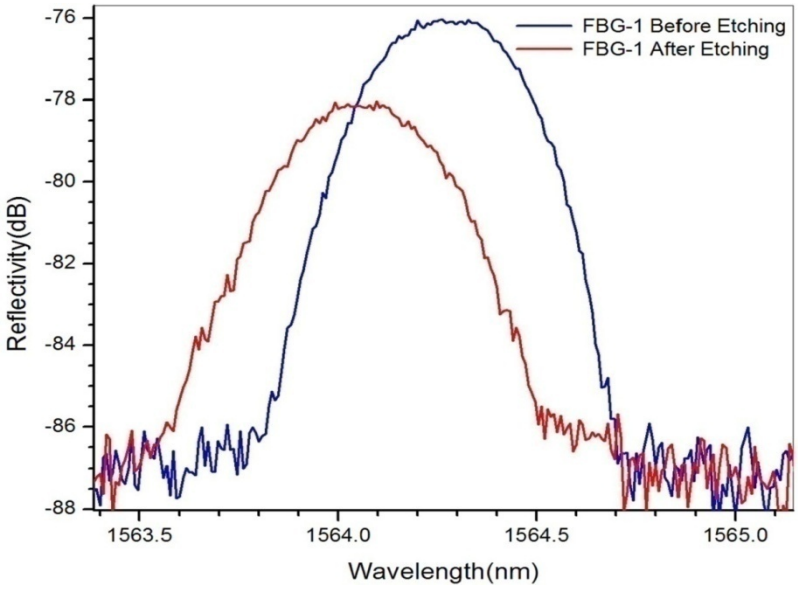


***Figure 5.18:*** *Spectrum of the FBG-1 before and after the HF etching.*

After an etching time of 35.46 minutes the refractive index sensitivity of FBG-1 was assessed by immersing it into different samples of varying refractive indices.

### 5.7.1.2 Spectral Shift of FBG-2 During Etching Process

The FBG-2 was chemically etched for a period of 31.58 minutes in 48% HF solution. Figure 5.19 shows the spectral shift of FBG-2 written in Newport fiber. For the first 30.46 minutes, the spectrum slowly moves towards longer wavelengths. The red shift during etching process was only 0.14 nm, which is very low compared to FBG -1. After 30.46 minutes of etching, the Bragg wavelength shows an abrupt blue shift. Figure 5.20 shows the relative peak reflectivity observed during the final stages of etching process. To stop the etching process at the desired fiber diameter, the HF solution was removed and to restrict the etching activity the Teflon tube was filled with deionized water after 31.58 minutes.

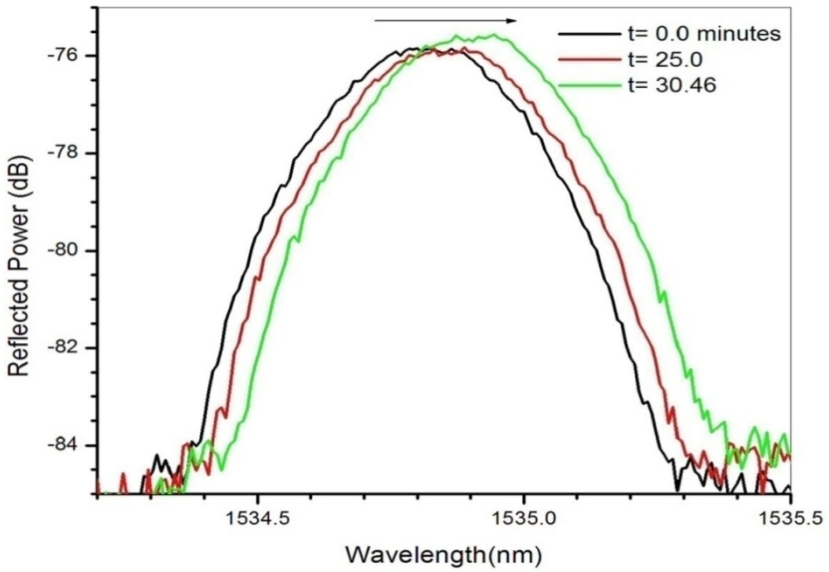


***Figure 5.19:*** *Bragg reflectivity versus wavelength shift (red shift) during the etching process of FBG-2.*

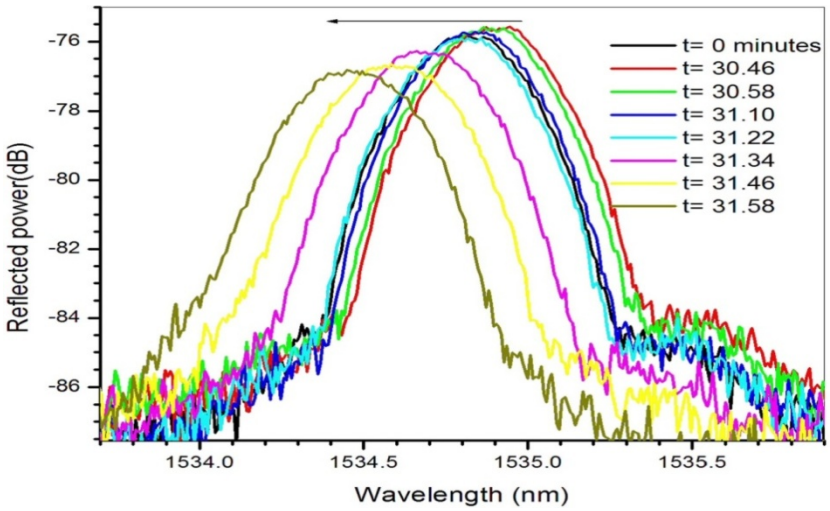


***Figure 5.20:*** *Bragg reflectivity versus wavelength (blue shift) for final period of the etching process of FBG-2.*

A final shift of 0.35 nm in the Bragg wavelength between unperturbed and etched grating with air as external medium has been measured. The spectrum of FBG-2 before etching and after partial etching of the cladding is depicted in Fig. 5.21.

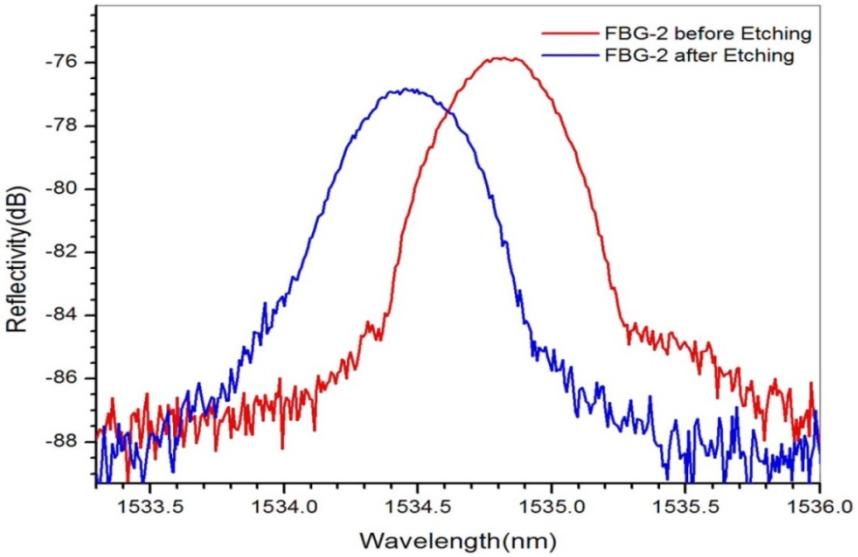


***Figure 5.21:*** *Spectrum of the FBG-2 before and after the HF etching.*

## 5.8 Spectral Shift of Etched FBGs with Change in External Refractive Index

### A. Surrounding Refractive Index Sensitivity of FBG-1 (RI-cladding: 1.4563, RI-core: 1.463)

Experimental characterization of the sensor response to external refractive indices varying in the range 1.000–1.4680 has been carried out by using a white light source and an optical spectrum analyzer. Figure 5.22 plots the behavior of etched FBG-1 versus outer medium refractive indices. An etched fiber has a core and some portion of the original cladding. Before each measurement, the sensor was submerged into isopropyl alcohol to clean any residue left out from the previous measurement. Since the principle of operation relies on the interaction between the evanescent wave of the fundamental guided mode and the surrounding medium, it is obvious to expect the effective refractive index variations, and then, the corresponding Bragg wavelength shift. For an external RI around 1.33, the guided mode is well confined in the core region, leading to a weak evanescent wave and thus

low surrounding refractive index sensitivity. As the surrounding medium RI increases, higher sensitivity is observed, since the fundamental mode is less confined in the core region leading to a higher evanescent field and thus to a more efficient interaction with the external medium [2,14,19].

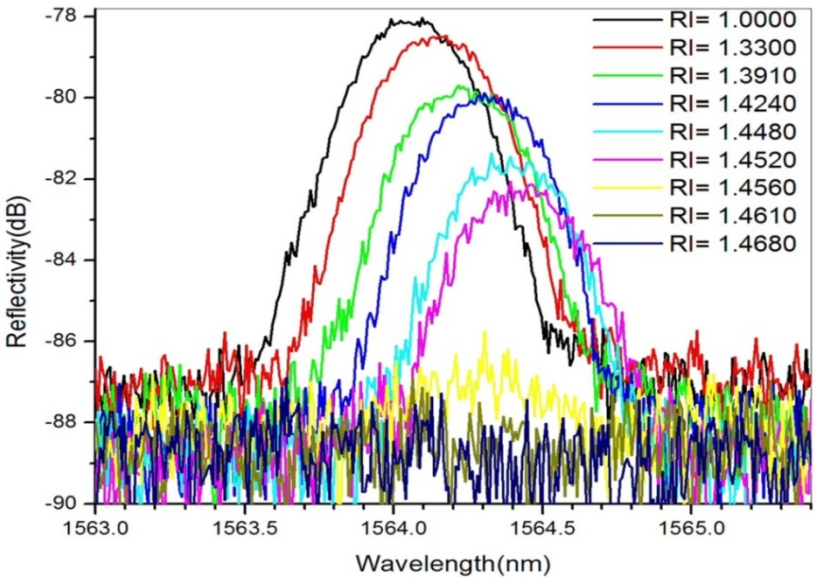


***Figure 5.22:*** *Bragg wavelength of the etched FBG-1 with changes in surrounding medium refractive index.*

From the results it can be seen that the Bragg wavelength increases, as the surrounding index increases and approaches the core refractive index. The rate of change in wavelength with surrounding index also increases as the surrounding index approaches the fiber cladding index (1.4563). The FBG-1 exhibited a total red shift of approximately 0.35 nm when the value of surrounding medium was gradually changed from 1.0 to 1.4520. It can also be seen that the reflected power decreases as the spectrum shows red shift with increase in RI. This effect can be explained by considering the difference in the numerical aperture between the un-etched and thinned optical fibers [2]. When the outer RI becomes equal or greater than the cladding RI, the guided wave becomes leaky and no reflection will be

obtained. As Fig. 5.22 illustrates, there was no reflection when the outer RI becomes equal or greater than the effective RI of core as expected.

The large value of the sensitivity obtained in the sensor can be used to measure small changes in refractive index of the surrounding medium. This can also be used to measure the presence and amount of chemical or biological agents with an excellent degree of accuracy [20-25].

## B. Surrounding Refractive Index Sensitivity of FBG-2 ( RI-cladding: 1.446, RI-core: 1.45)

The changes of the FBG-2 reflection spectra with the changes in the RI of the external medium are shown in Fig. 5.23. When we changed the SRI from 1 to 1.4410, a shift of the resonance bands towards the longer wavelength (red shift) side can be seen. This wavelength shift occurs due to the increase in the SRI which in turn increases $n_{eff}$ of the FBG. The highest RI sensitivity of FBG is observed when the external medium index is close to that of the cladding index (1.446).

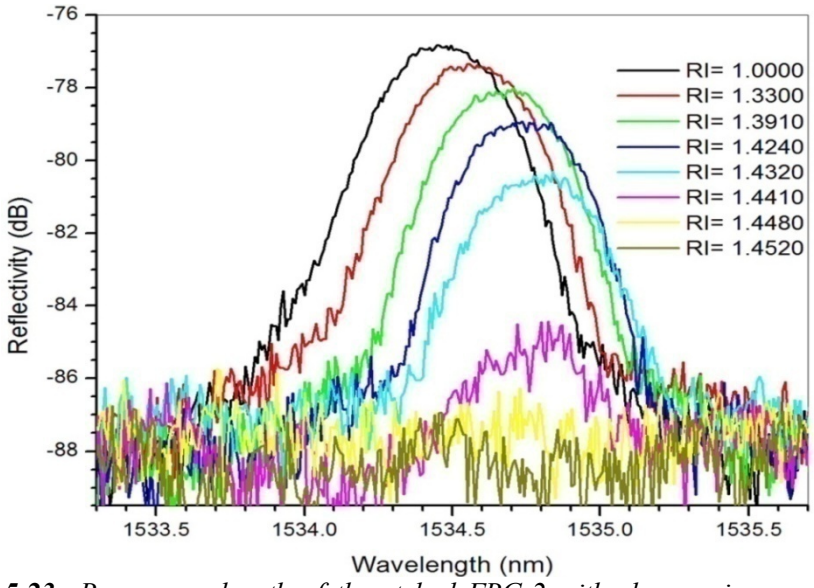


***Figure 5.23:*** *Bragg wavelength of the etched FBG-2 with changes in surrounding medium refractive index.*

There is no reflection when the ambient index is higher than that of the cladding. Unlike FBG-1, the reflection spectra of FBG-2 disappeared for external refractive index values greater than 1.4480. The FBG-1 was fabricated in a CGCRI made photo sensitive fiber for which cladding index is 1.4563 and FBG-2 in a Newport made photo sensitive fiber for which cladding index is only 1.446. So the FBGs will give different external refractive index responses based on the RI of cladding.

## 5.9 Conclusions

In conclusion, highly sensitive etched fiber Bragg grating sensors have been demonstrated which detect the change of index of the surrounding medium by measuring the change of the Bragg wavelength. Bragg wavelength showed a red shift as the surrounding index increased and the rate of change in wavelength with RI also increased as the surrounding index approached the fiber cladding index. The reduction in reflected optical power with increase in surrounding RI is explained on the basis of mismatch of the numerical aperture between the un-etched and etched FBG. Although there are many RI sensors based on etched FBG in the literature, they are very difficult to fabricate and careful handling is also required as a very thin FBG portion is used for sensing. Although it gives very high sensitivity, it can break very easily and is prone to micro-bending.

This chapter also investigated the strain and temperature responses of FBGs. The dependence of the red-shift of the Bragg wavelength of the FBG on the applied strain was measured to be 0.39 pm/μstrain. During temperature measurement the wavelength shift was found linear and repeatable within the range of 30-150$^0$C. The dependence of the red-shift of the Bragg wavelength of the FBG on increasing temperature was measured to be 0.0095 nm/ °C. The developed RI sensor can be used to detect chemical or biological changes in the surrounding media. These sensors can be used for medical, pharmaceutical, and food industry applications.

## References


[1]. A. Asseh, S. Sandgren, H. Ahlfeldt, B. Sahlgren, R. Stubbe and G. Edwall, "*Fiber optical Bragg grating refractometer*", Fiber and Integrated Optics, **17**, pp. 51–62 (1998).

[2]. A. Iadicicco, A. Cusano, S. Campopiano, A. Cutolo and M. Giordano, "Thinned fiber Bragg gratings as refractive index sensors", IEEE Sensors Journal, **5**, pp. 1288-1295 (2005).

[3]. A. N. Chryssis, S. M. Lee, S. B. Lee, S. S. Saini, and M. Dagenais, "High sensitivity etched core fiber Bragg grating sensors," IEEE Photonics Technology Letters, **17**, pp. 1253–1255 (2005).

[4]. R. C. Kamikawachi , I. Abe, A. S. Paterno, H. J. Kalinowski, M. Muller, J. L. Pinto and J. L. Fabris, "*Determination of thermo-optic coefficient in liquids with fiber Bragg grating refractometer*", Optics Communications, **281**, pp. 621–625 (2008).

[5]. D. A. Pereira, O. Frazão and J. L. Santos, "*Fiber Bragg grating sensing system for simultaneous measurement of salinity and temperature*", Optical. Enineering, **43**, pp. 299-304 (2004).

[6]. U. S. Raikar, A. S. Lalasangi, V. K. Kulkarni and J. F. Akki, "*Concentration and Refractive Index Sensor for Methanol Using Short Period Grating Fiber*", International Journal for Light and Electron Optics, **122**, pp. 89-91 (2011).

[7]. A.D. Kersey, M.A. Davis and H.J. Patrick, *"Fiber grating sensors",* Journal of Lightwave Technology, **15**, pp. 1442 -1463 (1997).

[8]. L. Ren, J. Chen, H. N. Li, G. Song and X. Ji, "*Design and application of a fiber Bragg grating strain sensor with enhanced sensitivity in the small scale dam model*", Smart Materials and Structures, **18**, pp. 035015 (2009).

[9]. J. Yang, Y. Zhao, B. J. Peng, X. Wan, "*Temperature-compensated high pressure FBG sensor with a bulk-modulus and self-demodulation method*", Sensors and Actuators A: Physical, **118**, pp. 254–258 (2005).

[10]. V. Bhatia and A. M. Vengsarkar, "*Optical fiber long period gratings sensors*", Optics Letters, **21**, pp. 692 – 694 (1996).

[11]. X. Shu and D. X. Huang, "*High sensitive chemical sensor based on the measurement of the separation of dual resonant peaks in a 100 μm period fiber grating*", Optics Communications, **171**, pp. 65–69 (1999).

[12]. X. Shu, X. L. Zhang and I. Bennion, "Sensitivity characteristics of long-period fiber gratings," J. Lightwave Technology, **20**, pp. 255–266 (2002).

[13]. J. A. Barnes, R. S. Brown, A. H. Cheung, M. A. Dreher, G. Mackey and H. P. Loock, "*Chemical sensing using a polymer coated long-period fiber grating interrogated by ring-down spectroscopy*", Sensors and Actuators B: Chemical, **148**, pp. 221–226 (2010).

[14]. A. Iadicicco, A. Cusano, A. Cutolo, R. Bernini and M. Giordano, "*Thinned fiber Bragg gratings as high sensitivity refractive index sensor*", IEEE Photonics Technology Letters, **16**, pp. 1149-1151 (2004).

[15]. A. Iadicicco, S. Campopiano, A. Cutolo, M. Giordano and A. Cusano, "*Self temperature referenced refractive index sensor by non-uniform thinned fiber Bragg gratings*", Sensors and Actuators B: Chemical, **120**, pp. 231–237 (2006).

[16]. W. Liang, Y. Y. Huang, Y. Xu, R. K. Lee and A. Yariv, "*Highly sensitive fiber Bragg grating refractive index sensors*", Applied Physics Letters, **86**, pp. 151122-24 (2005).

[17]. H. Xue Feng, C. Zhe Min, S. Li Yang, C. Ke Fa, S. De Ren, C. Jun and Z. Hao, "*Design and characteristics of refractive index sensor based on thinned and microstructure fiber Bragg grating*", Applied Optics, **47**, pp. 504-511 (2008).

[18]. A. Cusano, A. Iadicicco, S. Campopiano, M. Giordano and A. Cutolo, "*Thinned and micro-structured fibre Bragg gratings: towards new allfibre high-sensitivity chemical sensors*", Journal of Optics A: Pure and Applied Optics, **7**, pp. 734-741 (2005).

[19]. K. Zhou, X. Chen, L. Zhang, I. Bennion, "*Implementation of optical chemsensors based on HF-etched fibre Bragg grating structures*", Measurement Science and Technology, **17**, pp. 1140-1145 (2006).

[20]. V. V. Spirin, M. G. Shlyagin, S. V. Miridonov, F. J. M. Jimenez and R. M. L. Gutierrez, "*Fiber bragg grating sensor for petroleum hydrocarbon leak detection*", Optics and Lasers in Engineering, **32**, pp. 497–503 (1999).

[21]. Q. Jiang, D. B. Hu and M. Yang, "*Simultaneous Measurement of Liquid Level and Surrounding Refractive In-dex Using Tilted Fiber Bragg Grating*", Sensors and Actuators A: Physical, **170**, pp. 62-65 (2011)

[22]. J. Kumar, R. Mahakud, O. Prakash and S. K. Dixit, "*Study on hydrofluoric acid-based clad etching and chemical sensing characteristics of fiber Bragg gratings of different reflectivity fabricated under different UV exposure times*", Optical Engineering, **52**, pp. 054402-07 (2013).

[23]. F. K. Coradin, G. R. C. Possetti, R. C. Kamikawachi, M. Muller and J. L.Fabris, "*Etched fiber Bragg gratings sensors for water-ethanol mixtures: A comparative study*", J. Microwave optoelectronics electromagnetic applications, **9**, pp. 131–143 (2010).

[24]. J. Kumar, R. Mahakud, O. Prakash and S. K. Dixit, "*HF based clad etching of fibre Bragg grating and its utilization in concentration sensing of laser dye in dye–ethanol solution*", Pranama-Journal of Physics, **82**, pp. 265–269 (2014).

[25]. B. N. Shivananju, M. Renilkumar, G. R. Prashanth, S. Asokan and M. M. Varma, "*Detection Limit of Etched Fiber Bragg Grating Sensors*", Journal of Lightwave Technology, **31**, pp. 2441-2447 (2013).

[26]. Y. Yuan, L. Wang, L. Ding and Y. Chenhui Wu., "*Theory, experiment, and application of optical fiber etching*", Applied Optics, **51**, pp. 5845–5849 (2012).

[27]. N. Chen, B. Yun, Y. Wang and Y. Cui, "*Theoretical and experimental study on etched fiber Bragg grating cladding mode resonances for ambient refractive index sensing*", Journal of the Optical Society of America B, **24**, pp. 439–445 (2007).

[28]. N. Chen, B. Yun and Y. Cui, "*Cladding mode resonances of etch eroded fiber Bragg grating for ambient refractive index sensing*", Applied Physics Letters, **88**, pp. 133902 (2006).

[29]. Q. Zhou, T. Ning, L. Pei, C. Li, "*Spectral characterization of fiber Bragg grating with etched fiber cladding*", Optoelectronics Letters, **8**, pp. 328–331 (2012).

[30]. H. K. Bal, Z. Brodzeli, N. M. Dragomir, S. F. Collins and F. Sidiroglou, "*Uniformly thinned optical fibers produced via HF etching with spectral and microscopic verification*", Applied Optics, **51**, pp. 2282–2287 (2012).

[31]. B. Sutapun, M. Tabib-Azar and A. Kazemi, "*Pd-coated elastooptic fiber optic bragg grating sensors for multiplexed hydrogen sensing*", Sensors and Actuators B: Chemical, **60**, pp. 27–34 (1999).

[32]. L. Ai, J. C. Mau, W. F. Liu, T. C. Chen and W. K. Su, "*A volatile solvent gas fiber sensor based on polyaniline film coated on superstructure fiber Bragg gratings*", Measurement Science and Technology, **19,** pp. 017002-017006 (2008).

[33]. A. N. Chryssis, S. S. Saini, S. M. Lee, Y. Hyunmin, W. E. Bentley and M. Dagenais "*Detecting Hybridization of DNA by Highly Sensitive Evanescent Field Etched core Fiber Bragg Grating Sensors*", IEEE J. Selected Topics: Quantum Electronics, **11**, pp. 864–872 (2005).

[34]. S. S. Saini, C. Stanford, S.M. Lee, J. Park, P. Deshong, W. E. Bentley and M. Dagenais, "*Monolayer detection of Biochemical agents using etched-core fiber Bragg grating sensors*", IEEE Photonics Technology Letters, **19**, pp. 1341–1343 (2007).

[35]. V. Mishra, N. Singh, U. Tiwari and Pawan Kapur, "*Fiber grating sensors in medicine: Current and emerging applications*", Sensors and Actuators A: Physics, **167**, pp. 279–290 (2011).

[36]. G. Ryu, M. Dagenais, M. T. Hurley and P. Deshong, "*High specificity binding of lectins to carbohydrate-functionalized fiber Bragg gratings: A newmodel for biosensing applications*", IEEE Journal of Quantum Electronics, **16**, pp. 647–653 (2010).

Chapter 6

# Etched and DNA Coated Fiber Bragg Grating Sensing System for Protein Concentration Measurement

*Abstract*

*In this chapter, we propose a novel method for measuring the concentration of protein (Bovine Serum Albumin) present in bio-chemical samples. The bio sensor exploits the inherent characteristics of the Fiber Bragg Grating (FBG) coated with a biopolymer, deoxyribonucleic acid (DNA). For increased sensitivity, the fiber with FBG was etched with hydrofluoric acid (HF) prior to coating with the DNA. The etched FBGs are sensitive to an external analyte by evanescent field interaction. The sensing mechanism is based on the interaction of the protein with the biopolymer film, which changes the film refractive index resulting in a shift in the Bragg wavelength. By analyzing the Bragg wavelength shift, we can calculate the amount of protein present in the sample solution. A complete experimental analysis, based on the use of an etched and coated FBG for protein concentration measurement, is being presented.*

T. M . Libish *et al*., Optoelectronics and Advanced Materials-Rapid Communications, 9 (11), pp. 1401-1405 (2015).

## 6.1 Motivation

Proteins form a major class of biomolecules and there is much interest to detect proteins because they are widely employed to diagnose the presence of diseases. Today, the protein concentration measurement is very important and has significant applications in medical diagnostics, drug discovery, food and biotechnology. Currently analytical techniques like Gas Chromatography- Mass Spectroscopy (GC-MS) and High Performance Liquid Chromatography-Mass Spectroscopy (HPLC-MS) are commonly used. But most of these techniques have the disadvantage that they are expensive, time consuming and require skilled and well-trained technicians to perform the analysis. So, a fiber optic based biosensor will be a promising alternative to the classical analytical methods due to its simplicity, relatively low cost, inherent specificity, ability to perform sensing using a small amount of sample and rapid response. FBG sensors are one of the most exciting developments in the field of optical fiber sensors in recent years[1-5]. FBGs make promising candidates as sensors because of their significant sensing advantages, the most important of which is that the information on a measurand is encoded in the reflected or transmitted wavelength from the grating. Thus problems associated with source power fluctuations, bending losses and reflection losses are eliminated.

To use the FBG as an effective refractometric sensor element, the cladding radius around the grating region must be reduced, allowing the effective refractive index of the fiber core to be significantly affected by the refractive index of the external medium [7-9]. As a consequence, shifts are expected in the Bragg wavelength combined with a modulation of the reflected amplitude. A very simple method to reduce the cladding can be the uniform chemical etching of the Bragg grating section of the fiber using hydrofluoric acid [10,11]. The sensitivity of the sensor depends on the change in the effective index of the core mode, which is related to the change in the refractive index of the biological or chemical sample

under test [12-20]. The etched FBGs can be made to detect extremely low concentrations of biochemical target molecules by applying suitable material coatings on their surface. These coatings selectively react with specific target molecules and result in the refractive index change. The presence of a specific target molecule is detected by analyzing the Bragg wavelength shift of the FBG reflection spectra. Therefore, FBGs are ideal candidates for biomolecular and chemical sensing applications [21-26], if properly complemented with suitable chemically sensitive materials or biorecognition elements.

The bio sensing device demonstrated in this chapter consists of an etched FBG coated with a biopolymer material, DNA. The selective interaction of the protein with DNA leads to a change in refractive index of the material coating. This interaction may also exert some small strain on the underlying fiber. Contribution to the wavelength shift by the strain is reported to be negligibly small [27]. As a result, both shift in the Bragg wavelength and reflectivity can be attributed to the concentration of protein in bio samples. Protein concentration measurement can be done by analyzing the relation between Bragg wavelength shift and amount of protein present in test solutions. The basic configuration of the sensor is shown in Fig. 6.1.

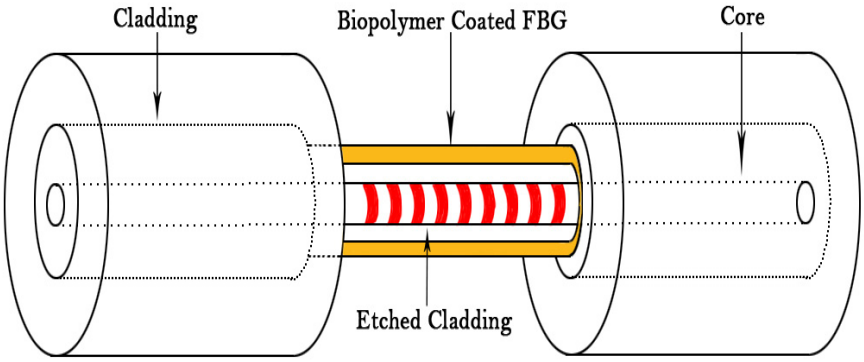


***Figure 6.1:*** *Structure of the biopolymer coated etched FBG sensor.*

## 6.2 Experiments

### 6.2.1 Materials and methods

The DNA used for our experiment was commercially made available from Sigma Aldrich, USA. The available DNA was a double stranded and was rich in sodium salt. The extracted DNA was in white fibrous form and was used without any further purification. It was found that this DNA, from salmon fish was soluble only in water. This property is not amenable for DNA to be dip coated into FBGs, as the resulting coating will be vulnerable to water absorption and will affect the mechanical strength of coated FBGs. Therefore, it is necessary to perform certain processing steps [28], so that the DNA will become suitable for fiber coating. DNA is naturally negatively charged due to the phosphate groups in the backbone of the double helical structure. They form electrostatic charged pairs with the sodium cations in aqueous solution. The processing techniques involve the removal of sodium salt by precipitating with a cationic surfactant, hexadecyltrimethylammonium bromide (CTAB). This surfactant replaces the cationic sodium salt with its long alkyl chain containing positively charged nitrogen by an ion exchange reaction, forming DNA-CTMA (hexadecyltrimethylammonium). The displaced sodium cation then ionically bonds with the bromide anion of CTAB forming NaBr as the byproduct. The CTAB was chosen for our studies because of its long alkyl chain (>16). A shorter chain might induce poor mechanical property and a longer one would damage the double helical structure of DNA by breaking the hydrogen bonds of the base pairs.

The coating material preparation was done as follows. First, the DNA was dissolved in demineralized water at a concentration of 4g/L by allowing it to dissolve for a day. Magnetic stirring was also done to speed up the process. The DNA solution should be stored at a temperature in the range 20°C to 25°C. CTAB was also prepared by dissolving it in water at a slightly higher concentration

(> 4g/L). This ensured that all sodium cations were replaced by the alkyl chain of CTAB. The surfactant solution was added drop by drop to the DNA solution, while stirring was done continuously. The DNA-CTMA lipid complex then begins to precipitate in the solution. The solution was stirred for few hours and the precipitate was seperated by filtration in vacuum using a nylon filter with a pore size of 0.45µm. During filtration, additional 3-4 liters of distilled water was made to run to ensure that any CTAB, that did not bind to DNA was washed away. The precipitate was then dried in vacuum at 40°C overnight. The resulting DNA-CTMA lipid complex was not soluble in water; however it is soluble in organic solvents such as methanol, ethanol and butanol. So we dissolved the lipid complex in butanol and again filtered using a nylon syringe filter of pore size 0.45µm. During this filtration process the temperature was maintained at $60^0$C [29]. The final solution was quite viscous and suitable as the coating material around FBGs. The measured refractive index of the coating solution was found to be 1.398. The protein powder, Albumin Bovine Fraction V (BSA) was supplied by Sisco research Laborataries (SRS). The test samples were prepared by dissolving BSA in distilled water in different proportions (50 µg/mL to 300 µg/mL.). CTAB was supplied by Ranbaxy fine chemicals Ltd.

### 6.2.2 Fabrication of the sensor and Experimental set up

The processes for producing a fiber grating based bio sensor include fiber hydrogen loading, FBG fabrication, fiber cladding etching and film coating. The fabrication of the sensor has been carried out using an FBG with Bragg reflectivity at 1564.28 nm before etching. FBG was written on the middle of the stripped section of a B-Ge co-doped photosensitive single-mode fiber by the phase mask technique, using a KrF laser operating at 248 nm. The single-mode fiber used had a cladding diameter of 125 micron and a numerical aperture of 0.14. The core and the cladding refractive indices were 1.463 and 1.4563, respectively. To enhance the

photosensitivity, the fiber was hydrogen loaded at 100°C and 1500 psi of pressure for 24 hours before the FBG fabrication.

To make the FBGs sensitive to changes in the surrounding refractive index, the cladding diameter around the grating region was reduced by wet chemical etching in a buffered hydrofluoric acid (HF 48%) solution. For this purpose HF solution was taken in a special Teflon mount, which is non reactive to HF. The behavior of the FBG during the etching process is explained in chapter 5, section 5.7. The experimental set-up for monitoring and for recording the Bragg wavelength shift with variation in protein concentration, is shown in Fig. 6.2. It comprises of a white light source ([Yokogawa] AQ 4305), a 3dB coupler to collect the reflected spectrum from the sensor head, a Teflon mount and an optical spectrum analyzer ([Yokogawa] AQ 6319) for spectral measurements. The Teflon mount has an inlet and outlet provision and the dimensions were suitably selected to facilitate the process of etching and sensor operation. To stop the etching process at the desired fiber diameter, the HF solution was removed and to restrict the etching activity the Teflon mount was filled with deionized water. After an etching time of 33 minutes, a final blue shift of 0.28 nm in the Bragg wavelength was observed between unperturbed and etched grating with air as external medium and is shown in Fig. 6.3. The etched fiber was cleaned by repeatedly washing with isopropyl alcohol and methnol. The FBG was then dipped in DNA coating solution for two minutes using a dip coating machine and withdrawn at a speed slow enough to produce a uniform coating without bead formation. Residual stress and refractive index change after the film deposition was observed which produced a red shift of 0.26 nm and is shown in Fig. 6.3. For precise measurement, the experimental setup and sample solution temperature were maintained at 25.0 ±0.5 °C.

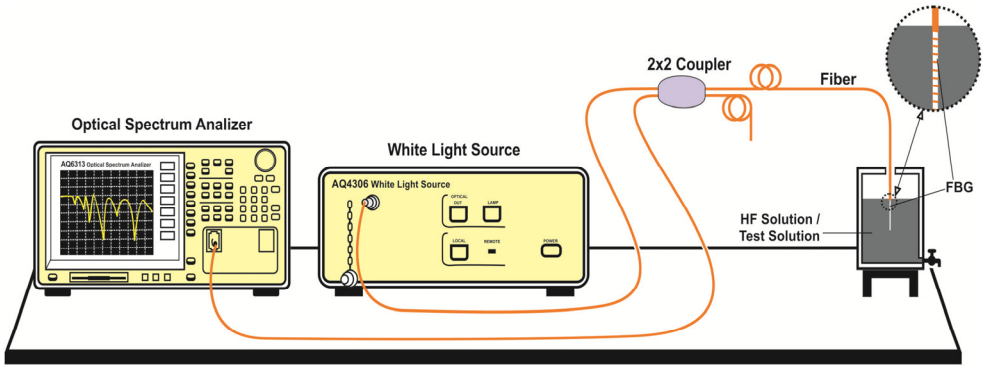


***Figure 6.2:*** *Experimental setup for FBG etching/protein concentration measurement*

.

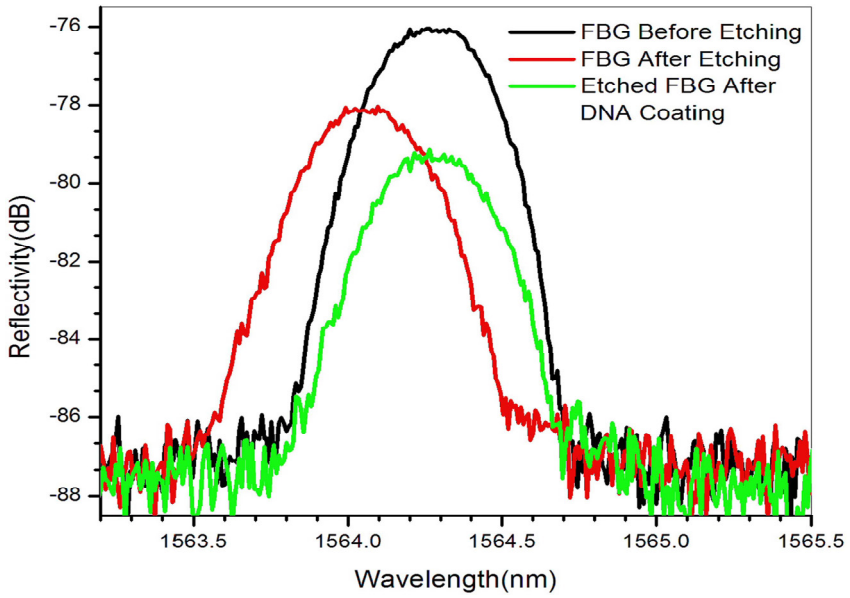


***Figure 6.3:*** *Bragg wavelength and reflectivity before and after the etching.*

## 6.3 Results and Discussion

In our experiment, the Bragg wavelength of the bio polymer coated FBG was monitored, while samples with different protein concentrations were in contact with the sensing region. Since the principle of operation relies on the interaction

between the evanescent wave of the fundamental guided mode and the surrounding medium, it is obvious to expect the effective refractive index variations with change in BSA concentration, and the corresponding Bragg wavelength shift. The concentration of BSA used ranged from 50 µg/mL to 300 µg/mL. Before each measurement, the sensing element was immersed in deionized water to clean any residue left out from the previous measurement. After this cleaning and proper drying, when we exposed the DNA-coated FBG to air, the Bragg wavelength returned to its original wavelength without any deformation in the transmission spectral shape. This demonstrates the reversibility and reusability of the bio sensor. This is verified by performing the experiments repeatedly. Sensor responded to concentration changes as soon as new samples were introduced to the Teflon cell. But, to get a stabilized output, all readings were taken one minute after the FBG was immersed in the solution.

Reflection spectra of the sensor as a function of protein concentration are shown in Fig. 6.4. From the figure, it can be seen that the Bragg wavelength of the sensor showed a red shift when it was exposed to a higher protein concentration. The FBG exhibited a total red shift of approximately 0.141 nm when the BSA concentration was gradually changed from 50 µg/mL to 300 µg/mL. Apart from the red shift, there was a reduction in the reflected power with increasing protein concentration. When we expose the bio sensor to protein test samples it selectively reacts with DNA coating. This causes a modulation of refractive index at the surface and leads to a change in FBG reflection spectrum. As a result, both red shift in the Bragg wavelength and reduction in reflectivity are observed based on the concentration of protein present in bio samples. Hence the amount of the Bragg wavelength shift can be directly related to the protein concentration. The reduction in reflectivity can be explained by considering the difference in the

numerical aperture of the sensing region of the fiber between successive sample measurements [11].

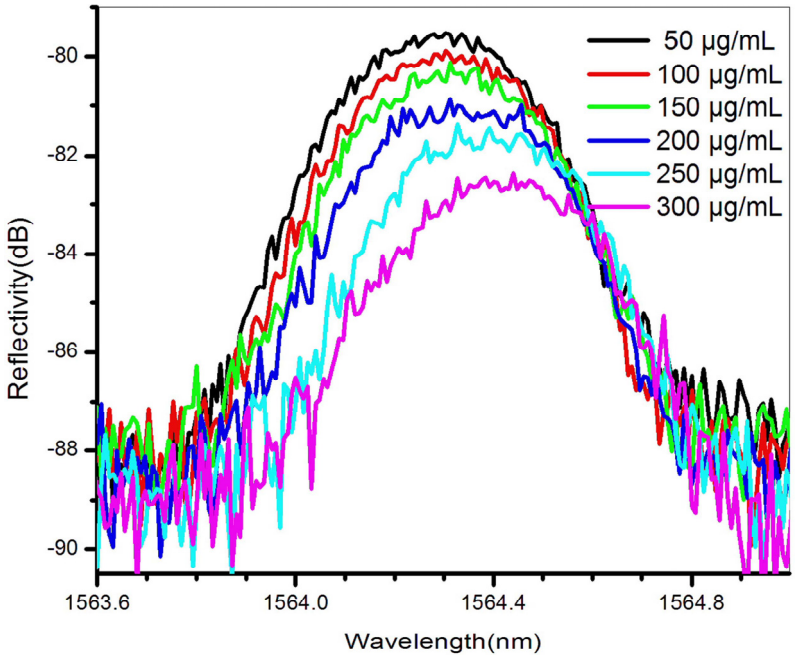


***Figure 6.4:*** *The spectral response of FBG for different concentrations of protein solutions.*

The sensitivity of the coated FBG, when used as a sensor for various weight percentage of protein in distilled water is shown in Fig. 6.5. It can be seen from the graph that the sensitivity of the sensor increases with increase in protein concentration. The FBG sensor sensitivity was around 0.180 pm/µgmL$^{-1}$ of protein in the lower concentration measurement range and 0.820 pm/µgmL$^{-1}$ of protein in the higher measurement range (150-300 µg/mL).

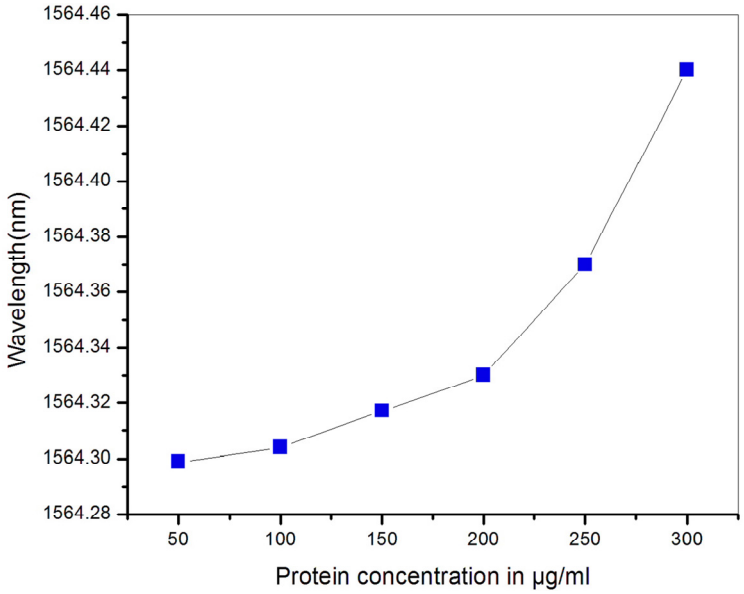


***Figure 6.5:*** *Bragg wavelengths of the FBG sensors as a function of protein concentrations.*

## 6.4 Conclusions

In conclusion, we have designed, fabricated and then experimentally evaluated a protein concentration sensor based on biopolymer coated FBG refractometer. Fabrication of the sensor was made by etching the grating region with HF solution (48%). The bio sensor can measure the amount of protein by monitoring the Bragg wavelength shift which is induced by the selective interaction of protein with DNA biopolymer coating. The advantages of this type of grating sensor are easy interrogation, it does not involve the use of toxic chemicals, requires a small volume of sample for analysis and provides the response in real time. This sensor has also shown very good repeatability. The measurement system may be used to detect biological or chemical changes in the surrounding media. The simplicity and high sensitivity of the sensor make it worthy for medical diagnostics, pharmaceutical and biomedical sensing applications

## References


[1]. A. D. Kersey, M. A. Davis, H. J. Patrick, M. LeBlac, K. P. Koo, C. G. Askins, M. A. Putnam and E. J. Friebele, *"Fiber grating sensors",* Journal of Lightwave Technology, **15**, pp. 1442 -1463 (1997).

[2]. A. Kerrouche, W. J. O. Boyle, T. Sun and K.T.V. Grattan, "*Design and in the field performance evaluation of compact FBG sensor system for structural health monitoring applications*", Sensors and Actuators A: Physical, **151**, pp. 107-112 (2009).

[3]. J. Yang, Y. Zhao, B.J. Peng and X. Wan, "*Temperature-compensated high pressure FBG sensor with a bulk-modulus and self-demodulation method*", Sensors and Actuators A: Physical, **118**, pp. 254–258 (2005).

[4]. Y. J. Rao, "*In-fiber Bragg grating sensors*", Measurement Science and Technology, **8**, pp. 355-375 (1997).

[5]. A. Othonos, "*Fiber Bragg gratings*", Review of Scientific Instruments, **68**, pp. 4309-4341 (1997).

[6]. Raman Kashyap, J. M. Lopez Higuera, "*Handbook of optical fiber sensing technology; Fiber Grating Technology: Theory, Photosensitivity, Fabrication and characterization*", John Wiley & Sons, pp. 349-377 (2002).

[7]. A. Iadicicco, A. Cusano, A. Cutolo, R. Bernini and M. Giordano, "*Thinned fiber Bragg gratings as high sensitivity refractive index sensor*", IEEE Photonics Technology Letters, **16**, pp. 1149-1151 (2004).

[8]. A. N. Chryssis, S. M. Lee, S. B. Lee, S. S. Saini and M. Dagenais, "*High sensitivity etched core fiber Bragg grating sensors*", IEEE Photonics Technology Letters, **17**, pp. 1253–1255 (2005).

[9]. J. Kumar, R. Mahakud, O. Prakash and S. K. Dixit, "*Study on hydrofluoric acid-based clad etching and chemical sensing characteristics of fiber Bragg gratings of different reflectivity fabricated under different UV exposure times*", Optical Engineering, **52**, pp. 054402-07 (2013).

[10]. W. Liang, Y. Huang, Y. Xu, R.K. Lee and A. Yariv, "*High sensitive fiber Bragg grating refractive index sensor*", Applied Physics Letters, **86**, pp. 151122-151124 (2005).

[11]. A. Iadicicco, A. Cusano, S. Campopiano, A. Cutolo and M. Giordano, "*Thinned fiber Bragg gratings as refractive index sensors*", IEEE Sensors Journal, **5**, pp. 1288-1295 (2005).

[12]. R. C. Kamikawachi , I. Abe, A. S. Paterno, H. J. Kalinowski, M. Muller, J. L. Pinto and J. L. Fabris, "*Determination of thermo-optic coefficient in liquids with fiber Bragg grating refractometer*", Optics Communications, **281**, pp. 621–625 (2008).

[13]. H. Xue Feng, C. Zhe Min, S. Li Yang, C. Ke Fa, S. De Ren, C. Jun and Z. Hao, "*Design and characteristics of refractive index sensor based on thinned and microstructure fiber Bragg grating*", Applied Optics, **47**, pp. 504-511 (2008).

[14]. A. Cusano, A. Iadicicco, S. Campopiano, M. Giordano and A. Cutolo, "*Thinned and micro-structured fibre Bragg gratings: towards new all fibre high-sensitivity chemical sensors*", Journal of Optics A: Pure and Applied Optics, **7**, pp. 734-741 (2005).

[15]. U. S. Raikar, A. S. Lalasangi, V. K. Kulkarni and J. F. Akki, "*Concentration and Refractive Index Sensor for Methanol Using Short Period Grating Fiber*", International Journal for Light and Electron Optics, **122**, pp. 89-91 (2011).

[16]. K. Zhou, X. Chen, L. Zhang, I. Bennion, "*Implementation of optical chemsensors based on HF-etched fibre Bragg grating structures*", Measurement Science and Technology, **17**, pp. 1140-1145 (2006).

[17]. J. Kumar, R. Mahakud, O. Prakash and S. K. Dixit, "*HF based clad etching of fibre Bragg grating and its utilization in concentration sensing of laser dye in dye–ethanol solution*", Pranama-Journal of Physics, **82**, pp. 265–269 (2014).

[18]. F. K. Coradin, G. R. C. Possetti, R. C. Kamikawachi, M. Muller and J. L.Fabris, "*Etched fiber Bragg gratings sensors for water-ethanol mixtures: A comparative study*", J. microwaves optoelectronics electromagnetic applications, **9**, pp. 131–143 (2010).

[19]. V. V. Spirin, M. G. Shlyagin, S. V. Miridonov, F. J. M. Jimenez and R. M. L. Gutierrez, "*Fiber bragg grating sensor for petroleum hydrocarbon leak detection*", Optics and Lasers in Engineering, **32**, pp. 497–503 (1999).

[20]. Q. Jiang, D. B. Hu and M. Yang, "*Simultaneous Measurement of Liquid Level and Surrounding Refractive In-dex Using Tilted Fiber Bragg Grating*", Sensors and Actuators A: Physical, **170**, pp. 62-65 (2011)

[21]. K. Schroeder, W. Ecke, and R. Willsch, "*Optical fibre Bragg grating hydrogen sensor based on evanescent-field interaction with palladium thin-film transducer*", Optics and Lasers in Engineering, **47**, pp.1018–1022 (2009).

[22]. Cong, X.M. Zhang, K.S. Chen and J. Xu, "*Fiber optic Bragg grating sensor based on hydrogels for measuring salinity*", Sensors and Actuators B: Chemical, **87,** pp. 487–490 (2002).

[23]. A. N. Chryssis, S. S. Saini, S. M. Lee, Y. Hyunmin, W. E. Bentley and M. Dagenais "*Detecting Hybridization of DNA by Highly Sensitive Evanescent Field Etched core Fiber Bragg Grating Sensors*", IEEE Journal of Selected Topics in Quantum Electronics, **11**, pp. 864–872 (2005).

[24]. S. S. Saini, C. Stanford, S.M. Lee, J. Park, P. Deshong, W. E. Bentley and M. Dagenais, "*Monolayer detection of Biochemical agents using etched-core fiber Bragg grating sensors*", IEEE Photonics. Technology Letters, **19**, pp. 1341–1343 (2007).

[25]. V. Mishra, N. Singh, U. Tiwari and Pawan Kapur, "*Fiber grating sensors in medicine: Current and emerging applications*", Sensors and Actuators A: Physical, **167**, pp. 279–290 (2011).

[26]. L. Ai1, J. C. Mau, W. F. Liu, T. C. Chen and W. K. Su, "*A volatile-solvent gas fiber sensor based on polyaniline film coated on superstructure fiber Bragg gratings*", Measurement Science and Technology, **19**, pp. 017002 (2008).

[27]. G. Ryu, M. Dagenais, M. T. Hurley and P. DeShong, "*High specificity binding of lectins to carbohydrate-functionalized fiber Bragg gratings: A new model for biosensing applications*", IEEE Journal of Selected Topics in Quantum Electronics, **16**, pp. 647-653 (2009).

[28]. M. Heckman, Joshua A. Hagen, Perry P. Yaney, James G. Grote and F. Kenneth Hopkins, "*Processing techniques for deoxyribonucleic acid: Biopolymer for photonics applications*", Applied Physics Letters, **87**, pp. 211115 (2005).

[29]. L. Wang, J. Yoshida, N. Ogata, S. Sasaki and T. Kamiyama, "*Self-assembled supramolecular films derived from marine deoxyribonucleic acid (DNA) – cationic lipid complexes: large-scale preparation and optical and thermal properties*", Chemistry of Materials, **13**, pp. 1273-1281 (2001).

# Chapter 7

# Summary and scope for future study

*Abstract*

*This chapter concludes the thesis by summarizing the results and presenting suggestions on further work based on this research. This research work focused on the study of fiber gratings based sensors for chemical and bio-sensing applications.*

## 7.1 Summary

Design and development of fiber grating based chemical and bio-sensors form the focal theme of this thesis. Before the discussion on the design and development of optical fiber sensors, an outline of the different types of fiber optic sensors with special emphasis on the principle and operation of grating based sensors have been given in initial two chapters. Recently fiber grating based optical sensors have received a great interest because of their unique wavelength encoded characteristics. The basic principle of FBGs, types of FBGs and sensing characteristics of FBGs were detailed in chapter 2. Further, we introduced the sensing capabilities of Long-Period Gratings. The LPG theory and the basic principle of operation of LPG based sensors were discussed and the mechanism behind the spectral shifts in the resonance band was explored.

In the third chapter, an experimental analysis of LPG transmission spectra with variation in temperature and surrounding medium refractive index was discussed. We first studied the effect of grating length and annealing on the transmission spectrum of LPG written in hydrogen loaded standard single mode fiber. We observed that the annealing of the LPG after their fabrication is a very essential process for stabilizing the grating spectrum and for obtaining good quality LPG for sensing applications. We have studied the temperature sensitivities of different mode orders using LPGs inscribed in B–Ge co-doped fiber and standard single mode fiber and verified the theoretical descriptions with good accuracy. The difference in temperature sensitivity between the SMF-28 and B-Ge co-doped fiber is explained on the basis of the thermo-optic coefficients of the respective core and the cladding materials of the two fibers. We have also presented a detailed investigation of the LPG spectra when the external index of refraction is lower or higher than that of the cladding glass. We have demonstrated that the changes in wavelength and attenuation dip of an LPG attenuation band with external index of

refraction are highly dependent on the grating period. The shorter period LPG showed more sensitivity; when the RI of the surrounding medium was lower than that of the cladding of the fiber. But the longer period LPG showed more sensitivity, when the RI of the surrounding medium was higher than that of the cladding of the fiber.

The refractive index sensitivity of long period gratings has been exploited to demonstrate an edible oil adulteration detection sensor in chapter 4. The obtained results have exhibited the LPG's potential for measurement of adulterant in pure coconut oil and olive oil. Detection limit of adulteration was found to be 3% for coconut oil- paraffin oil binary mixture and 4 % for olive oil- sunflower oil binary mixture. The LPG sensor sensitivity was around 0.15 nm/vol% of paraffin oil in the measurement range. The developed sensor is user-friendly, reusable and allows instantaneous determination of the percentage concentration of adulterant in an edible oil sample without involving any chemical analysis. The newly developed sensor also showed good reversibility and repeatability. This work could be considered as an important step towards foodstuff quality control and industrial applications.

Chapter 5 provided the details of the fabrication process of FBGs used in this thesis. A RI sensor based on etched FBG was discussed and tested experimentally. Simple and low cost fabrication technique involving wet chemical etching in a buffered HF solution has been carried out for sensor fabrication. The Bragg wavelength shifted to longer wavelength as the ambient refractive index increased in the range of 1 to fiber cladding index and the rate of change in wavelength with RI also increased as the surrounding index approached the fiber cladding index. The reduction in reflected optical power with increase in surrounding RI is explained on the basis of mismatch of the numerical aperture between the un-etched and etched FBGs. We believe that the etched core fiber Bragg grating sensor can

be a powerful and versatile sensor to detect chemical and biological reagents, and can be used for the in situ monitoring of bioprocesses.

In chapter 6, a fiber optic based protein concentration sensor is demonstrated by coating an etched FBG with a DNA bio polymer material. The RI change induced in the biopolymer film during its interaction with protein depends on the concentration of protein present in test samples. Using a real time monitoring set-up, we recorded the Bragg wavelength changes with changes in protein concentration. By analyzing the Bragg wavelength shift, we calculated the concentration of protein present in a liquid sample. The FBG sensor sensitivity was around 0.180 pm/$\mu gmL^{-1}$ of protein in the lower concentration measurement range and 0.820 pm/$\mu gmL^{-1}$ of protein in the higher measurement range (150-300 μg/mL). The simplicity and high sensitivity of the sensor make it worthy for medical diagnostics, pharmaceutical and biomedical sensing applications.

## 7.2 Scope for future study

The main aim of this research work was to develop fiber grating based refractive index sensors and evaluate them for two major sensing areas, viz. chemical and bio-sensing. A number of areas of future research have arisen from the experimental work and the most significant of them are outlined below.

- Further studies can be extended to the development of coated LPGs for bio-sensing and gas sensing applications and identification of suitable coating materials for enhancing the selectivity and sensitivity of such sensors. If a suitable film of the appropriate thickness is laid onto the surface of the cladding, then a small RI change could induce a large wavelength shift, which offers the possibility for developing a highly sensitive sensor [1-7].

- The sensitivity of LPG based refractive index sensor can be increased appreciably by etching the cladding of the fiber[8-10]. We believe a better sensitivity of our designed sensor can be achieved by the optimization of key parameters such as grating length, grating period and thickness of cladding etched.
- Although there are many RI sensors based on etched FBG in the literature, the author believes that they are very difficult to fabricate and careful handling is also required as a very thin FBG portion is used for sensing. Although it gives very high sensitivity, it can break very easily and is prone to micro-bending. Hence developing a packaging system for etched FBGs also assumes great importance.

## References

[1]. L. Coelho, D. Viegas, J.L. Santos and J. M. M. M. de. Almeida, "*Detection of Extra Virgin Olive Oil Thermal Deterioration Using a Long Period Fibre Grating Sensor Coated with Titanium Dioxide",* Food and Bioprocess Technology, **8**, pp. 1211-1217 (2015).

[2]. P. Pilla, V. Malachovská, A. Borriello, A. Buosciolo, M. Giordano, L. Ambrosio, A. Cutolo and A. Cusano, "*Transition mode long period grating biosensor with functional multilayer coatings",* Optics Express, **19,** pp.512-526 (2011).

[3]. F. Zou, Y. Liu, C. Deng, Y. Dong, S. Zhu and T. Wang, "Refractive index sensitivity of nano-film coated long-period fiber gratings", Optics Express, **23**, pp. 1114-1124 (2015).

[4]. L. Coelho, D. Viegas, J.L. Santos and J. M. M. M. de. Almeida, "Enhanced refractive index sensing characteristics of optical fibre long period grating coated with titanium dioxide thin films", **202**, Sensors and Actuators B: Chemical, pp. 929-934(2014).

[5]. P. Pilla, C. Trono, F. Baldini, F. Chiavaioli, M. Giordano and A. Cusano, *"Giant sensitivity of long period gratings in transition mode near the dispersion turning point: an integrated design approach",* Optics Letters, **37**, pp. 4152- 4154 ( 2012).

[6]. T. Wang, S. Korposh, S. James, R. Tatam and S. W. Lee, "Optical fiber long period grating sensor with a polyelectrolyte alternate thin film for gas sensing", Sensors and Actuators B: Chemical, **185**, pp. 117-124(2013).

[7]. L. Melo, G. Burton, B. Davies, D. Risk and P. Wild, *"Highly sensitive coated long period grating sensor for $CO_2$ detection at atmospheric pressure",* Sensors and Actuators B: Chemical, **202**, pp. 294-300(2014).

[8]. I. D. Villar, *"Ultrahigh-sensitivity sensors based on thin-film coated long period gratings with reduced diameter, in transition mode and near the dispersion turning point",* Optics Express, **23**, pp. 8389-8398 (2015).

[9]. S.M. Tripathi, W.J. Bock, P. Mikulic and R. Chinnappan, *"Long period grating based biosensor for the detection of Escherichia coli bacteria"*, Biosensors and Bioelectronics, **35,** 308–312 (2012).

[10]. H. Hen and Z. Gu, " *Design of a gas sensor based on a cladding-reduced long period fiber grating coated with a sensitive film* ", Optik, **124**, pp. 219-224 (2013).

*"Each time the discovery of new facts, the reversal or extension of accepted theories, reminded us that science is never finished."*

**Charles Fabry (1867-1945)**